WORLD METEOROLOGICAL ORGANIZATION

GLOBAL ATMOSPHERE WATCH

WORLD DATA CENTRE FOR GREENHOUSE GASES

WMO WDCGG DATA SUMMARY

WDCGG No. 32

GAW DATA

Volume IV-Greenhouse Gases and Other Atmospheric Gases

PUBLISHED BY
JAPAN METEOROLOGICAL AGENCY
IN CO-OPERATION WITH
WORLD METEOROLOGICAL ORGANIZATION

MARCH 2008

Acknowledgements

The present issue of *Data Summary* summarizes the latest status of greenhouse gases and related gases in the global atmosphere. The Data Summary was prepared by the World Meteorological Organization (WMO) World Data Centre for Greenhouse Gases (WDCGG) in cooperation with the WMO using the data from the global observation network that consists of many contributors (Appendix: LIST OF CONTRIBUTORS). These organizations and individuals are involved in observations and research at stations and laboratories which measure greenhouse gases and other atmospheric gases within the framework of the WMO Global Atmosphere Watch (GAW), and other cooperative monitoring and research programmes. The WDCGG thanks all of the organizations and individuals for their efforts in maintaining the observation programme and for their continuous provision of data, particularly the National Oceanic and Atmospheric Administration (NOAA) global air sampling network. Some contributors may not be explicitly acknowledged in this publication owing to lack of space, but it should be noted that all of the organizations and individuals that have submitted data to the WDCGG equally contributed to this new issue of *Data Summary*.

CONTENTS

Summary

This issue of *Data Summary* reports the results of basic analyses of greenhouse gas mole fraction data submitted to the WMO World Data Centre for Greenhouse Gases (WDCGG). The observations range from 1968 to 2006 and only data which the WDCGG accepted by October 2007 are analyzed. This *Data Summary* includes analyses of global, hemispheric and 30° latitudinal zone monthly mean mole fractions of greenhouse and related gases, and also provides useful information on the state of mole fractions of these gases.

Only monthly mean mole fraction data were used here for analyses. WDCGG greatly appreciate that some stations submit daily and hourly mean mole fractions, which are important for analyzing the variations on various time-scales. All the data submitted to WDCGG are available on the WDCGG web site http://gaw.kishou.go.jp/wdcgg.html.

In this issue, units ppm, ppb and ppt corresponding to the SI units μmol/mol, nmol/mol and pmol/mol respectively, are used to quantify mole fractions for convenience.

Variations in mole fraction of some greenhouse gases in the atmosphere are presented on seasonal cycles and deseasonalized long-term trends. Growth rates are presented as time derivatives of the long-term trends. The analytical results are summarized below for each greenhouse and related gas.

1. Carbon Dioxide (CO_2)

The level of carbon dioxide (CO_2), which of all greenhouse gases contributes the most to global warming, has been increasing since the pre-industrial period. The global average mole fraction of this gas reached a new high of 381.2 ppm in 2006, which is 136% of that in the pre-industrial period. The increase of 2.0 ppm from 2005 to 2006 is larger than the average for the 1990s (about 1.5 ppm/yr).

The global growth rate of CO_2 varies markedly interannually and was 1.93 ppm/year on average for the period 1996-2006. The high growth rates in 1987/1988, 1997/1998,2002/2003 and 2005, which exceeded 2 ppm/year, resulted from warmer conditions caused by the El Niño-Southern Oscillation (ENSO). An anomalously strong El Niño event in 1997/1998 resulted in worldwide high increases in 1998. The large growth rates in 2006 may be related with global high temperature in 2006. The exceptionally low growth rates in 1992, including negative values for northern high-latitude, were caused by low global temperature following the eruption of Mt. Pinatubo in 1991. Variations in CO_2 mole fraction can be seen on both a seasonal scale and a long-term scale. Amplitudes of the seasonal cycle are markedly large in northern high and mid-latitudes and small in the Southern Hemisphere. The seasonal cycle in the Northern Hemisphere mainly reflects seasonal variations in the absorption/emission in the biosphere there, while the seasonal cycle in the Southern Hemisphere reflects oceanic variations and biomass burning in addition to the influence of activities in the biosphere. In southern low latitudes, an annual cycle cannot be clearly determined but a semiannual cycle can. This is probably due to two opposing factors — the direct influence of sources and sinks there and the propagation of the out-of-phase seasonal variation from the Northern Hemisphere.

2. Methane (CH_4)

Methane (CH_4) is the second most significant greenhouse gas whose level has been increasing since the beginning of the 19th Century. Global mean mole fractions reflect an annual increase, and the annual averaged mole fraction was 1782 ppb in 2006, a decrease of 1 ppb since 2005 and of 2 ppb since 2003, respectively. The mole fraction is now of 255% of that in the pre-industrial period.

The latitudinal gradient of CH_4 mole fraction is large from the mid-latitudes in the Northern Hemisphere to the Tropics, suggesting that the major sources are in the high and mid northern latitudes

Growth rates decreased significantly in some years, including 1992, when negative values were recorded in northern high and mid-latitudes. However, both hemispheres experienced high growth rates in 1998, caused by an exceptionally high global mean temperature. The global growth rates decreased to almost zero in 2000-2001, suggesting that the global CH_4 budget seemed to have been in a steady-state. The growth rates temporally increased again in 2002 and 2003 with the occurrence of the 2002 /2003 El Niño event.

The global growth rate was 11.5 ppb/year on average for the period 1984-1990, but the rates decreased markedly in the 1990s. The global growth rate for the period 1996-2006 was 2.4 ppb/year. Some theories for the cause of this decreasing growth rate have been proposed but the issue remains unresolved.

Monthly mean mole fractions have a seasonal variation with high mole fractions in winter and low mole fractions in summer. Unlike CO_2, amplitudes of the seasonal cycle of CH_4 are large, not only in the Northern Hemisphere but also in southern high and mid-latitudes. In southern low latitudes, a distinct semi-annual component with a secondary maximum in boreal winter overlays the annual component. This is attributed to the large-scale transportation of CH_4 from the Northern Hemisphere.

3. Nitrous Oxide (N_2O)

Nitrous oxide (N_2O) is an important greenhouse gas whose level is increasing on a global scale. N_2O data submitted to the WDCGG show that mole fractions are increasing in both hemispheres. Global mean mole fraction reached a new high of 320.1 ppb in 2006, which is an increase of 0.8 ppb over the year before. The mean growth rate of the global mean mole fraction over the period 1996 - 2006 was 0.76 ppb/year. This mole fraction is corresponds to 119% of that in the pre-industrial period.

4. Halocarbons

Halocarbons, most of which are anthropogenic, are effective greenhouse gases and some also act as ozone-depleting compounds. Levels of some halocarbons (CFCs, etc.) increased in the 1970s and 1980s, but have now almost ceased increasing as a result of regulation of production and emission under the Montreal Protocol on Substances that Deplete the Ozone Layer and its Adjustments and Amendments.

Mole fractions of CFC-11 peaked around 1992 and then started decreasing. The growth rate of CFC-12 has declined since around 1990 and is now nearly zero. CFC-113 growth stopped in the 1990s, and has shown a slight decreasing trend over the last decade. Mole fractions of HCFC-22, HCFC-141b and HCFC-142b, which are the industrial replacements of CFCs, are increasing. Mole fractions of CCl_4 were at a maximum around 1991. Since then, they have been decreasing slowly. Mole fractions of CH_3CCl_3 peaked around 1992 and thereafter they are clearly decreased.

5. Surface Ozone (O_3)

Ozone (O_3) plays important roles in the atmospheric environment through radiative and chemical processes. It absorbs solar UV radiation in the stratosphere, influencing making a vertical temperature profile, and circulates the atmosphere with its absorbed energy. It also absorbs terrestrial IR radiation contributing to the greenhouse effect as a greenhouse gas.

Variation in the mole fraction of O_3 near the surface, so-called surface ozone, reflects various processes there. While some of the O_3 in the troposphere comes from the stratosphere, the rest is chemically produced in the troposphere through oxidation of CO or hydrocarbons in the presence of rich NO_x.

Many stations at various locations measure the mole fraction of surface ozone. However, it is difficult to identify a global long-term trend of surface O_3 due to its very uneven geographic distribution.

6. Carbon Monoxide (CO)

Carbon monoxide (CO) is not a greenhouse gas itself, but influences the mole fractions of greenhouse gases by affecting hydroxyl radicals (OH). Its mole fraction in northern high latitudes has been increasing since the mid-19th Century. The mean global mole fraction was about 94 ppb in 2006. The mole fraction is high in the Northern Hemisphere and low in the Southern Hemisphere, suggesting substantial anthropogenic emissions in the Northern Hemisphere.

Although the global mole fraction of CO was increasing until the mid-1980s, growth ceased or the mole fraction subsequently decreased thereafter (WMO, 1999a). There was large fluctuation in the growth rate, however, with high positive rates followed by high negative rates in northern latitudes and southern low latitudes from 1997 to 1999. The growth rates in the Northern Hemisphere increased again in 2002.

Monthly mean mole fractions show a seasonal variation with large fluctuations in the Northern Hemisphere and small fluctuations in the Southern Hemisphere. This seasonal cycle is driven by industrial emissions, biomass burning, large-scale transportation, and variations in the OH mole fraction which acts as a sink.

7. Nitrogen Monoxide (NO) and Nitrogen Dioxide (NO_2)

Nitrogen oxides (NO_x, i.e., NO and NO_2) are not greenhouse gases, but influence mole fractions of important greenhouse gases by affecting OH. In the presence of NO_x, CO and hydrocarbons are oxidized to produce ozone (O_3), which affects the Earth's radiative balance as a greenhouse gas and the oxidization capacity of the atmosphere by reproducing OH.

Most of the stations reporting NO_x data to the WDCGG are located in Europe. NO_x has large temporal and geographic variability, and it is difficult to identify a long-term trend. In Europe, NO_2 mole fractions are generally higher in southern regions than in northern regions.

8. Sulphur Dioxide (SO_2)

Sulphur dioxide (SO_2) is not a greenhouse gas but a precursor of atmospheric sulphate aerosol. Sulphate aerosol is produced by SO_2 oxidation through photochemical gas-to-particle conversion. SO_2 has also been a major source of acid rain and deposition throughout industrial times.

Most of the stations reporting SO_2 data to the WDCGG are located in Europe. Generally, in Europe, SO_2 mole fractions are higher in southern regions than in northern regions.

1. Introduction

Human activities have been shown to have major impacts on the global environment. Since the beginning of the industrial revolution, mankind has increasingly made use of land, water, minerals and other natural resources, and future population and economy growths will result in further increases in our impact on the environment. As the global climate, biogeochemical processes and natural ecosystems are closely interlinked, changes in any one of these systems may affect the others and be detrimental to humans and other organisms. Emissions of man-made gaseous and particulate matter alter the energy balance of the atmosphere, and consequently affect interactions between the atmosphere, hydrosphere, and biosphere. Nevertheless, we do not yet have a sufficient understanding of either the chemical processes that occur within the atmosphere or the interrelationships between the atmosphere, the hydrosphere, and the biosphere. Our lack of understanding of the chemical processes of the atmosphere and the oceans is mainly due to lack observation data.

The World Meteorological Organization (WMO) launched the Global Atmosphere Watch (GAW) Programme in 1989 to promote systematic and reliable observation of the global environment, including greenhouse gases (CO_2, CH_4, CFCs, N_2O, *etc.*) and other related gases (*e.g.*, CO, NO_x, and SO_2) in the atmosphere. In October 1990, the WMO established the World Data Centre for Greenhouse Gases (WDCGG) at the Japan Meteorological Agency (JMA) in Tokyo as one of the GAW World Central Facilities to collect, archive, and distribute data regarding greenhouse and related gases in the atmosphere and oceans. In August 2002, the WDCGG took over the role of the Data Centre for Surface Ozone from the Norwegian Institute for Air Research (NILU) and began to collect surface ozone data from a number of observation sites throughout the world participating in GAW and other scientific monitoring programmes (Appendix: LIST OF OBSERVING STATIONS).

With regard to issues involving global warming, the Kyoto Protocol, in which quantified emission limitations and reductions were agreed upon based on the United Nations Framework Convention on Climate Change, came into force in February 2005. The WMO commenced annual publications of the WMO Greenhouse Gas Bulletin in March 2006. The second and third issues of a series of the bulletins were published in November of 2006 and 2007, respectively. The bulletin briefly summarizes the state of greenhouse gases in the atmosphere. The WDCGG is needed for swifter and smoother exchange of such data.

Since its establishment, the WDCGG has provided its users with data and other information through its regular publications: *Data Report*, *Data Catalogue*, *Data Summary,* and *CD-ROM* (Appendix: LIST OF WMO WDCGG PUBLICATIONS). All data and information are now available on the WDCGG web site, which aims to improve accessibility to data, information, and products in line with the GAW Strategic Plan: (2008-2015) (WMO, 2007a). Furthermore, the WDCGG published the Data Submission and Dissemination Guide in 2007 (WMO, 2007b). It would be helpful for submission of observation data and access to Archived data in the WDCGG.

The GAW Strategic Plan requests World Data Centres to assist users of atmospheric chemistry observations. To this end, the WDCGG provides diagnostic information on global greenhouse gases. Performing global and integrated diagnostics on the state of greenhouse gases is one of the important tasks of the WDCGG. Other important tasks include revision and improvement of the contents of *Data Summary* based on comments from data contributors and scientists, and provision of advanced analytical information to scientists and policy makers. The WDCGG invites comments and suggestions regarding *Data Summary* or any other publications. We hope the diagnostic information presented here will both stimulate the use of data on greenhouse and other gases and increase appreciation of the GAW programme.

All users are required to accept the following conditions set forth by the Commission for Atmospheric Sciences (CAS) WG and supported by the Thirteenth Session of CAS: "For scientific purposes, access to these data is unlimited and provided without charge. By their use you accept that an offer of co-authorship will be made through personal contact with the data providers or owners whenever substantial use is made of their data. In all cases, an acknowledgement must be made to the data providers or owners and to the data centre when these data are used within a publication." The WDCGG requests data users to make acknowledgements appropriately. Data users should refer to the GAW Station Information System (GAWSIS) which can be found at the GAW website (http://www.wmo.ch/web/arep/gaw/gaw_home.html) or see WDCGG website for details on GAW Country Contacts, what measurements are being made, and the investigators responsible. The information at the GAWSIS and World Data Centres is updated in cooperation with the WMO Secretariat.

Finally, the WDCGG would like to express thanks to all data contributors, including those involved in measurement at the numerous sites worldwide, for their efforts in maintaining the observation programme and for their continuous provision of data.

Mailing address:
WMO World Data Centre for Greenhouse Gases (WDCGG)
c/o Japan Meteorological Agency

1-3-4, Otemachi, Chiyoda-ku, Tokyo 100-8122, Japan
E-mail: wdcgg@met.kishou.go.jp
Telephone: +81-3-3287-3439
Facsimile: +81-3-3211-4640
Web Site: http://gaw.kishou.go.jp/wdcgg.html

2. Analysis

The WDCGG collects, archives and provides observation data regarding mole fractions of greenhouse gases, and also provides diagnostic results on the greenhouse gases using collected data.

For CO_2, CH_4 and CO, long-term trends and seasonal variations in mole fractions derived for global and zonal means are presented. For N_2O, global trends are presented. For surface O_3, global long-term trends can not been determined because the stations measuring the mole fraction of surface O_3 are not unevenly geographically distributed. For halocarbons, NO_x and SO_2, only time series of monthly mean mole fractions are presented as few sites have submitted observation data.

For convenience, units ppm, ppb, and ppt corresponding to SI units μmol/mol, nmol/mol, and pmol/mol, respectively, are used.

The following sections explain the methods used for analysis of CO_2, CH_4, CO and N_2O. The global analysis method used for CO_2, CH_4, and N_2O by WDCGG is also summarized in the Technical Document (The Global Analyses Method by the WDCGG Using the Archived Data) and posted on the WDCGG website. Refer to the respective chapters for the other parameters.

2-1. Site selection for global, hemispheric and zonal mean mole fractions

For CO_2, the diagnostic statistics, such as global, hemispheric and zonal means, are based on data from the selected sites whose standard gases have traceability to the WMO standard gas kept at the Central Calibration Laboratory (CCL). The WMO standard for CH_4 was established in 2005, so the standard is now prevalent. Thus, for CH_4, the statistics are derived not only from the selected sites that employ the WMO standard gas but also from the sites that use standard gases whose differences from the WMO standard gas have been determined. The same is also true regarding N_2O .

As ground-based sites observe air at a lower boundary layer, the measured mole fractions of gases, such as CO_2, CH_4 and CO, which have sources or sinks on the Earth's surface, may show localised characteristics in a lower boundary layer depending on weather conditions, *etc.*.

These data provide very useful information for investigating the power of local sources and sinks. However, for global scale analysis, it is necessary to use data that can be considered as representative mole fractions averaged over a reasonable geographical area and in a whole boundary layer, *i.e.*, background data. In this study, for CO_2, CH_4 and CO, observation sites that were considered to offer such background data were selected.

Site selection was performed objectively as described below, based on data in a reasonably scattered range of the total data in the same latitudinal zone. The latitudinal distribution of the annual mean mole fractions normalised with respect to the South Pole, which were calculated from the monthly mean mole fractions, was fitted to the LOESS model curve (Cleveland *et al.*, 1988). Sites with mole fractions lying more than $\pm 3\sigma$ from this curve were rejected and this process was iterated until all of the remaining sites lay within $\pm 3\sigma$ from the fitted curve. The sites selected according to certain scales and/or background criteria are marked with asterisks in Plate 3.1 for CO_2, Plate 4.1 for CH_4, Plate 5.1 for N_2O and Plate 8.1 for CO. A list of the selected sites for CO_2, CH_4 and N_2O is available on the WDCGG web site (http://gaw.kishou.go.jp/wdcgg.html).

2-2. Trend analysis

The time series of greenhouse gas mole fractions, which is produced by removing local effects with very short-term variations, represents integration of variations on different time scales. The two major components of variation in the CO_2 mole fraction are seasonal variation and long-term trends. Many researchers have attempted to decompose observation data into these two components by objective curve fitting (Keeling *et al.*, 1989), digital filtering (Thoning *et al.*, 1989; Nakazawa *et al.*, 1991), or both (Conway *et al.*, 1994; Dlugokencky *et al.*, 1994).

Trend analysis approximating variations in the sum of seasonal variations by Fourier harmonics and long-term trends by low-pass filtering with a cut-off frequency of 0.48 cycles/year was performed for each selected site. Refer to WDCGG Data Summary No. 22 (2000) for details.

2-3. Estimation of value for periods without data for zonal mean calculation

The number of sites used for trend analysis outlined above varied during the analysis period. Moreover, data were frequently missing due to pauses in the observation. When the calculations are performed without considering these situations, the values, such as the zonal growth rate, fluctuate with the change in the number of available sites and data. These fluctuations were particularly evident in the early period when few sites were available.

However, if we select only those sites for which data are available throughout the whole analysis period, the data from many newly established sites will not be reflected in the analysis. To use as many sites as possible and to avoid gaps accompanying changes in

the number of sites, the estimated values for the periods for which no data were included in the zonal mean calculations. These were estimated by interpolation and extrapolation as follows:

First, sites requiring interpolation were selected. A provisional seasonal variation was calculated from the longest consecutive data set for each site with all the same Lanczos filters (Duchon, 1979) as described in the previous Summary. Then, linear interpolation was performed for the data from which the provisional seasonal variation was subtracted. The complete variation was then retrieved by adding the provisional seasonal variation.

Next, the sites requiring extrapolation were selected. The provisional long-term trend and the seasonal variation were calculated from the interpolated data set with the same filter. Extrapolation was then performed for the long-term trend as its growth rate traces the zonal mean growth rate calculated from those of the other sites in the same latitudinal zone. Subsequently, the complete variation was retrieved by adding the site's own provisional seasonal variation. Here, each zone was created every 30° of latitude.

The zonal mean mole fractions were calculated from the continuous data set, derived in the above procedure, by determining the arithmetic mean for the sites included in each latitudinal zone for every 20° or 30°. The zonal mean in the early stage of the analysis period may be less accurate than that in the latest stage. Although the data sets were partly estimated, the completeness of data was assumed to be advantageous for trend analysis of the zonal mean.

2-4. Calculation of global and hemispheric means

Global and hemispheric means were calculated by averaging the zonal means, taking into consideration the area ratio of each latitudinal zone.

The deseasonalised long-term trend and growth rate for the globe, both hemispheres and each latitudinal zone were calculated again with the filter from the global, hemispheric and zonal means. To derive the trend for the whole period, we assumed that provisional data extending from both ends followed the linear trend for the whole period. Therefore, analyzed trends at both ends may depart from the actual values.

Here, we summarise the characteristics of global, hemispheric and zonal mean mole fractions by presenting the time series of monthly mean mole fractions, deseasonalised long-term trends, annual growth rates and the averaged seasonal cycle.

3.

CARBON DIOXIDE

(CO_2)

● : CONTINUOUS STATION

△ : FLASK STATION

□ : FLASK MOBILE (SHIP)

▼ : REMOTE SENSING STATION

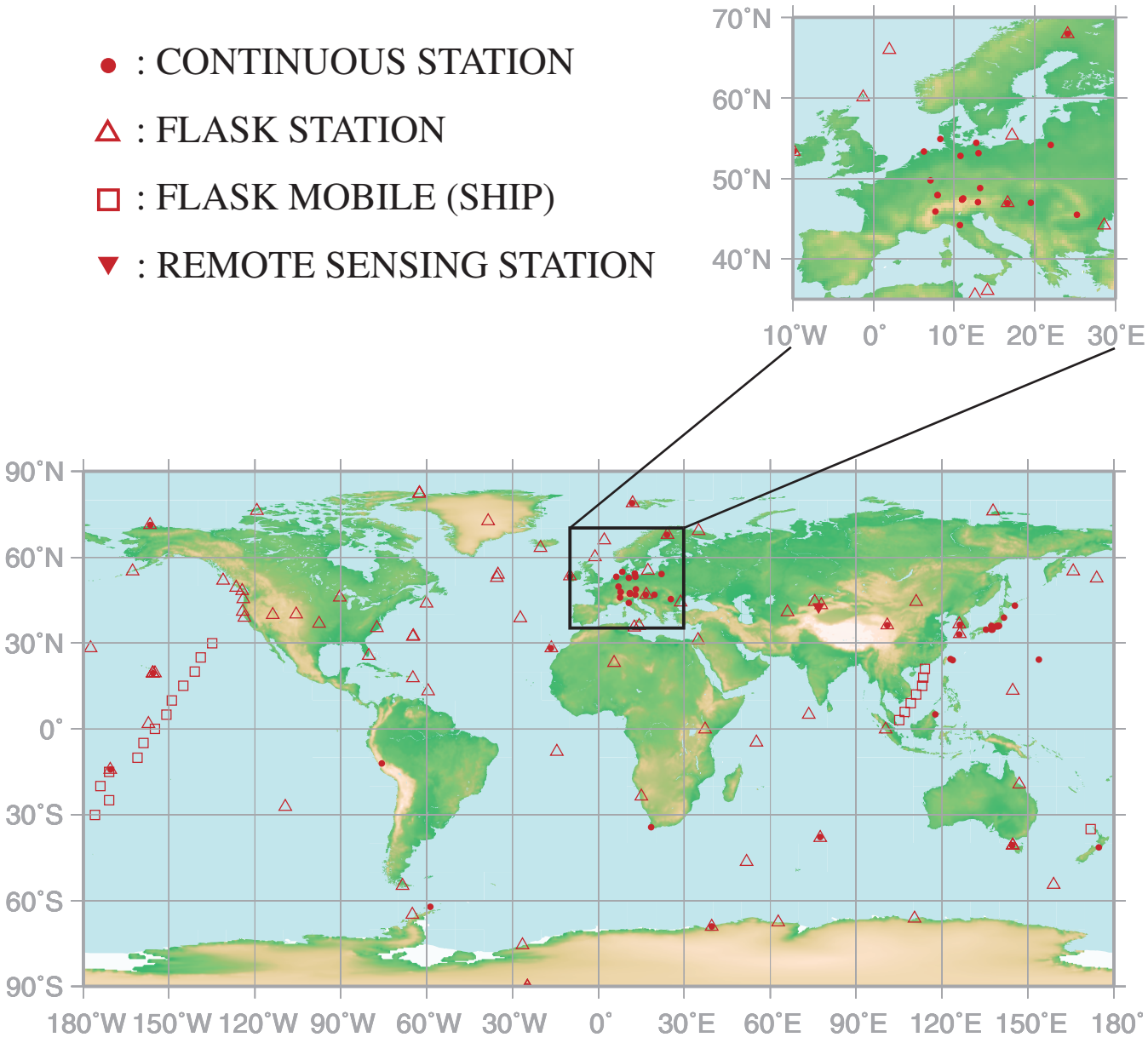

This map shows locations of the site where the monthly mean mole fractions are submitted.

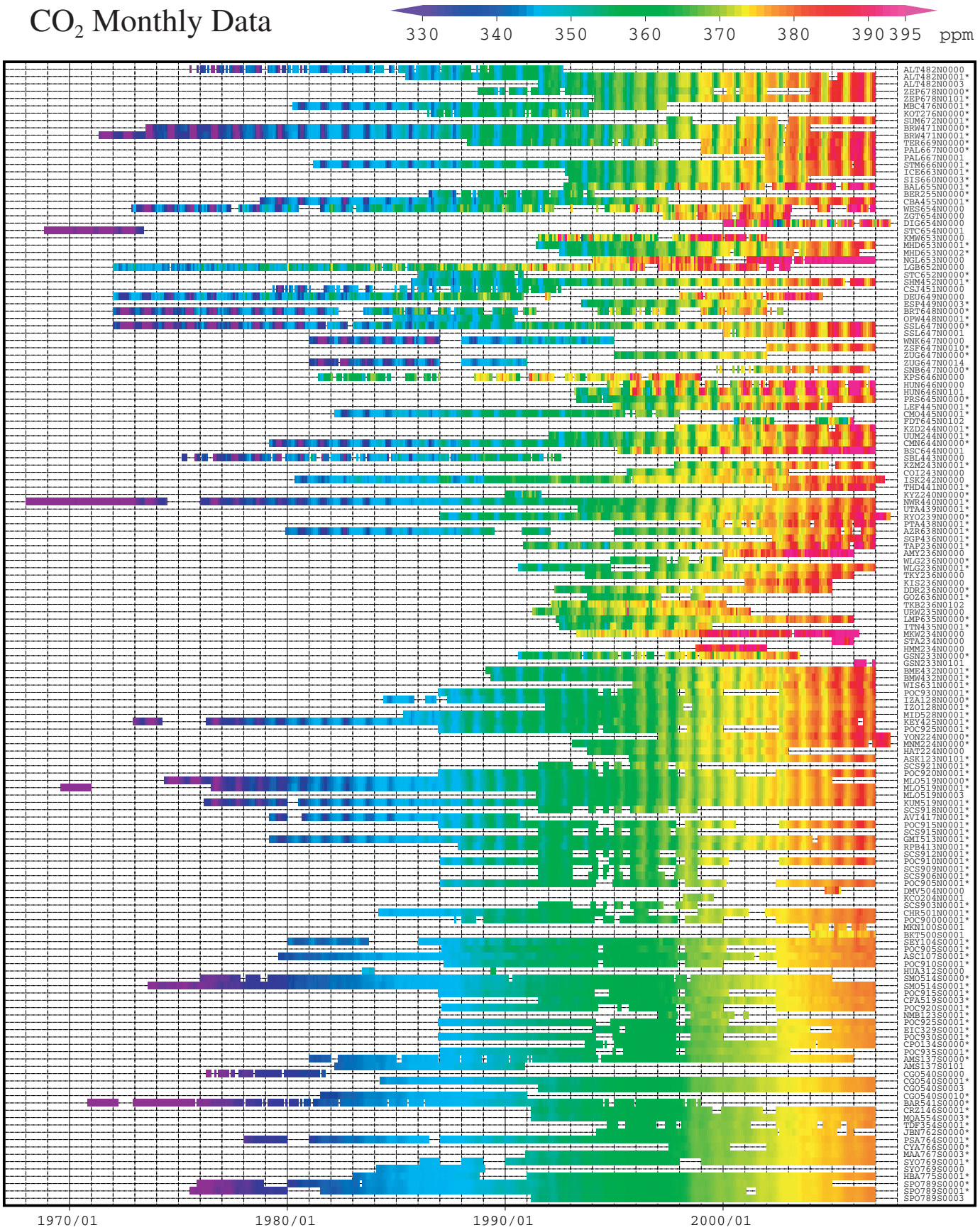

Plate 3.1 Monthly mean CO_2 mole fractions for all sites reported to the WDCGG illustrated in colors that change with the mole fraction. The sites are set from north to south. Though some stations reported data at two or three different altitudes, only data at the highest altitudes are illustrated. The monthly value at the site which has submitted only original (hourly) data before selection is calculated by the WDCGG as an arithmetric mean, and may become high for reflecting the mole fraction influenced in plant breathing at nighttime in the lower boundary layer. Filename code with an asterisk shows the data used in the analysis shown in Plate 3.2. (see Chapter 2)

CO_2 mole fraction

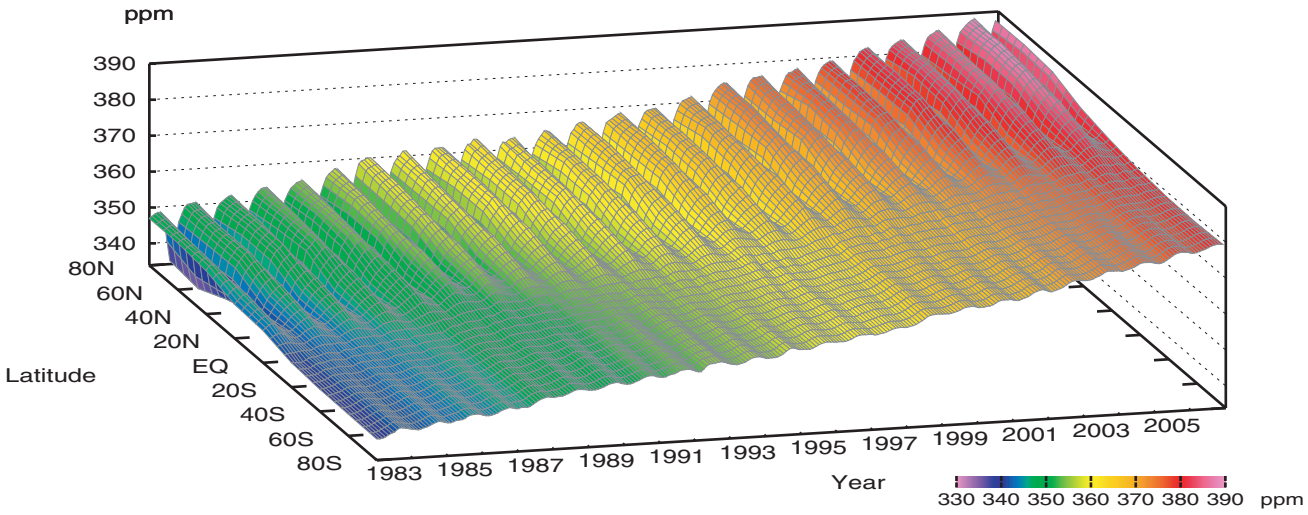

CO_2 deseasonalized mole fraction

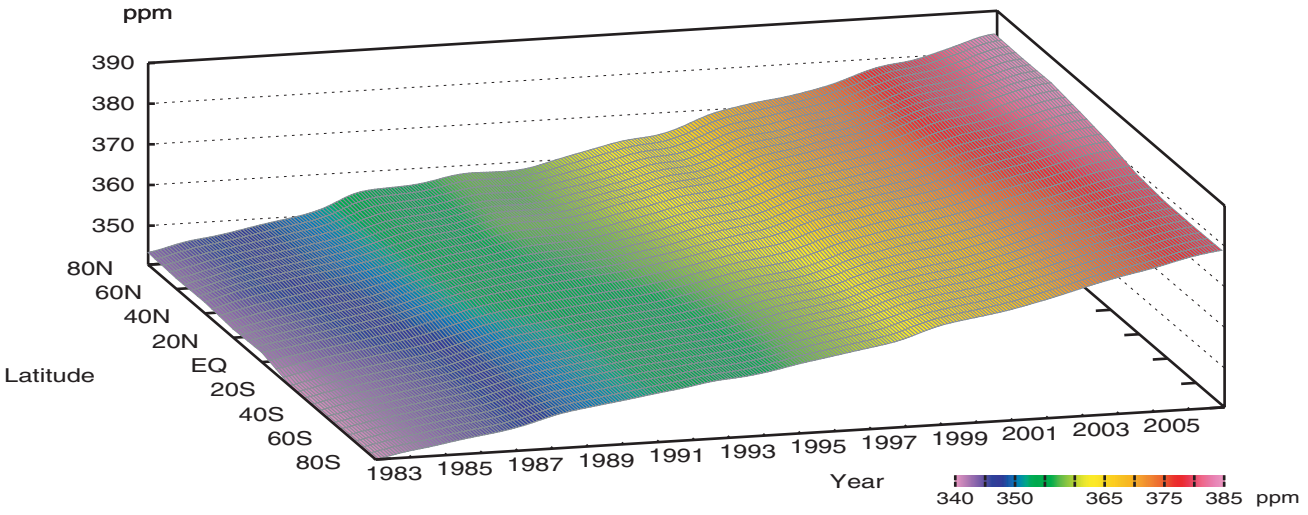

CO_2 growth rate

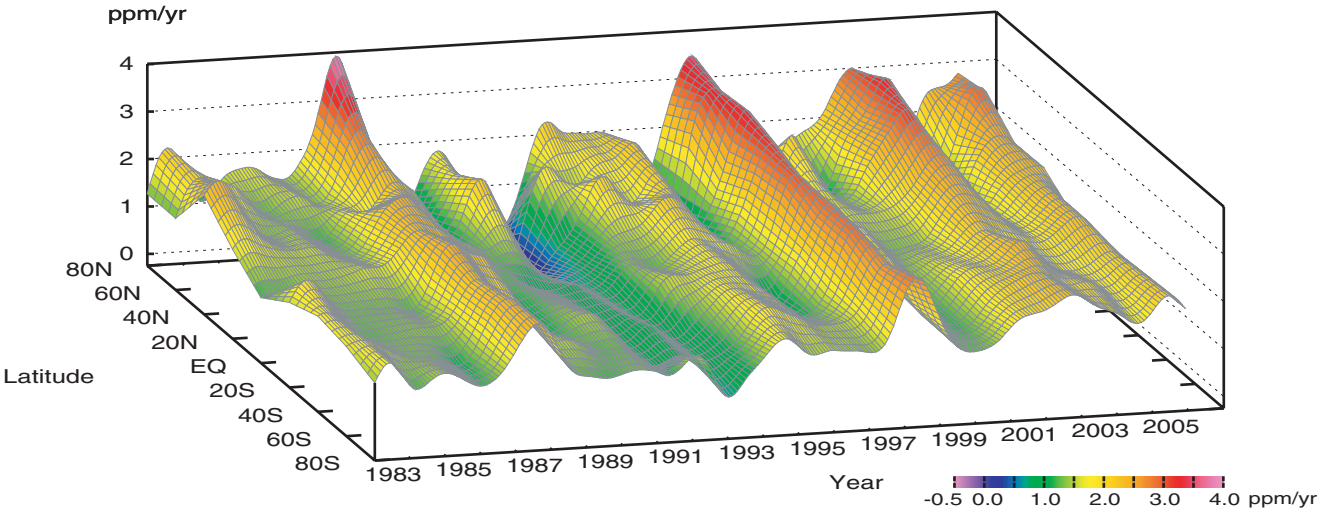

Plate 3.2 Variation of zonally averaged monthly mean CO_2 mole fractions (top), deseasonalized mole fractions (middle), and growth rates (buttom). Zonally averaged mole fractions are calculated for each 20° zone. Deseasonalized mole fractions and growth rates are derived as described in Chapter 2.

3. Carbon Dioxide (CO_2)

Basic information on CO_2 with regard to environmental issues

Carbon dioxide (CO_2) has strong absorption bands in the infrared region and is the biggest contributor to the greenhouse effect. It contributed 63% of the radiative forcing caused by the increase in well-mixed greenhouse gases from 1750 to 2005 (IPCC, 2007).

The balance between its emission and absorption at the surface of the earth or oceans determines the mole fraction of CO_2 in the atmosphere. About 762 Gigatonnes of carbon exist in the atmosphere as CO_2. This carbon is exchanged with two other large reservoirs, the terrestrial biosphere and the oceans. The CO_2 is exchanged between the atmosphere and terrestrial biosphere mainly through absorption by photosynthesis and emission from plant respiration and decomposition of organic soils. These biogenic activities vary with season, resulting in large seasonal variations in CO_2 levels. CO_2 is transported between the atmosphere and the ocean, with direction determined by relative CO_2 mole fractions which also vary with time and geography.

Current mole fractions of atmospheric CO_2 far exceed pre-industrial values dating back 650,000 years according to the publication IPCC AR4 (Solomon *et al*., 2007). Based on results of ice core studies, the mole fraction of atmospheric CO_2 in the pre-industrial level was about 280 ppm (IPCC, 2007). Emissions of CO_2 due to human activities have been increasing from the beginning of the industrial era, and have been distributed into the atmosphere, oceans and terrestrial biosphere. The global carbon cycle, which is comprised mainly of CO_2, is not fully understood. About half of the anthropogenic CO_2 emission has stayed in the atmosphere, the rest having been removed by sinks, including the terrestrial biosphere and ocean. However, the amount that the sinks remove from the atmosphere varies widely with time (Figure 3.1).

Carbon isotopic studies have demonstrated the importance of the terrestrial biosphere and oceans as sources and sinks (Francey *et al.*, 1995; Keeling *et al.*, 1995; and Nakazawa *et al.*, 1993, 1997a). On the other hand, the atmospheric O_2 content is dependent mainly on O_2 removal by burning of fossil fuels, and O_2 release from the terrestrial biosphere. Therefore, the uptake of carbon by the terrestrial biosphere and ocean can be evaluated from O_2 (O_2/N_2) measurements combined with CO_2 measurements (IPCC, 2001). IPCC AR4 showed that the ocean and the terrestrial biosphere respectively absorbed about 31% and 12% of CO_2 emitted from the burning of fossil fuel in 2000-2005, while the remaining 57% contributed to the annual increase in CO_2 level in the atmosphere (Solomon *et al*., 2007).

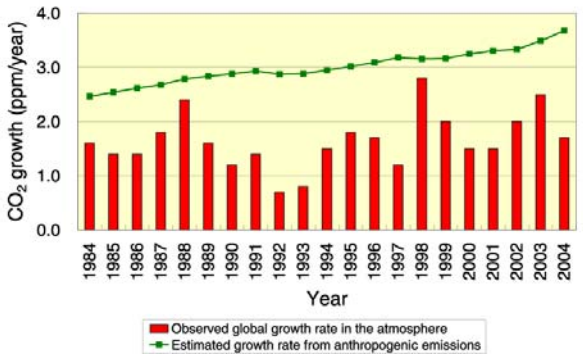

Fig. 3.1 Time series of annual mean CO_2 growth rates in the atmosphere calculated from observation data (red column) and from anthropogenic emission data (green curve). CO_2 emissions were calculated by CDIAC based on the United Nations Energy Statistics, and the observed growth rate was calculated by the WDCGG. Note that observational CO_2 abundance in the atmosphere is expressed by mole fraction with respect to dry air, but CO_2 mole fraction from anthropogenic emission is calculated based on the atmosphere including water vapor that is usually less than 1% in mole fraction.

Large amounts of CO_2 are exchanged among these reservoirs, and the global carbon cycle is coupled with the climate system on seasonal, interannual and decadal time scales. Accurate understanding of the global carbon cycle is essential for the estimation of future CO_2 mole fractions in the atmosphere.

The map at the beginning of this chapter shows observation sites that submitted CO_2 mole fraction data to the WDCGG by October 2007. These sites include *in situ* stations performing continuous measurement as well as flask-sampling stations, such as those in the NOAA/GMD network. In addition to such fixed stations, mobile stations on ships and aircraft, and other stations that measure event data also report their data to the WDCGG (see Appendix: LIST OF OBSERVATION STATIONS).

Annual variations in CO_2 in the atmosphere

The monthly mean of CO_2 data from all stations that submitted to the WDCGG are shown in Plate 3.1. In this plate, mole fraction levels are illustrated in different colours. Global, hemispheric and zonal mean background mole fractions were analysed based on selected stations (see the caption to Plate 3.1). The three-dimensional representations of latitudinal distribution of the atmospheric CO_2 mole fraction, deseasonalized mole fractions and the growth rates are shown in Plate 3.2. These three-dimensional

representations (CO_2 carpets) indicate that the amplitudes of seasonal mole fraction variations are large in the northern mid- and high-latitudes, but the seasonal variation is indistinct in the Southern Hemisphere; the increases in mole fraction occur in the Northern Hemisphere prior to the Southern Hemisphere, and propagate to the Southern Hemisphere, and the inter-annual variation of growth rates occurs largely in the Northern Hemisphere.

Figure 3.2 shows the global monthly mean mole fractions with the long-term trends and growth rate from 1983 to 2006. The global average mole fraction reached a new high in 2006 at 381.2 ppm which corresponds to 136% of the pre-industrial level. The increase from 2005 to 2006 was 2.0 ppm, which was larger than the average for the 1990s (about 1.5 ppm/yr).

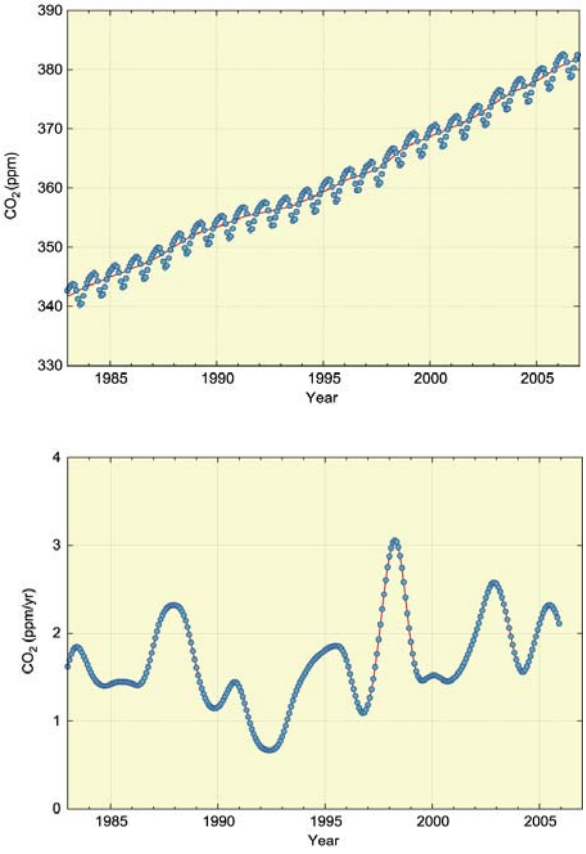

Fig. 3.2 Monthly mean mole fractions (dots) and deseasonalized long-term trends (line) (top), and growth rate (bottom) from 1983 to 2006 for the globe.

The mean annual global growth rate of CO_2 for the 10 years 1996–2006 was 1.93 ppm/year. There was large inter-annual variation with 3.1 ppm/year in April 1998 and 0.7 ppm/year in June 1992, respectively. Growth rates exceeding 2 ppm/year were seen in 1987/1988, 1997/1998, 2002/2003 and 2005.

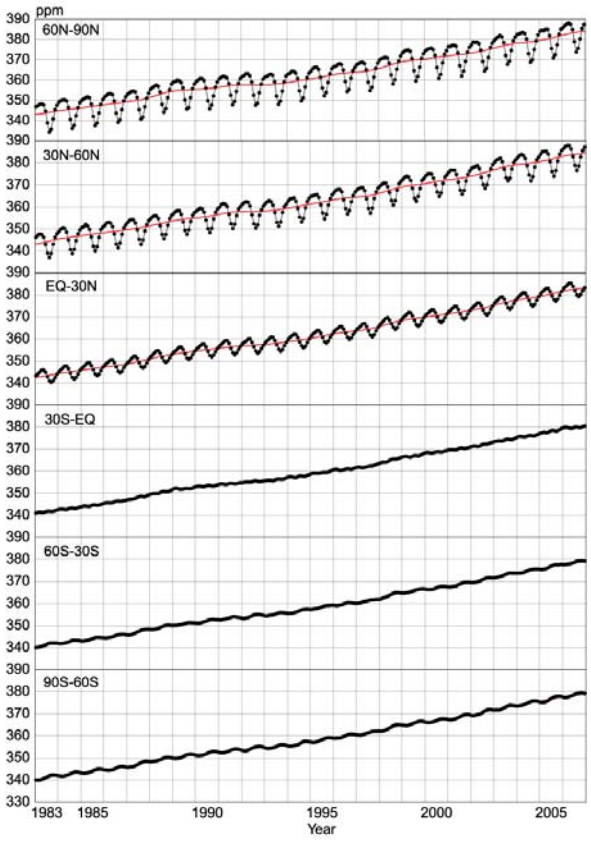

Fig. 3.3 Monthly mean mole fractions (thick lines and dots) and deseasonalized long-term trends (thin lines) from 1983 to 2006 for each 30° latitudinal zone.

Figure 3.3 shows the monthly mean mole fractions and long-term trends from 1983 to 2006 for each 30° latitudinal zone. Long-term increases in both hemispheres and seasonal variations in the Northern Hemisphere are clearly observed.

As shown in Figure 3.4, the growth rates for each 30° latitude zone fluctuated between –0.3 and 3.5 ppm/year with variability relatively large in northern high latitudes. In 1987/1988, 1997/1998, 2002/2003 and 2005, growth rates exceeding 2 ppm/year were observed for all 30° latitude zones. On the other hand, negative values were recorded in northern high latitudes in 1992.

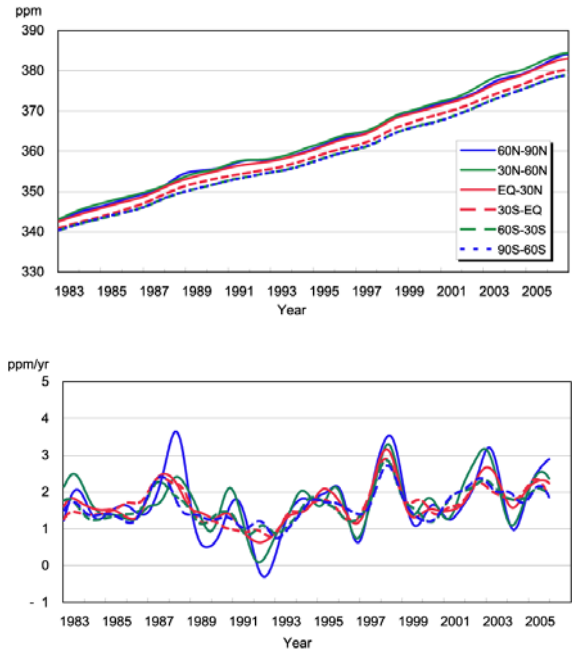

Fig. 3.4 Long-term trends (top) and growth rates (bottom) for each 30° latitudinal zone.

Changes in growth rate are known to be associated with El Niño-Southern Oscillation (ENSO). Apart from 1992, El Niño events that occurred in 1982/1983, 1986-1988, 1991/1992, 1997/1998 and 2002/2003 correspond with high growth rates. The high growth rates in 2005, when El Niño events did not occure, may be related to the global high temperature of 2005 especially in the northern hemisphere. In addition to those at the surface, CO_2 growth rates observed by aircraft flying at high altitudes (8-13 km) over the Pacific Ocean also have a similar relationship with ENSO (Matsueda *et al.*, 2002). Ordinarily, there is an up-welling area of CO_2-rich ocean water in the eastern equatorial Pacific,, however, El Niño events suppress this up-welling reducing CO_2 emission. On the other hand, El Niño events result in high temperature anomalies in many areas, particularly the Tropics, which increase CO_2 emission from the terrestrial biosphere via enhanced respiration of plants and decomposition of organic matter in the soil (Keeling *et al.*, 1995). Anomalously low precipitation, particularly in the Tropics, also enhances this effect by suppressing plant photosynthesis. These oceanic and terrestrial processes have opposite effects during El Niño events. However, Dettinger and Ghil (1998) suggested that the oceanic effect was limited to the eastern equatorial Pacific, while the terrestrial effect was more global. Thus, the global CO_2 response, which is almost synchronous with El Niño events, is due to terrestrial biosphere changes associated with temperature variations on a global scale.

Carbon isotope (^{13}C) studies have also shown that atmospheric CO_2 variations accompanying El Niño events are brought about by the flux between the terrestrial biosphere and the atmosphere, rather than between the ocean and the atmosphere (Keeling *et al.*, 1989; Nakazawa *et al.*, 1993; Morimoto *et al.*, 2000). The El Niño event during 1997/1998, which was one of the most severe in the 20th Century, brought about high temperatures and low precipitation levels on a global scale (WMO, 1999b), resulting in frequent wildfires and drought in Southeast Asia. Such meteorological conditions perturbed the global carbon cycle, and are considered to intensify CO_2 emission from the terrestrial biosphere. However, an exceptionally low CO_2 growth rate occurred during the El Niño event in 1991/1992.

The injection of 14-20 Mt of SO_2 aerosols into the stratosphere by the Mt. Pinatubo eruption in June 1991, which affected the radiation budget and atmospheric circulation (Hansen *et al.*, 1992; Stenchikov *et al.*, 2002), and resulted in a drop in the global temperature. The reduced CO_2 emission from consequent terrestrial vegetation respiration and decomposition of organic matter (Conway *et al.*, 1994; Lambert *et al.*, 1995; Rayner *et al.*, 1999), and enhanced CO_2 absorption by intensive photosynthesis due to the increase in diffuse radiation (Gu *et al.*, 2003) contributed to the low CO_2 growth rate despite this El Niño event (Angert *et al.*, 2004).

Figure 3.5 shows a time series of CO_2 growth rates in the tropical area (< ±30° from 1983 to 2005), the Southern Oscillation Index (SOI), Sea Surface Temperature (SST) anomaly in the eastern equatorial Pacific (5°N--5°S, 150°W-90°W) and temperature anomaly on land in the Tropics calculated from Japanese Re-Analysis 25 years (JRA-25: Onogi *et al.*, 2007) data. SOI and SST data are provided by the WMO DDBs (Distributed Data Bases). In the figure, the SOI, the SST anomaly and the temperature anomaly are processed as a five-month running mean to display the seasonal variation. The growth rate in the Tropics showed good correspondence to the SOI and SST anomalies with a time lag except in 1992. In addition, the growth rate in the Tropics also showed good correspondence to the temperature anomaly on land in the Tropics, including 1992. These results suggest that the growth rate is related to ENSO events and that temperature anomalies on tropical land have the closest relationship with CO_2 growth rate in the Tropics suggesting a strong influence of the tropical biosphere on tropical CO_2 mole fraction.

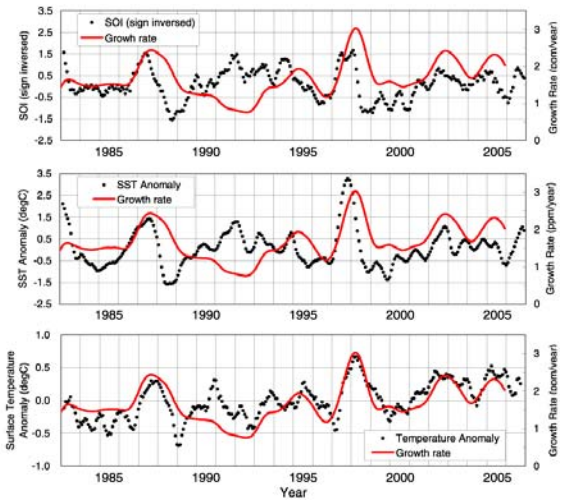

Fig. 3.5 Time series of growth rates in the Tropics (30°N-30°S) and a comparison with the Southern Oscillation Index inversed sign (top), SST anomaly in the eastern equatorial Pacific (5°N-5°S, 150°W-90°W) (middle) and temperature anomaly on land in the Tropics calculated from JRA-25 reanalysis data (bottom). The solid lines show the growth rates, and the dots show each element (5-month running mean).

Seasonal cycle of CO_2 in the atmosphere

Figure 3.6 shows average seasonal cycles for each 30° latitudinal zone from which the long-term trends were subtracted.

Amplitudes of seasonal cycles are clearly large in northern high and mid-latitudes and small in the Southern Hemisphere. Oceanic uptake (Ramonet *et al.*, 1996) and biomass burning (Wittenberg *et al.*, 1998) are thought to influence the seasonal variation. However, these large seasonal cycles in the Northern Hemisphere are characterized by rapid decreases from June to August and large returns from September to December. They are the result of the activities of the terrestrial biosphere, *i.e.*, CO_2 absorption by photosynthesis, emission by respiration of vegetation, and decomposition of organic matter by microbes in the soil (*e.g.*, Nakazawa *et al.*, 1997b).

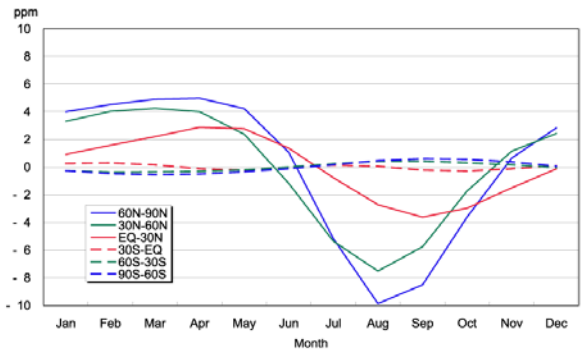

Fig. 3.6 Average seasonal cycles for each 30° latitudinal zone from which the long-term trends were subtracted.

In northern high and low latitudes, occurrences of maximum mole fractions are delayed by one or two months. Minimum mole fractions appeared in August in northern high and mid-latitudes and in September in northern low latitudes. The peak in low latitudes is delayed because seasonal variation in high latitudes takes time to reach low latitudes (Tanaka *et al.*, 1987), and the seasonal cycle of terrestrial biosphere activity at low latitudes is later than in mid-latitudes due to the wet and dry seasons (Nemry *et al.*, 1996).

In the Southern Hemisphere, seasonal variations showed small amplitudes with a half-year delay due to small amounts of net emission and absorption by the terrestrial biosphere. Seasonal variations of northern mid-latitudes and southern mid-latitudes seemed to be superimposed in the southern low latitudes (0-30°S), while the amplitude was small, suggesting that large seasonal variation in the Northern Hemisphere influences the Southern Hemisphere. The direct influence of sources and sinks in the Southern Hemisphere might be partially cancelled by propagation of the out-of-phase seasonal variation from the Northern Hemisphere.

Figure 3.7 shows the latitudinal distributions of CO_2 mole fractions in January, April, July and October in 2006. Latitudinal gradients around 30°N were positive (larger mole fractions in higher latitudes) in January and April, and negative (smaller mole fractions in higher latitudes) in July, corresponding to the large seasonal cycle in northern, mid- and high latitudes.

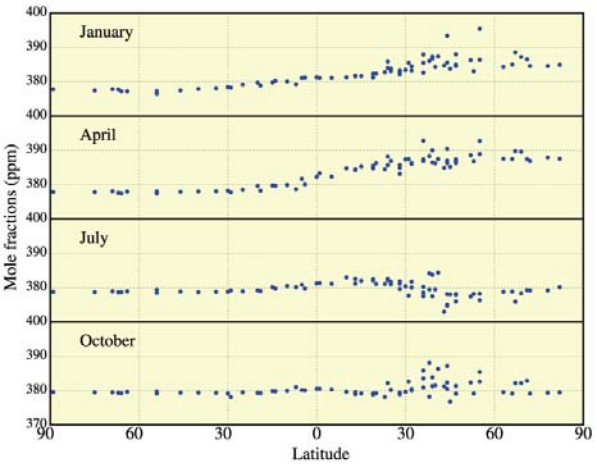

Fig. 3.7 Latitudinal distributions of monthly mean mole fractions in January, April, July and October 2006.

Annual variation of CO_2 in the upper atmosphere

The Meteorological Research Institute in JMA has carried out aircraft-based measurements of trace gases, such as CO_2, at altitudes of 8-13 km over the western Pacific using commercial flights between Japan and Australia in cooperation with Japan Airlines Foundation, the Ministry of Land, Infrastructure and Transport, and Japan Airlines since 1993. The observation data are submitted to the WDCGG every year. Fig. 3.8 shows the time series of the atmospheric CO_2 mole fractions, deseasonalized mole fractions and growth rates in the upper air obtained. Continuous data obtained by linear interpolation is used. The trend analysis is described in Chapter 2. CO_2 mole fractions increased with seasonal variation, similar to those on the surface. Seasonal variations observed over the Northern Hemisphere also reflected those on the surface, but the amplitudes were smaller.

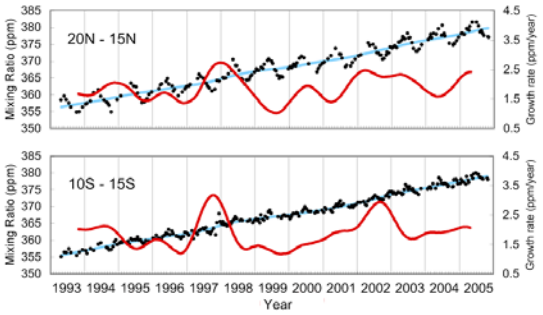

Fig. 3.8 Time series of CO_2 mole fractions (dots), deseasonalized mole fractions (dashed lines), and growth rates (solid lines) observed at latitudinal zones of 15-20°N and 10-15°S at altitudes of 8–13 km over the western Pacific.

4.

METHANE

(CH_4)

● : CONTINUOUS STATION

△ : FLASK STATION

□ : FLASK MOBILE (SHIP)

▼ : REMOTE SENSING STATION

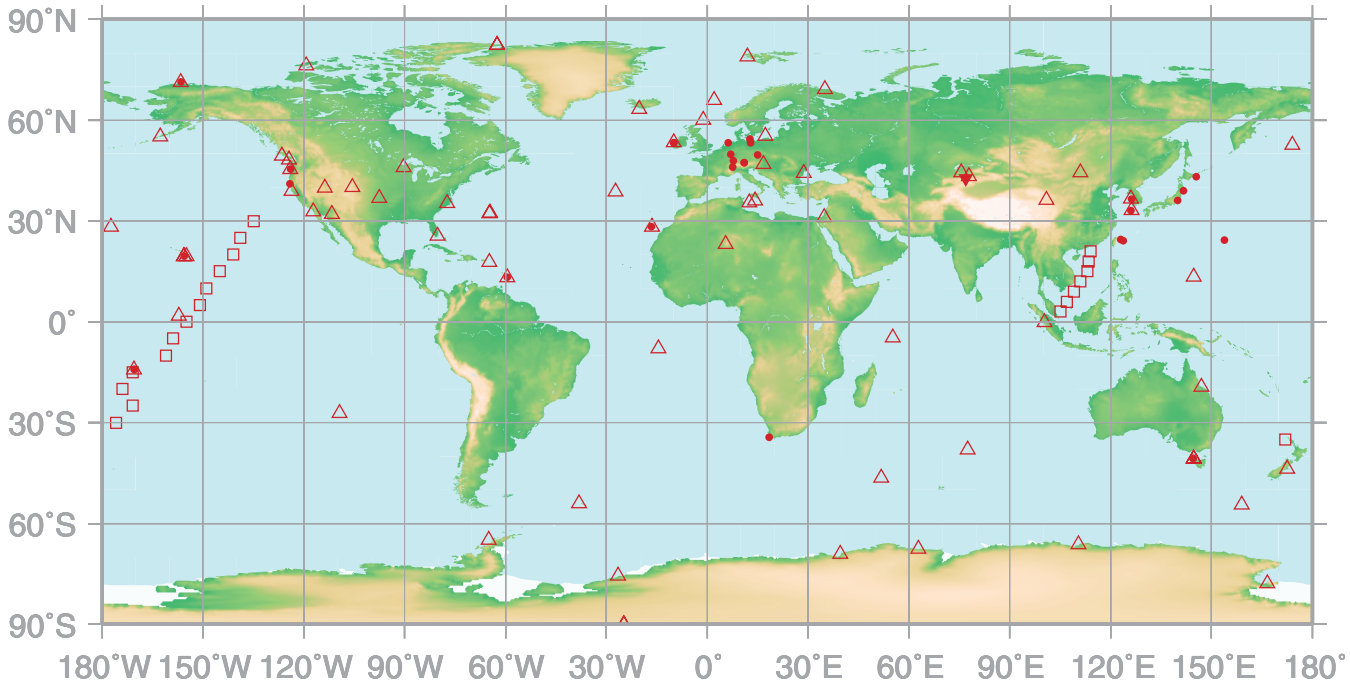

This map shows locations of the site where the monthly mean mole fractions are submitted.

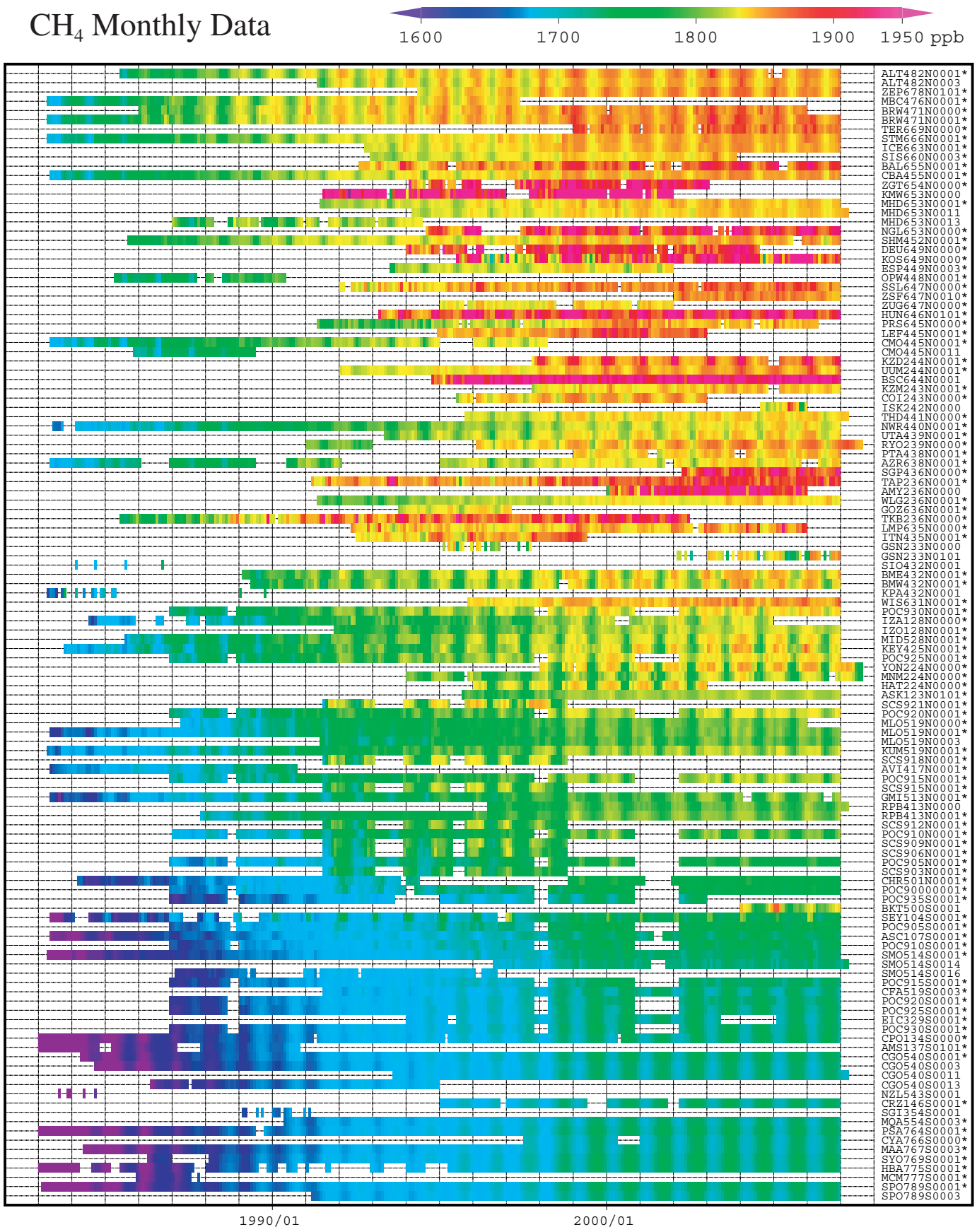

Plate 4.1 Monthly mean CH_4 mole fractions for all sites reported to the WDCGG illustrated in colors that change with the mole fraction. The sites are set from north to south. Though some stations reported data at two or three different altitudes, only data at the highest altitudes are illustrated. The monthly value at the site which has submitted only original (hourly) data before selection is calculated by the WDCGG as an arithmetic mean. Filename code with an asterisk shows the data used in the analysis shown in Plate 4.2. (see Chapter 2)

CH_4 mole fraction

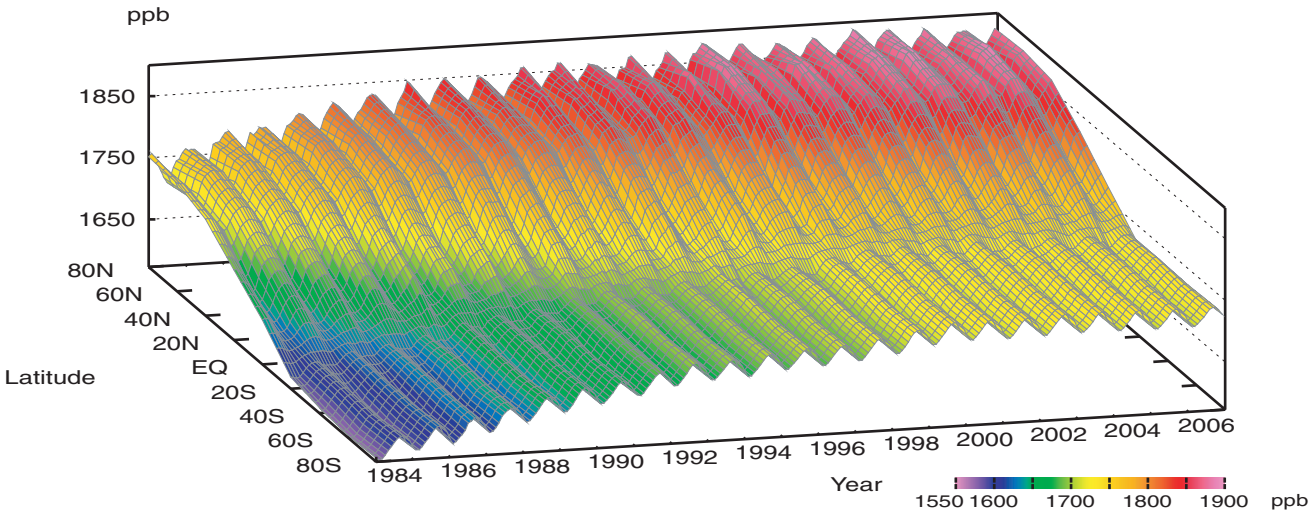

CH_4 deseasonalized mole fraction

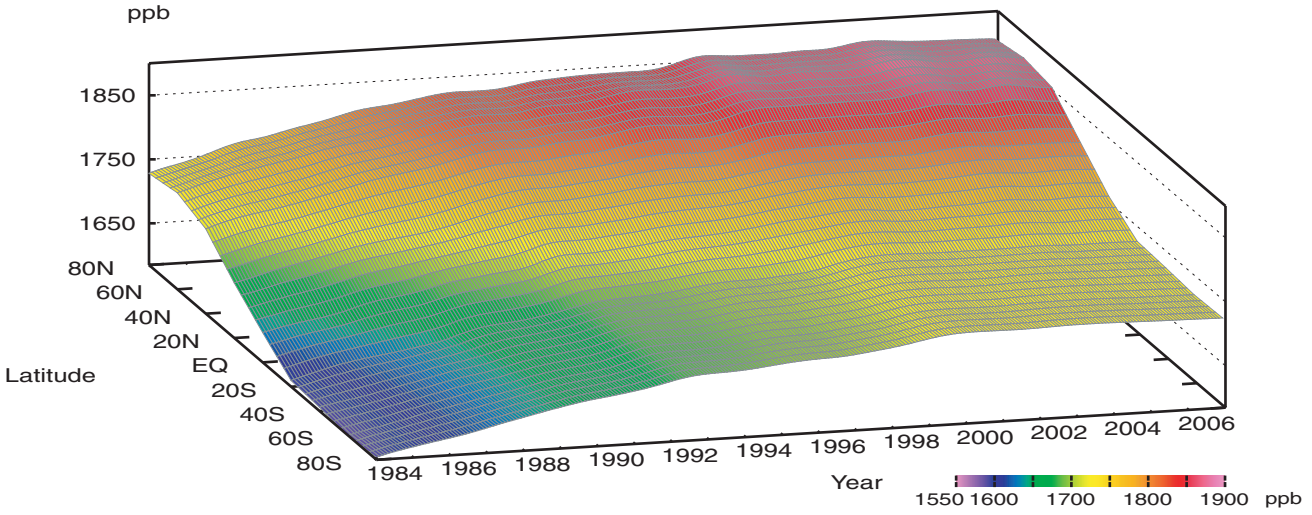

CH_4 growth rate

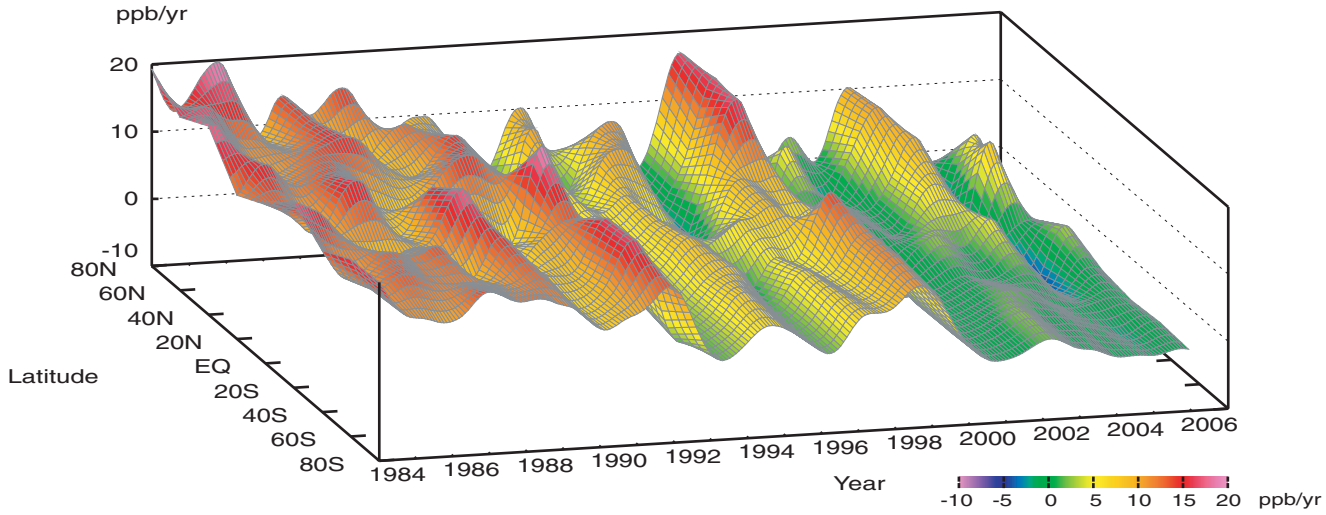

Plate 4.2 Variation of zonally averaged monthly mean CH_4 mole fractions (top), deseasonalized mole fractions (middle), and growth rates (buttom). Zonally averaged mole fractions are calculated for each 20° zone. Deseasonalized mole fractions and growth rates are derived as described in Chapter 2.

4. Methane (CH_4)

Basic information on CH_4 with regard to environmental issues

Methane (CH_4) is the second most significant greenhouse gas, but is estimated to have 23 times as much global warming potential for a 100 year horizon as CO_2 per molecule. It contributed 18% of the radiative forcing caused by the increase in well-mixed greenhouse gases from 1750 to 2005 (IPCC, 2007).

Analyses of air trapped in ice cores from the Antarctica and Arctic revealed current atmospheric CH_4 mole fraction to be the highest of the last 650,000 years according to the Fourth Assessment Report (AR4) of the Intergovernmental Panel on Climate Change (IPCC) (Solomon *et al.*, 2007b). The mole fraction of CH_4 remained steady at 700 ppb from 1000 AD until the start of the industrial revolution (Etheridge *et al.*, 1998), after which it began increasing. The rate of increase has slowed in the last few years. From the measurements of CH_4 mole fractions in ice cores from the Antarctica and Greenland, the mole fraction difference between the Northern and Southern Hemispheres was in the range of 24~58 ppb from 1000 to 1800 A.D. (Etheridge *et al*., 1998), but now it is about 150 ppb (see Fig. 4.3), reflecting more emissions in the Northern Hemisphere where major anthropogenic sources exist.

CH_4 is emitted from both natural and anthropogenic sources, including natural wetlands, oceans, landfills, rice paddies, enteric fermentation, gas drilling and biomass burning. Denman *et al.*(2007) estimated global emission at 582 teragrams (Tg) CH_4 per year. Of the various sources of emissions, more than 60% are estimated to be related to anthropogenic activities. CH_4 is destroyed by reaction with hydroxyl radicals (OH) in both the troposphere and the stratosphere, and by reaction with chlorine atoms and $O(^1D)$, an excited state of oxygen, in the stratosphere. CH_4 is one of the most important water vapour sources in the stratosphere and has atmospheric lifetime of about 12 years. However, the mole fraction of OH radicals is affected by ambient temperature and humidity. In addition, emissions from some sources are dependent on air temperature. Furthermore, Keppler *et al*. (2006) estimated that living plants and plant litter emit 62-236 and 1-7 Tg of methane per year, respectively. More information regarding sources and sinks of CH_4 must be collected to better estimate the atmospheric CH_4 budget.

The observation sites that submitted CH_4 mole fraction data to the WDCGG are shown on the map at the beginning of this chapter.

Annual variation in CH_4 levels in the atmosphere

The monthly mean CH_4 data from all the stations that submitted to the WDCGG are shown in Plate 4.1. In this plate, mole fraction levels are illustrated in different colours. Global, hemispheric and zonal mean background mole fractions were analysed based on selected stations (see the caption for Plate 4.1). The three-dimensional representations of latitudinal distribution of the atmospheric CH_4 mole fractions, deseasonalized mole fractions and the growth rate are shown in Plate 4.2. These three-dimensional representations (CH_4 carpets) indicate that the amplitudes of seasonal variation of mole fraction are larger in the Northern than the Southern Hemisphere; the increase in mole fraction starts in the Northern Hemisphere and then expands to the Southern Hemisphere. The variation in growth rate occurs on a global scale. These features are similar to those of CO_2 (see Section 3). The latitudinal gradient of CH_4 mole fraction is large from the mid-latitudes in the Northern Hemisphere to the Tropics, suggesting that the major sources are located in the high and middle northern latitudes and that CH_4 is destroyed with transportation to the Tropics where mole fraction of OH radicals is higher.

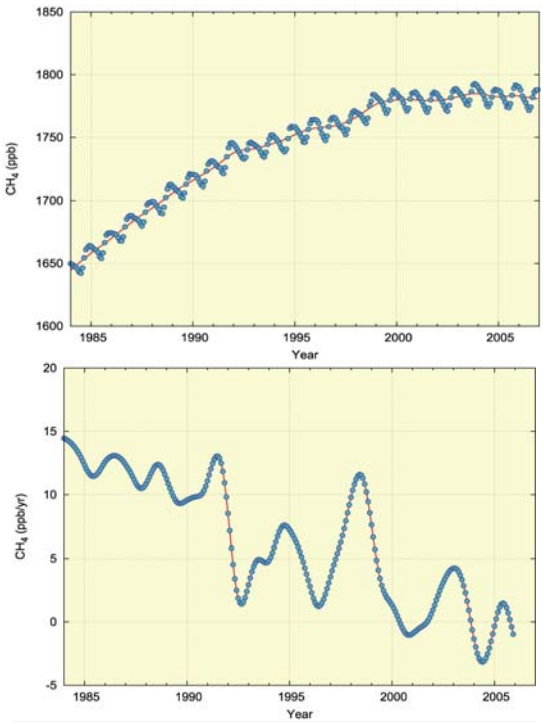

Fig. 4.1 Monthly mean mole fractions (thick line), deseasonalized long-term trends (thin line) (top) and growth rates (bottom) from 1984 to 2006 for the globe.

Figure 4.1 shows the global monthly mean mole fractions with deseasonalized long-term trends and the global growth rate from 1984 to 2006. The mean mole fraction was 1782 ppb in 2006, a decrease of 1 ppb since 2005 and 2 ppb since 2003, respectively. The mean growth rate was 2.4 ppm/year from 1996 to 2006. The current mole fraction is 255% of the pre-industrial level. Figure 4.2 shows the monthly mean mole fractions and their deseasonalized long-term trends from 1984 to 2006 for each of the 30° latitudinal zones. The seasonal variations were small in the latitudinal zone from the equator to 30°S.

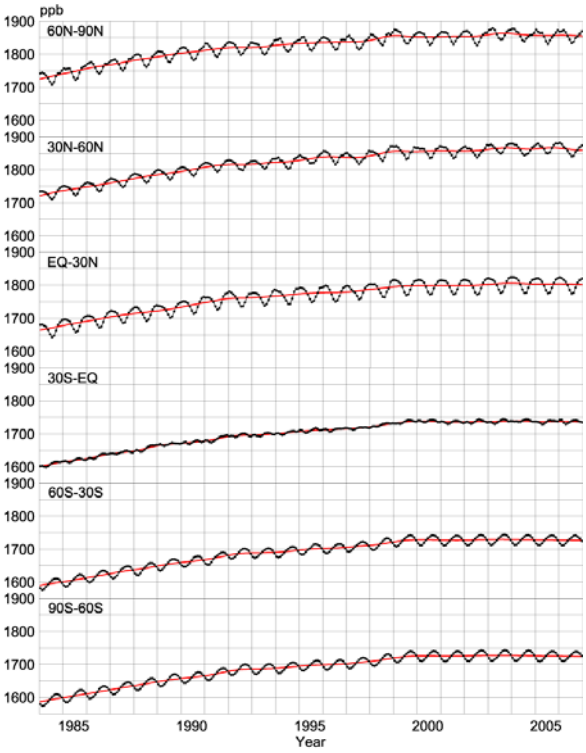

Fig. 4.2 Monthly mean mole fractions (thick line) and deseasonalized long-term trends (thin line) from 1984 to 2006 for each 30° latitudinal zone.

Figure 4.3 shows the deseasonalized long-term trends and growth rates for each of the 30° latitudinal zones. Deseasonalized long-term trends have the distinct feature of high mole fractions in northern high and mid-latitudes and low mole fractions in southern latitudes. Growth rates in all latitudinal zones clearly decreased in 1990s. The growth rates in the Southern Hemisphere and Northern Subtropics were high in 1991, but the global growth rate fell to about 1 ppb/year around 1992 and 1996. In 1998, the global growth rate increased to about 12 ppb/year, and the growth rates for northern high and mid-latitudes were over 15 ppb/year. In 2000 and 2001, the global growth rate decreased to around -1 ppb/year and the increase in mole fractions appeared to have stopped. Around 2002/2003, the growth rates increased in the Northern Hemisphere, especially in northern high and mid-latitudes where it reached about 10 ppb/year. The global growth rate was -3 ppb/year in 2004 and 1 ppb /year in 2005. Though the growth rates were large in 1998 and 2002/2003, which were affected by El Niño events as will be discussed later, the global growth rate during the last 10 years was lower than that in the 1990s.

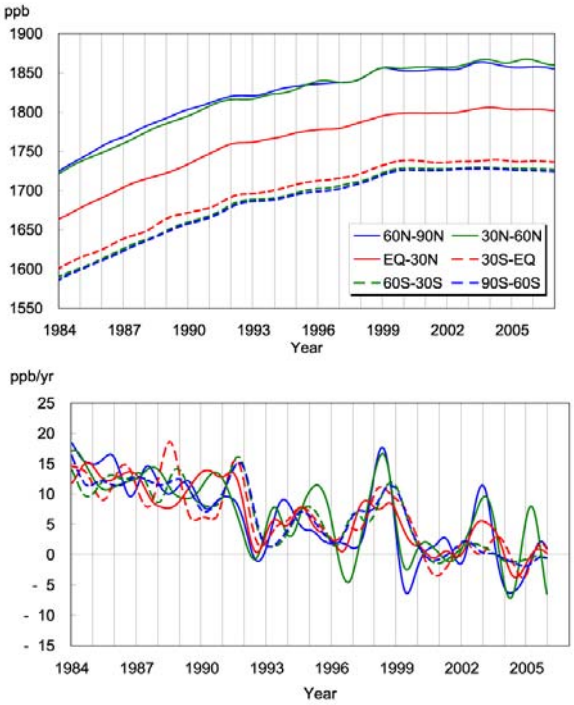

Fig. 4.3 Deseasonalized long-term trends (top) and growth rates (bottom) for each 30° latitudinal zone.

High temperature anomalies result in both increased CH_4 emission from wetlands and destruction by increased OH radical levels (Bekki and Low, 1997). The relationship between global growth rate and temperature anomalies showed that the former effect exceeds the latter globally. A study of the relationship between CH_4 mole fractions in ice cores or firn layers and global temperature anomalies also suggested that large growth rates for the CH_4 mole fraction follow high global mean temperatures (Etheridge *et al.*, 1998). Figure 4.4 shows interannual variations in global mean growth rate and global surface temperature anomaly. Global CH_4 growth rate fluctuated with global mean temperature anomalies in the 1990s, particularly during the period 1990-1998. However, apart from 1990-1998, interannual variations in global mean growth rate could have been caused by factors other than global temperature anomalies.

The large increase in CH_4 growth rate in 1991 may

have been caused by decreased levels of OH radicals due to reduced UV radiation as a result of the eruption of Mt. Pinatubo in 1991 (Dlugokencky *et al.*, 1996) and the subsequent decrease in 1992 may have been due to increased OH radical mole fraction as a result of stratospheric ozone depletion following the eruption (Bekki *et al.*, 1994). However, analysis of monsoon activity suggested that decrease in emission from wetlands and rice paddy fields, due to low temperatures, and more abundant decomposition due to dryness, may have been involved (Lelieveld *et al.*, 1998). On the other hand, carbon isotope observations suggested that the decrease in 1992 was probably caused by reduction in biomass burning at low latitudes (Lowe *et al.*, 1997).

Growth rates were large in 1998 for all latitudinal zones. Dlugokencky *et al.* (2001) suggested that this was due to increased emissions in the northern high latitudinal zones and tropical wetlands due to high temperatures and increased precipitation, and partly the influence of biomass burning of the boreal forest mainly in Siberia. On the other hand, Morimoto *et al.* (2006) estimated from isotope observations that the contribution of biomass burning to the 1998 increase was about a half of that of wetlands. Growth rates decreased afterward, but increased again upon occurrence of the 2002 /2003 El Niño event.

The cause of this long-term decreasing trend of CH_4 growth rate since 1991 remains unresolved. Lelieveld *et al.* (1998) noted that the decrease in global emission of CH_4 brought about a reduction in CH_4 growth rate in the 1990s. Bousquet *et al.* (2006) pointed out that the decreased growth rate in the 1990s was caused by reduced emission from anthropogenic sources, but after 1999 the increased anthropogenic emission may be offset by emission reduction from wetlands. On the other hand, Fiore *et al.* (2006) showed using the global tropospheric chemical transport model that the decrease in CH_4 growth rate resulted from an increase in tropospheric OH and a lower tropospheric warming that accelerates CH_4 destruction by OH radicals. They indicate that greater convective activity and subsequent production of NOx by lightning, increases the mole fraction of OH radicals in the troposphere.

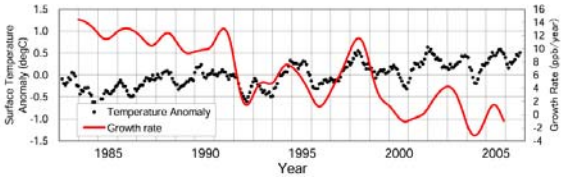

Fig. 4.4 Time series of the global mean CH_4 growth rates and their comparison with temperature anomalies on land from JRA-25 reanalysis data (Onogi *et al.*, 2007). The solid lines show the growth rates, and the dots show temperature anomalies (5-month running

Seasonal cycle of CH_4 in the atmosphere

Figure 4.5 shows average seasonal cycles for each of the 30° latitudinal zones. Seasonal cycles are brought about mainly by reaction with OH radicals, a major CH_4 sink in the atmosphere. The degree and timing of emission from CH_4 sources, such as wetlands and biomass burning along with transportation of CH_4, also affect the seasonal cycle. The amplitudes of the seasonal cycle were large in the Northern Hemisphere. Unlike CO_2, amplitudes were large in the Southern Hemisphere except at low latitudes. The CH_4 seasonal cycle showed a minimum in summer and a maximum in winter in both hemispheres. The seasonal variation of CH_4 is almost consistent with OH radicals reacting with the CH_4. Southern low latitudes have a distinct semi-annual component, which is superimposed on the annual component of the seasonal cycle at southern mid-latitudes. The secondary maximum occurred in boreal winter due to the trans-hemisphere transportation of CH_4 from the Northern Hemisphere. This phenomenon was seen at stations located in the western Indian Ocean, *e.g.,* Mahe Island and the Seychelles, and in the western and central equatorial Pacific, *e.g.,* Cape Matatula and Samoa.

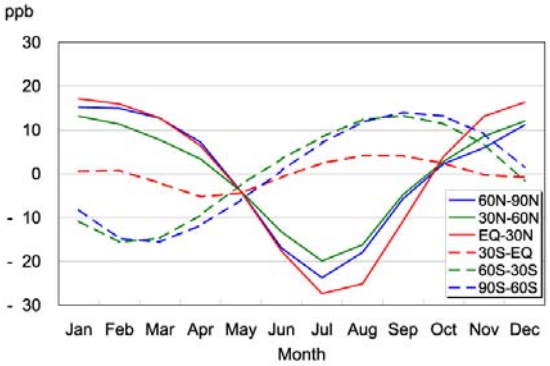

Fig. 4.5 Average seasonal cycles for each 30° latitudinal zone from which the long-term trends were subtracted.

5.

NITROUS OXIDE

(N_2O)

● : CONTINUOUS STATION

△ : FLASK STATION

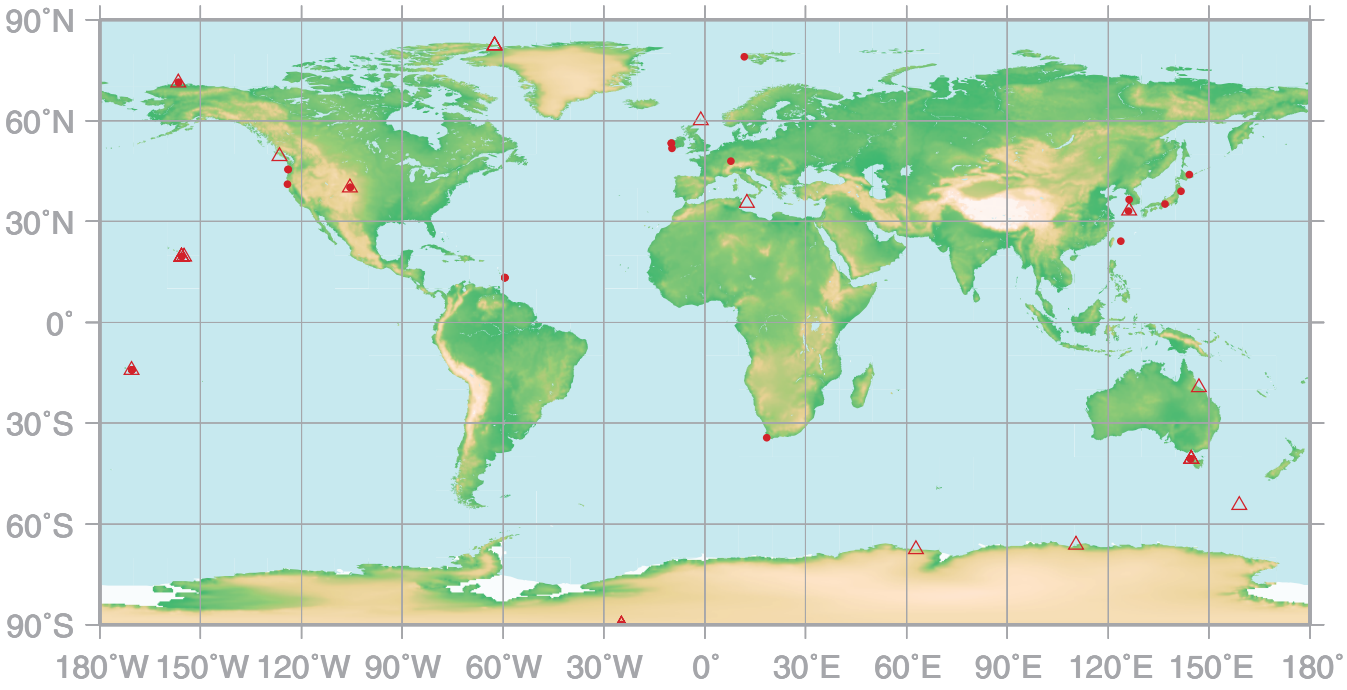

This map shows locations of the site where the monthly mean mole fractions are submitted.

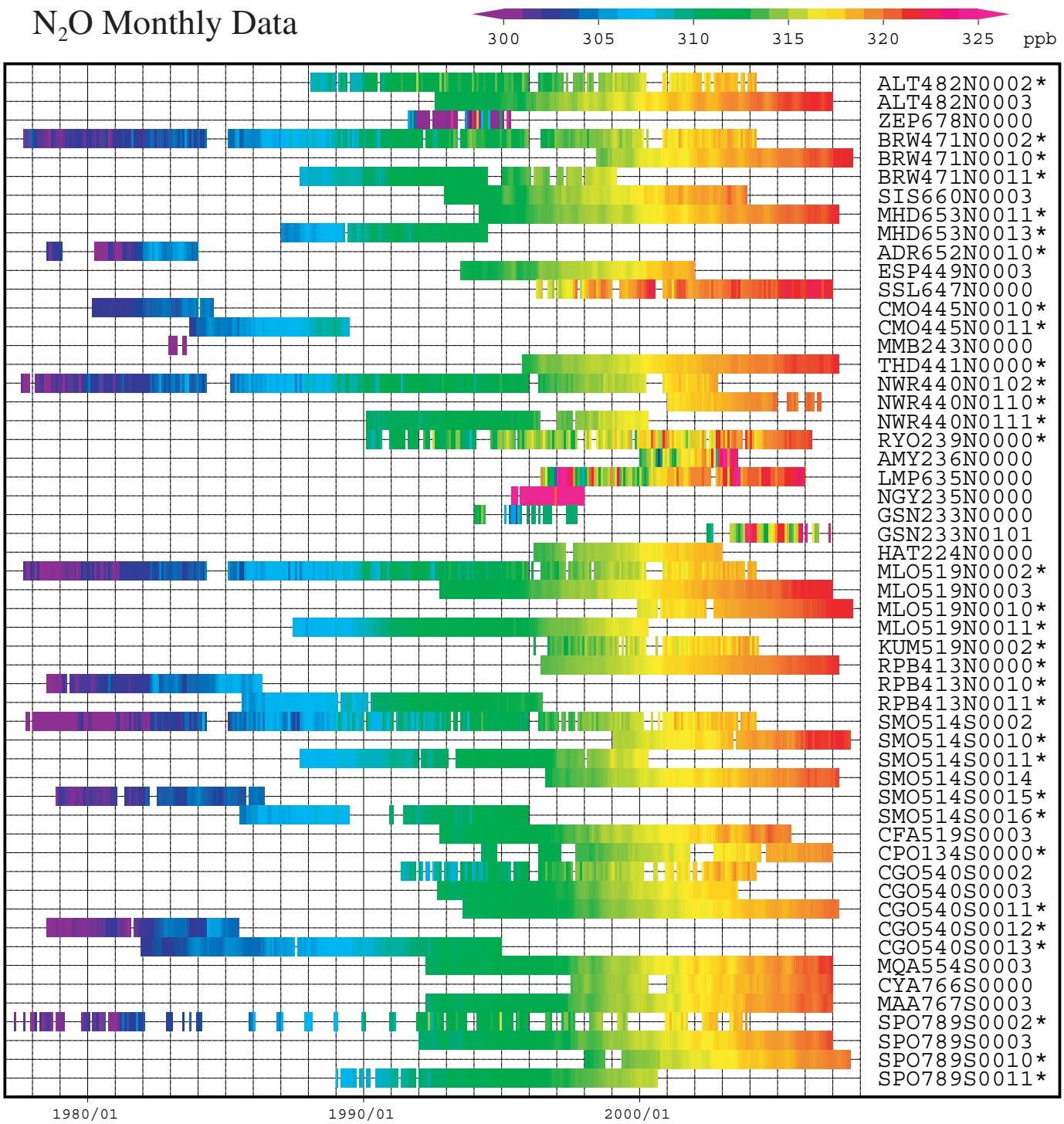

Plate 5.1 Monthly mean N_2O mole fractions for all sites reported to the WDCGG illustrated in colors that change with the mole fraction. The sites are set from north to south. Filename code with an asterisk shows the data used in the analysis shown in Fig. 5.1. (see Chapter 2)

5. Nitrous Oxide (N_2O)

Basic information on N_2O with regard to environmental issues

Nitrous oxide (N_2O) is a relatively stable greenhouse gas in the troposphere with an "adjustment-time" of 114 years. Radiative forcing due to the increase of N_2O from 1750 to 2005 is estimated at 0.16 W/m^2, which is 6% of that of all long-lived and globally mixed greenhouse gases (IPCC, 2007). The atmospheric mole fraction of N_2O has increased steadily from about 270 ppb in pre-industrial times and is now 19% higher than in 1750.

N_2O is emitted into the atmosphere from natural and anthropogenic sources, including the oceans, soil, combustion of fuels, biomass burning, fertiliser use and various industrial processes. One-third of the total amount of emission is considered to be from anthropogenic sources. N_2O is removed from the atmosphere mainly by photo-dissociation in the stratosphere. However, even at this stage, the estimated amounts from sources and sinks have not yet been determined.

Annual variation of N_2O levels in the atmosphere

The map at the beginning of this chapter shows observation sites that have submitted N_2O data to the WDCGG. The monthly mean N_2O data from all stations submitted to the WDCGG are shown in Plate 5.1. In this plate, mole fraction levels are illustrated in different colours. Data submitted to the WDCGG show that N_2O mole fractions are increasing in both hemispheres. Figure 5.1 shows global monthly mean mole fractions and the long-term trends from 1980 to 2006. The global mean mole fraction reached a new high of 320.1 ppb in 2006, which was an increase of 0.8 ppb over the year before. This mole fraction corresponds to 119% of the pre-industrial level. The mean increase rate of the global mean mole fraction during the period 1996-2006 was 0.76 ppb/year.

At some stations, the average growth rate (yearly difference of mole fraction) decreased considerably between 1991 and 1993, but then returned to almost the same rate as that observed during the 1980s. This was suggested to be due to a decrease in the use of nitrogen-based fertilisers, lower biogenic emissions and larger stratospheric losses due to volcanic-induced circulation changes (IPCC, 2001).

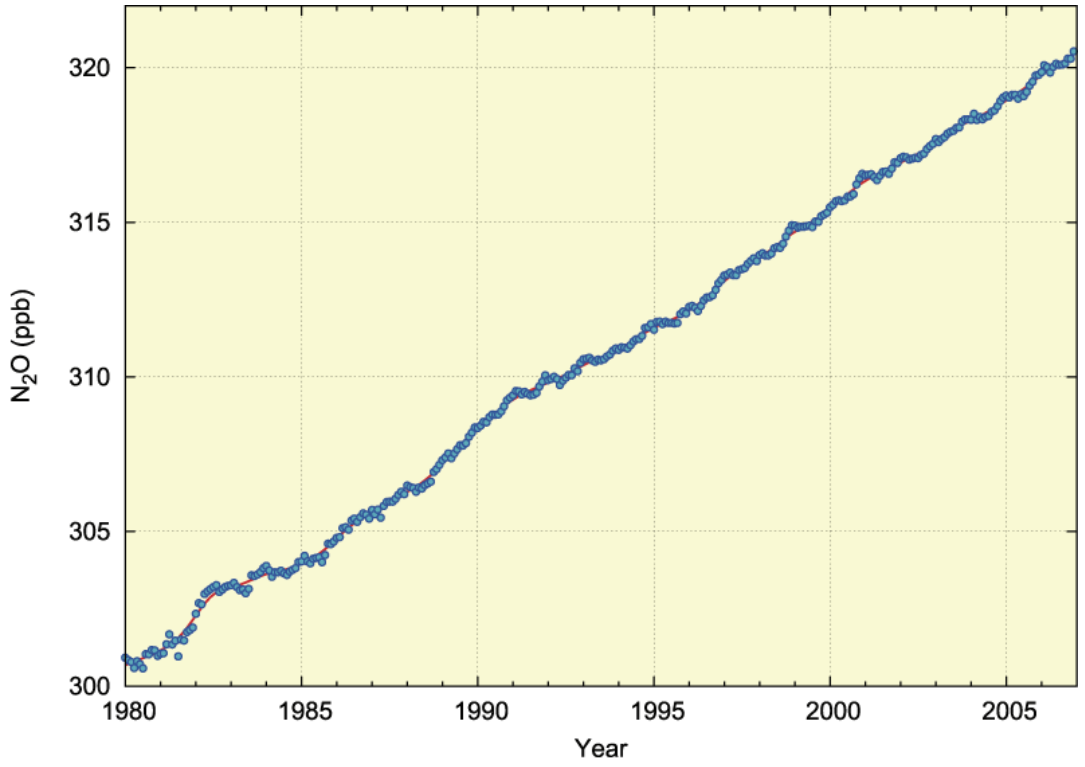

Fig. 5.1 Monthly mean mole fractions (dots) and deseasonalized long-term trends (lines) from 1980 to 2006 for the globe.

6.

HALOCARBONS

● : CONTINUOUS STATION

△ : FLASK STATION

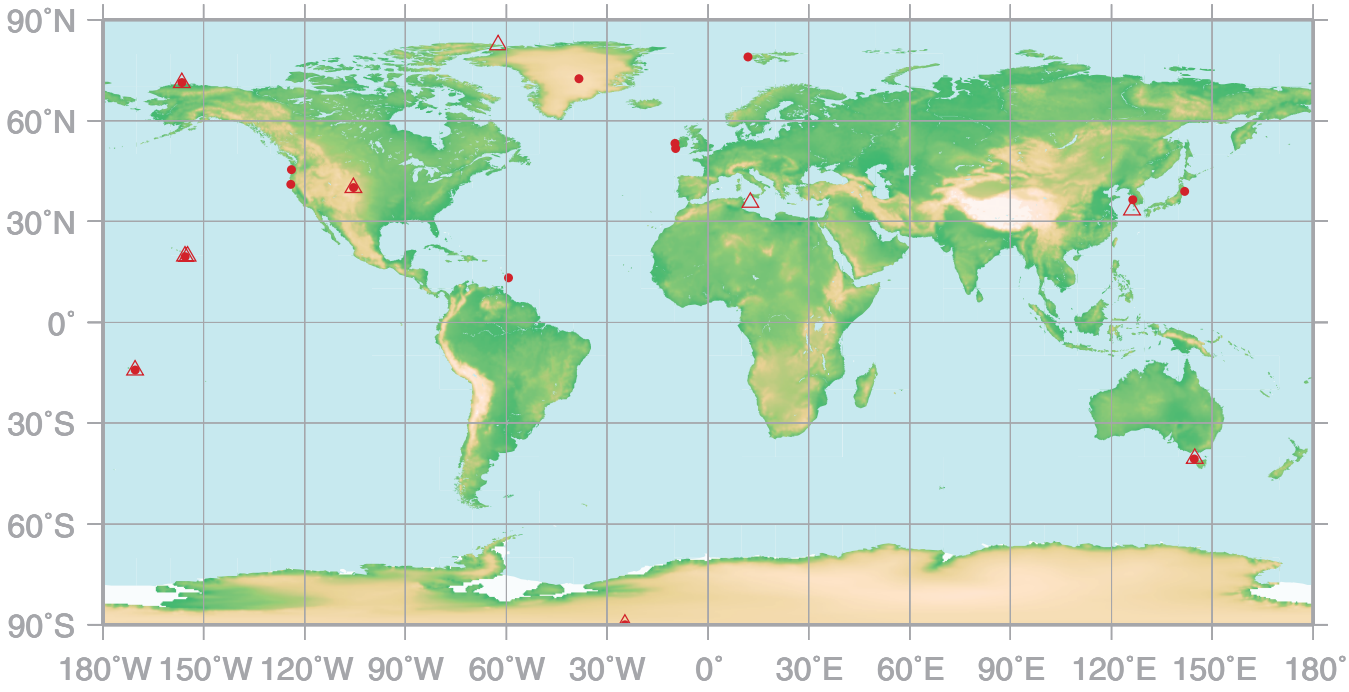

This map shows locations of the site where the monthly mean mole fractions are submitted.

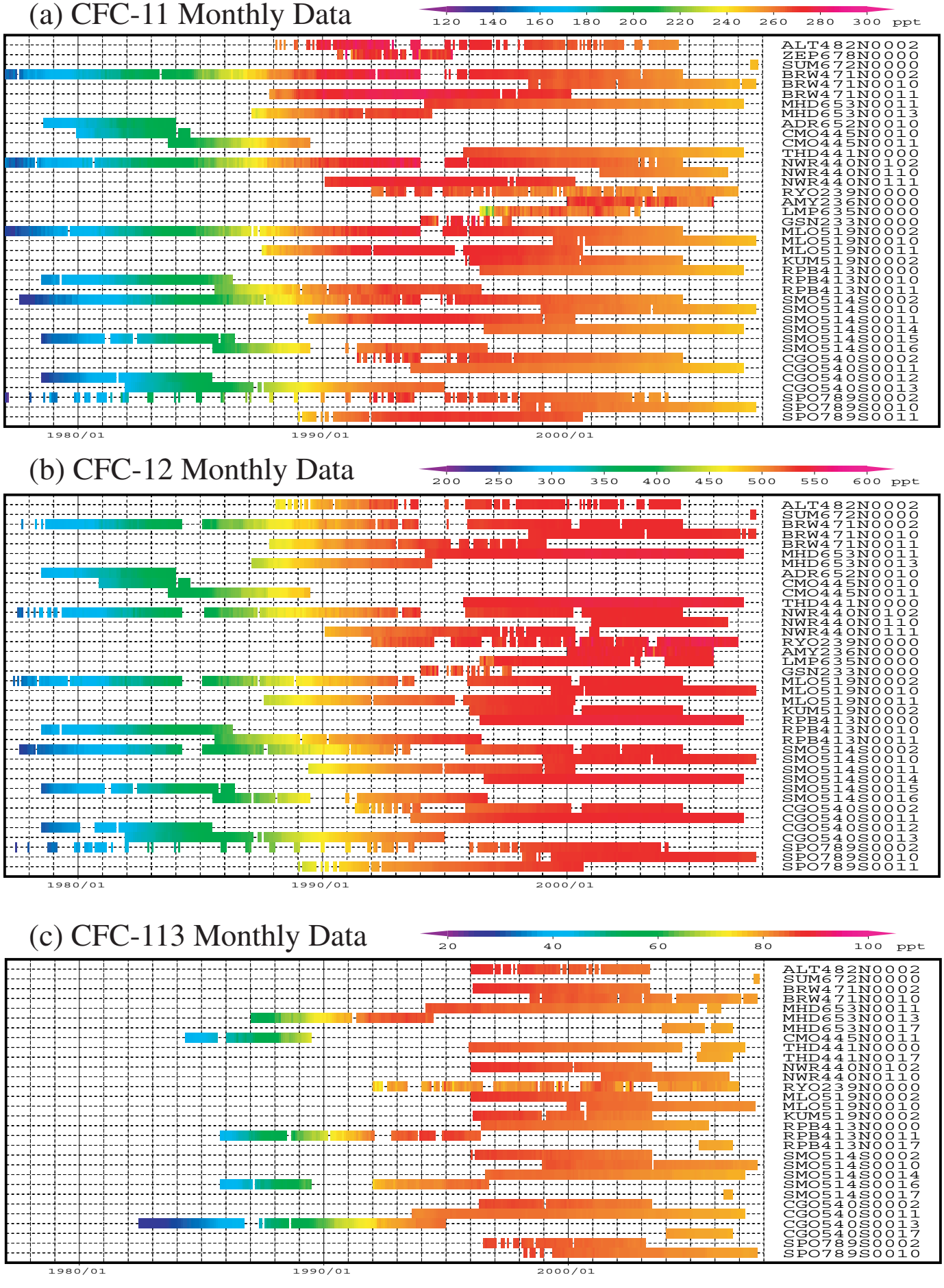

Plate 6.1 Monthly mean (a) CFC-11, (b) CFC-12, (c) CFC-113 mole fractions for all sites reported to the WDCGG illustrated in colors that change with the mole fraction. The sites are set from north to south.

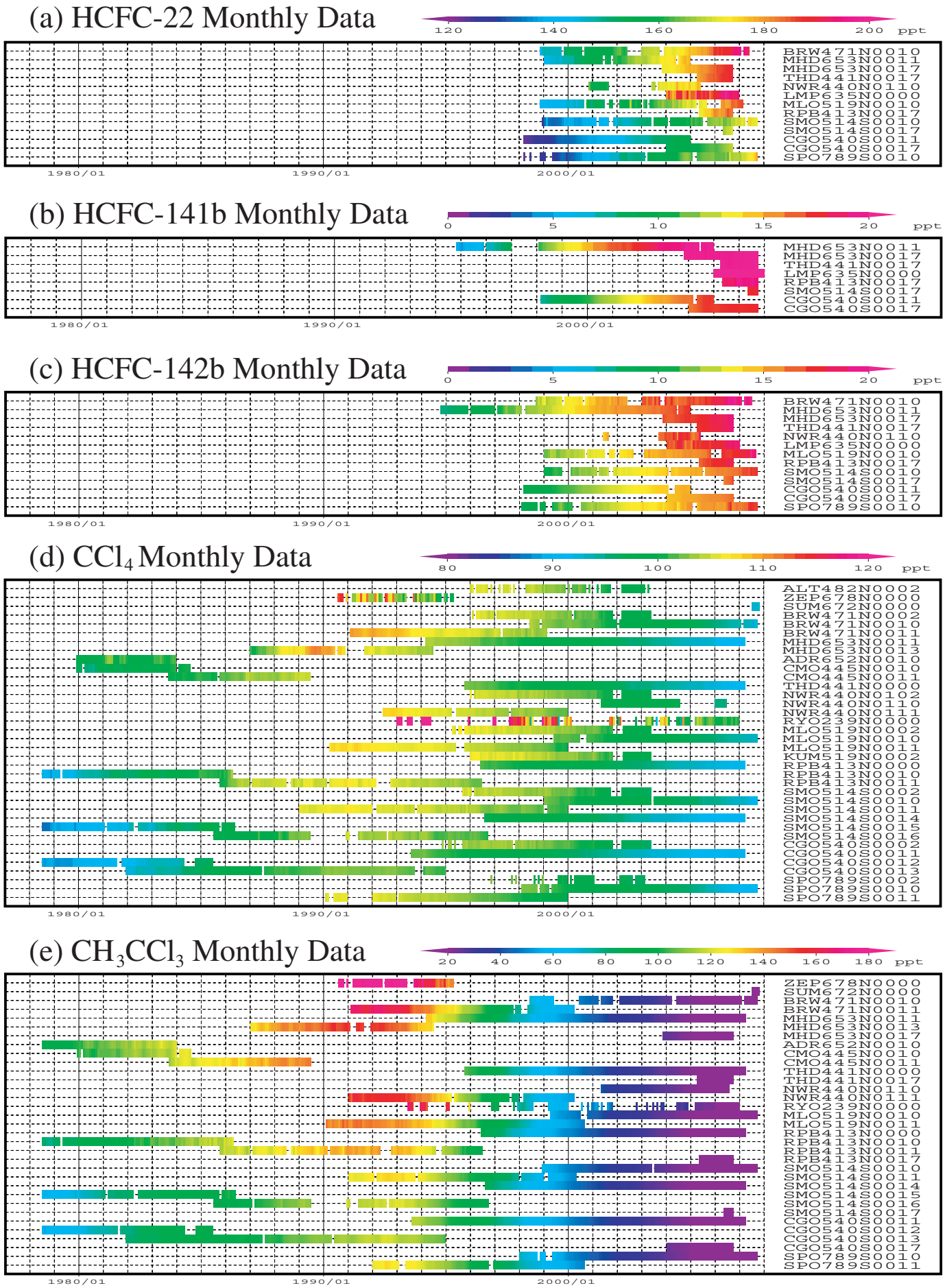

Plate 6.2 Monthly mean (a) HCFC-22, (b) HCFC-141b, (c) HCFC-142b, (d) CCl4, (e) CH3CCl3 mole fractions for all sites reported to the WDCGG illustrated in colors that change with the mole fraction. The sites are set from north to south.

6. Halocarbons (CFCs, HCFCs, CCl_4 and CH_3CCl_3)

Basic information on halocarbons with regard to environmental issues

"Halocarbons" are carbon compounds containing one or more halogens, *i.e.*, fluorine, chlorine, bromine or iodine and are mostly industrial products. The chlorofluorocarbons (CFCs) are halocarbons containing fluorine and chlorine but no hydrogen, while hydrochlorofluorocarbons (HCFCs) also contain hydrogen. Carbon tetrachloride (CCl_4) and methyl chloroform (CH_3CCl_3) are produced industrially, while methyl chloride and methyl bromide have natural sources. Although there are relatively low mole fractions of halocarbons in the atmosphere, most have high global warming potentials. Halocarbons contributed 13% of radiative forcing caused by the increase in levels of long-lived and globally mixed greenhouse gases from 1750 to 2005 (IPCC, 2007a).

Halocarbons are clear, odourless, and innocuous substances, which are readily gasified and liquefied and have low surface tension. Thus, they were commonly used as refrigerants, propellants and detergents for semiconductors, which resulted in a rapid increase in their atmospheric mole fractions until the mid-1980s. Halocarbons containing chlorine and bromine were found to deplete the ozone layer. The Montreal Protocol on Substances that Deplete the Ozone Layer and its Adjustments and Amendments regulate the production and transportation of ozone-depleting compounds. As a result, global mole fractions of CFC-11, CCl_4 and CH_3CCl_3 have begun to decrease; the global growth of CFC-113 stopped around 1996, and that of CFC-12 has decelerated substantially.

A decrease in stratospheric ozone leads to the cooling of the lower stratosphere. However, the increase in halocarbons has a net positive radiative forcing effect on global warming because the positive direct radiative forcing of halocarbons is greater than the negative indirect radiative forcing due to ozone depletion (WMO, 1999a).

CFCs are dissociated mainly by ultraviolet radiation in the stratosphere, and their lifetimes are generally long (*e.g.*, about 50 years for CFC-11). However, HCFCs and CH_3CCl_3, which contain hydrogen, react with hydroxyl radicals (OH) in the troposphere and have relatively short lifetimes (*e.g.*, about 5 years for CH_3CCl_3). As the reaction with OH in the troposphere is a major sink for CH_3CCl_3, global measurements of CH_3CCl_3 provide an accurate estimate of the global mole fraction of OH (Prinn *et al.*, 2001).

Annual variation of halocarbon levels in the atmosphere

The map at the beginning of this chapter shows observation sites that have submitted halocarbon data to the WDCGG. The monthly mean CFC-11, CFC-12, and CFC-113 data from all stations submitted to the WDCGG are shown in Plate 6.1. The monthly mean HCFC-22, HCFC-141b, HCFC-142b, CCl_4 and CH_3CCl_3 data from all stations submitted to the WDCGG are shown in Plate 6.2. Figure 6.1 shows the time series of monthly mean mole fractions of CFC-11, CFC-12 and CFC-113.

Figures 6.2 and 6.3 show the corresponding data for HCFCs, and CCl_4 and CH_3CCl_3, respectively. All monthly data from each station are plotted in these figures. The absolute values of mole fractions differ for some stations, suggesting that standard gases may not be traceable at those stations.

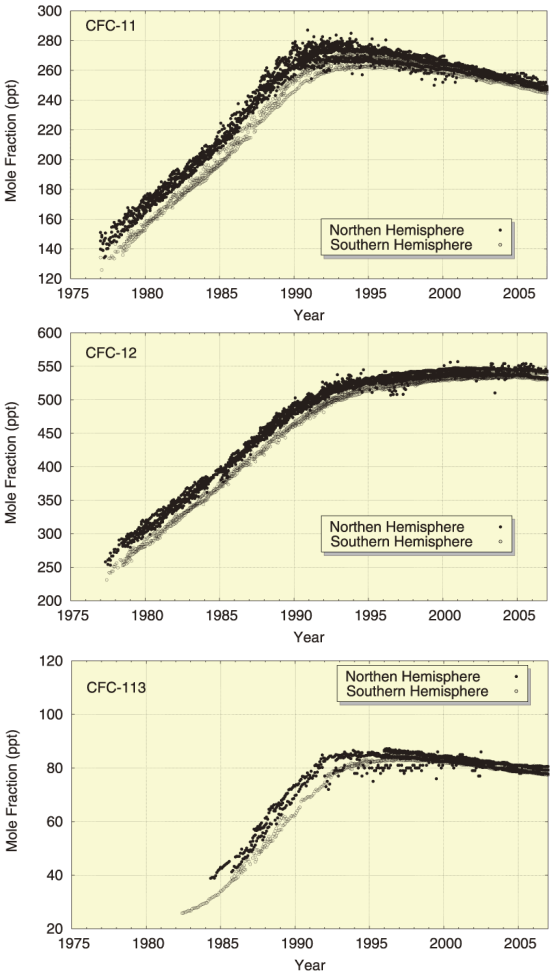

Fig. 6.1 Time series of monthly mean mole fractions of CFC-11, CFC-12 and CFC-113. Solid circles show the sites located in the Northern Hemisphere and open circles show the sites located in the Southern Hemisphere. Data from all sites that were reported to the WDCGG are shown.

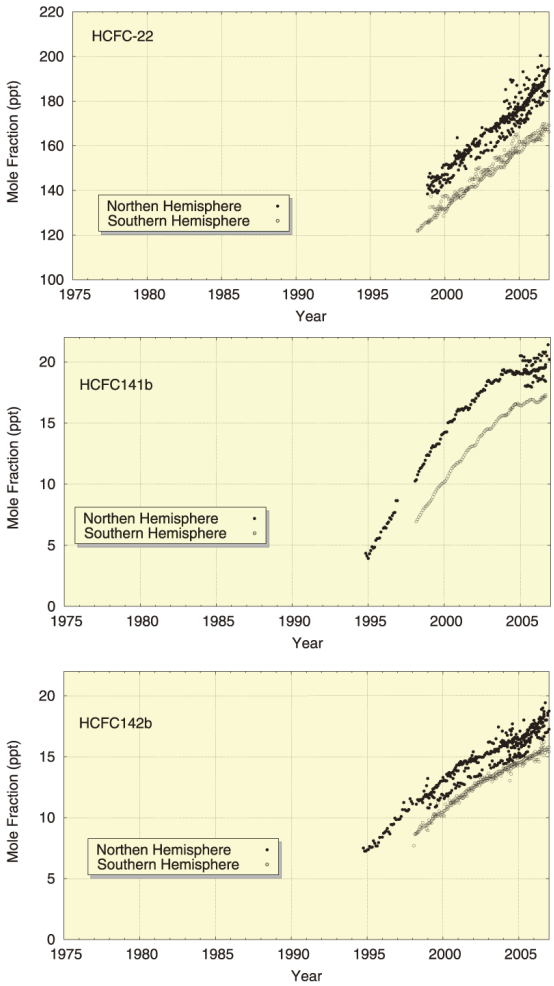

Fig. 6.2 Time series of monthly mean mole fractions of HCFC-22, HCFC-141b, and HCFC-142b. Solid circles show the sites located in the Northern Hemisphere and open circles show the sites located in the Southern Hemisphere. Data from all sites that were reported to the WDCGG are shown.

Figures 6.1 and 6.3 showed significant increases in mole fractions of all compounds during the 1980s in both hemispheres. Long-term trends since around 1990 for each compound are as follows:

CFC-11: Mole fractions were at a maximum around 1992 in the Northern Hemisphere and about one year later in the Southern Hemisphere. They have been decreasing slowly since then.

CFC-12: The growth rates have declined since around 1990 and are now nearly zero in both hemispheres.

CFC-113: Mole fractions were at a maximum around 1992 in the Northern Hemisphere and around 1997 in the Southern Hemisphere. Mole fractions are decreasing slowly in both hemispheres.

HCFC-22: Mole fractions are increasing.

HCFC-141b: Mole fractions are increasing.

HCFC-142b: Mole fractions are increasing.

CCl_4: Mole fractions were at a maximum around 1991 in both hemispheres. Since then, they have been decreasing slowly.

CH_3CCl_3: Mole fractions were at a maximum around 1992 in the Northern Hemisphere and around 1993 in the Southern Hemisphere. They have been decreasing since then.

Comparison of the stations using identical standard gases revealed that the mole fraction differences between the two hemispheres were large for all compounds except HCFCs in the 1980s. However, the differences have been decreasing for each since they peaked. The increases in mole fractions of HCFCs are the result of their continued use as substitutes for CFCs.

The mole fractions of HCFCs, which are some of the industrial replacements of CFCs, are increasing. Based on the special report from the Intergovernmental Panel on Climate Change (IPCC) and the Technology and Economic Assessment Panel (TEAP) (IPCC/TEAP, 2005), they are increasing at rapid rates of 3-7%, although their mole fractions are small.

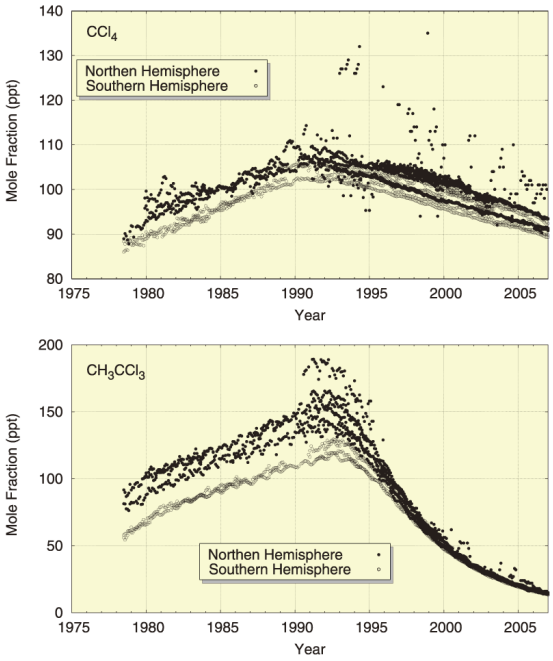

Fig. 6.3 Time series of monthly mean mole fractions of CCl_4 and CH_3CCl_3. Solid circles show the sites located in the Northern Hemisphere and open circles show the sites located in the Southern Hemisphere. Data from all sites that were reported to the WDCGG are shown.

7.

Surface OZONE

(O_3)

● : STATION

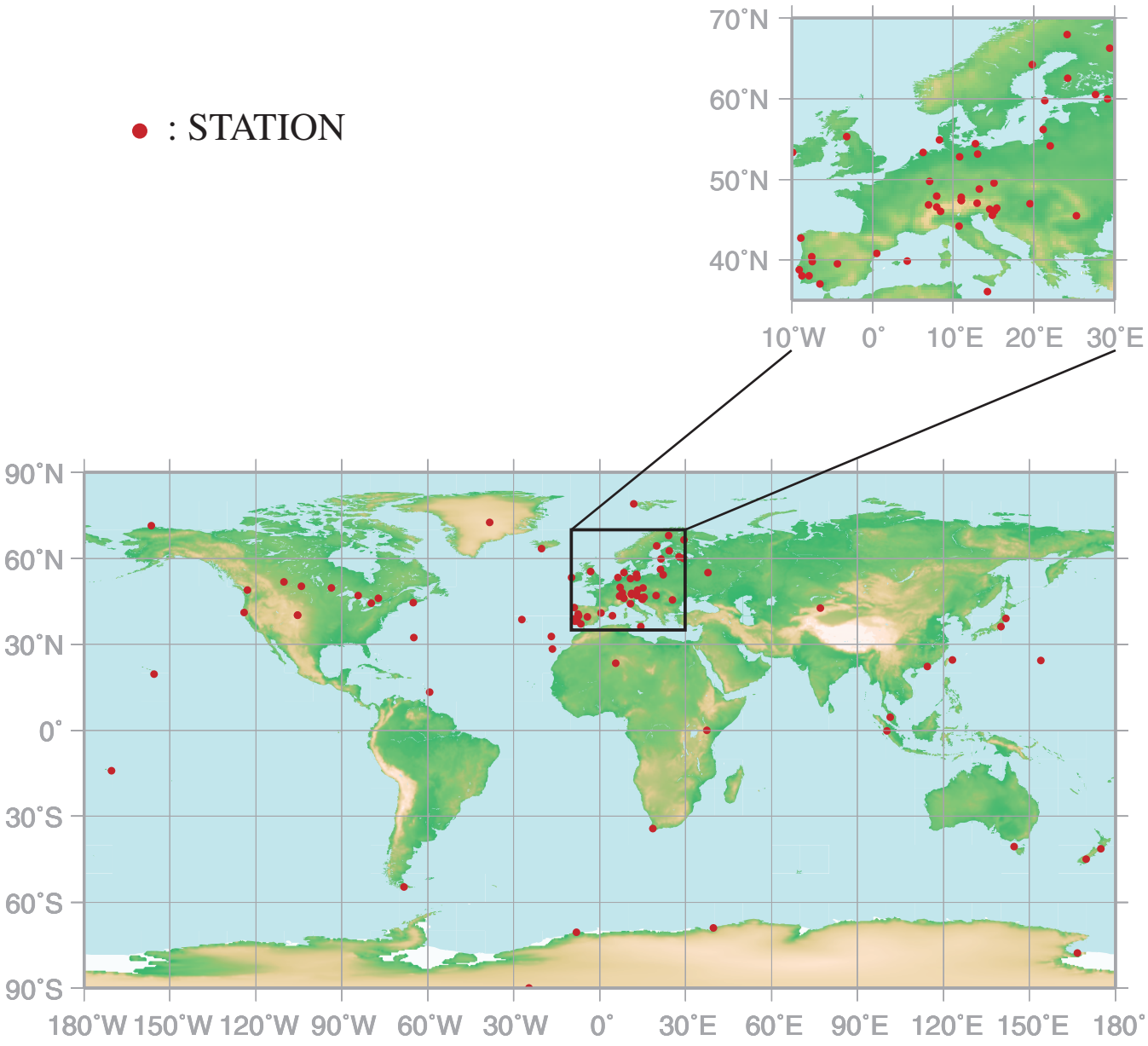

This map shows locations of the site where the monthly mean mole fractions are submitted.

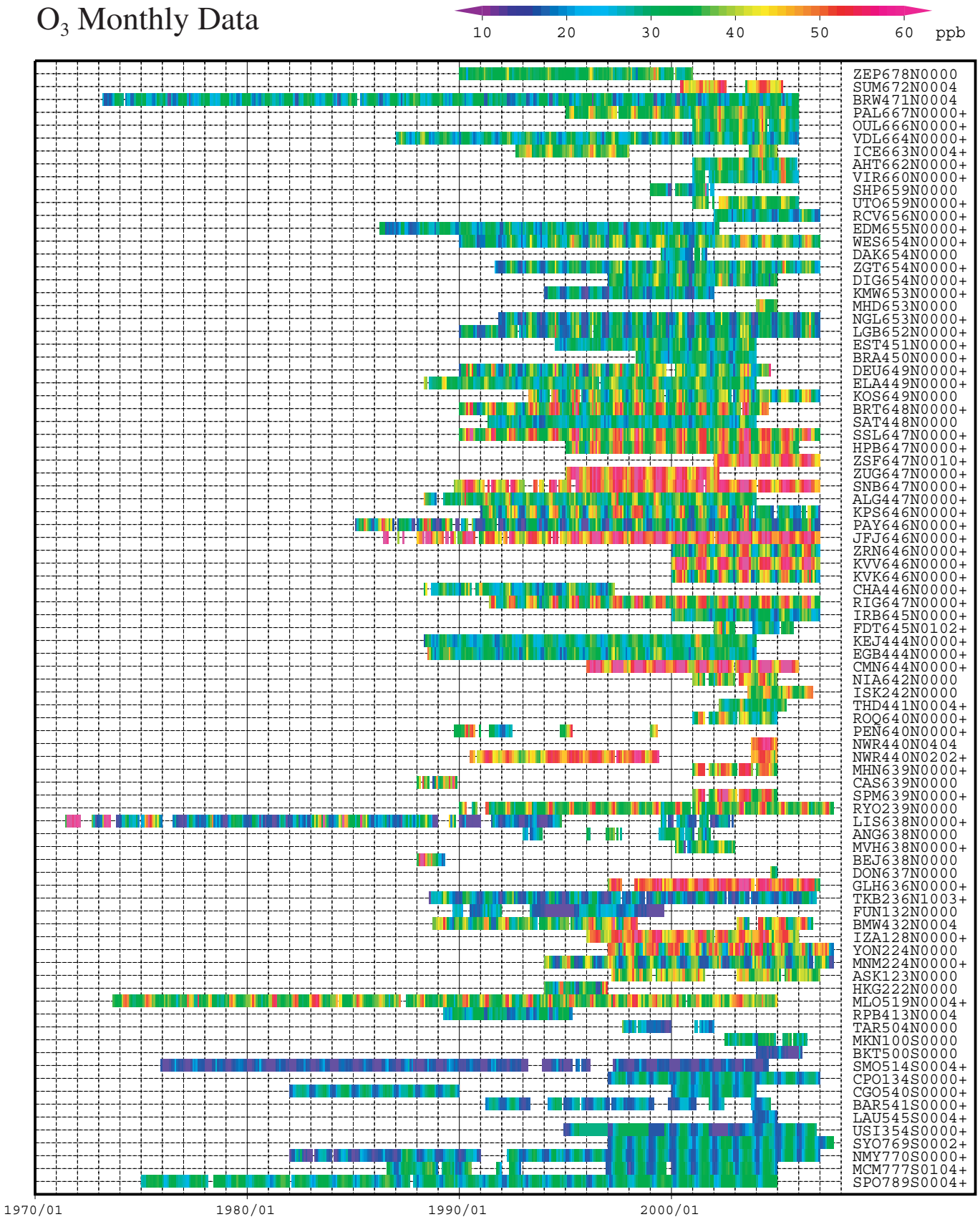

Plate 7.1 Monthly mean O_3 mole fractions for all sites reported to the WDCGG illustrated in colors that change with the mole fraction. The sites are set from north to south. It is shown that a cross incidental to station index is one peak type in the analysis shown in Fig 7.1.

7. Surface Ozone (O_3)

Basic information on surface ozone (O_3) with regard to environmental issues

Most ozone (O_3) in the atmosphere exists in the stratosphere, with less than 10% being in the troposphere. However, O_3 in the troposphere plays an important role in the atmospheric environment through radiative and chemical processes. O_3 absorbs UV radiation in the stratosphere, and this energy influences the temperature vertical profile and circulation in the stratosphere. O_3 also absorbs IR radiation, and is thus one of the greenhouse gases in the troposphere. This effect is more significant in the upper troposphere, and tropospheric O_3 is the third most important greenhouse gas after CO_2 and CH_4 according to the Fourth Assessment Report (AR4) of the Intergovernmental Panel on Climate Change (IPCC) (Denman *et al.*, 2007). In the tropics and the Arctic, where warming is accelerated compared with other regions, the tropospheric ozone originating from developing countries and the Northern extratropics could be playing significant role in addition to well-mixed greenhouse gases such as CO_2 and CH_4 (Shindell *et al*., 2006). O_3 constitutes most of the oxidants that form photochemical smog and high mole fraction of O_3 harm human respiratory organs and skin. Furthermore, O_3 produces OH radicals after reacting with water vapour under UV radiation. Since OH radicals control atmospheric mole fractions of many greenhouse gases, such as CH_4 through chemical reactions, tropospheric O_3 greatly impacts tropospheric chemistry.

Tropospheric O_3 is estimated to have increased 38% since pre-industrial times by IPCC AR4 (Denman *et al.*, 2007). From the comparison between the observation results at high altitudes from the end of the 19th Century to the first half of 20th Century and around 1990, global increases in tropospheric ozone were alarming as well as urban areas (Staehelin *et al.*, 1994). However, ozone sonde data in the troposphere show almost stable or decreasing trends in the middle latitudes of the Northern Hemisphere (Oltmans *et al*., 2006).

The sources of tropospheric O_3 are intrusions from the stratosphere and photochemical production. Major intrusions occur by tropopause folding accompanied with low pressure activity in the middle and high latitudes, and unstable mixing in the vicinity of the tropopause around cold vortexes, etc. These intrusions occur around meandering parts of the jet stream. *Photochemical production occurs by the reactions of nitrogen oxides with carbon monoxide (CO) and non-methane hydrocarbons under solar radiation (these substances are called "O_3 precursors"). At the same time, O_3 is destroyed mainly through chemical reactions with OH radicals and deposition at the Earth's surface. The lifetime of tropospheric ozone varies from one or a few days in the boundary layer to few tens of days or even a few months in the free troposphere.

The latitudinal distributions of O_3 in the middle troposphere have high mole fractions in the middle and high latitudes in both hemispheres, and low mole fractions in the tropics over the Atlantic Ocean (Marenco and Said, 1989) and Pacific Ocean (Tsutsumi *et al.,* 2003). As sources are localized and their lifetimes are generally short, the distribution of surface O_3 is also localized and time-variant.

Annual variation of surface O_3

The WDCGG took over the role of World Data Centre for surface O_3 in August 2002. The monthly means of O_3 data submitted by observation site around the world are shown in Plate 7.1 The map at the beginning of this chapter also shows observation sites that have submitted O_3 data to the WDCGG. In the plate, mole fraction levels are illustrated by different colours. Please note that the surface O_3 data is reported in two units, *i.e.*, mole fraction (ppb) and weight per volume ($\mu g/m^3$) at 25°C. Weight per volume ($\mu g/m^3$) is converted to mole fraction (ppb) as follows:

$$X_p\,[ppb] = (R * T / M / P_0) * 10 * X_g\,[\mu g/m^3]$$

where R is the molar gas constant (8.31451 [J/K/mol]),
T is the absolute temperature reported by an individual station,
M is the molecular weight of O_3 (47.9982), and
P_0 is the standard pressure (1013.25 [hPa]).

The mole fraction of surface O_3 varies from station to station, many of which are located in Europe. Moreover, the seasonal and interannual variation is relatively large at most stations and so it is difficult to identify a global long-term trend in surface O_3 mole fractions.

Figures 7.1 and 7.2 show average single and multi-peak type seasonal cycles, respectively, from which the long-term trends were subtracted for each 30° latitudinal zone. The seasonal cycles for each site can be divided into two types: a single-peak type that has a maximum monthly mean, and a multi-peak type that has more than one annual maximum. The maximum mole fraction of the single-peak type appears in April in northern high and low latitudes and in May in northern mid-latitudes. The delayed peak in the mid-latitudes may be attributed to air pollution in

Europe given that most mid-latitude stations are located on this continent. Relatively high spring maximum mole fractions were observed at Sonnblick, Niwot Ridge, Assekrem and Mauna Loa, all of which are located at high altitudes (above2700 m).

The second peak of the seasonal cycle of the multi-peak type for the 60N-30N zone around August is unclear because O_3 tends to be dispersed around this time.

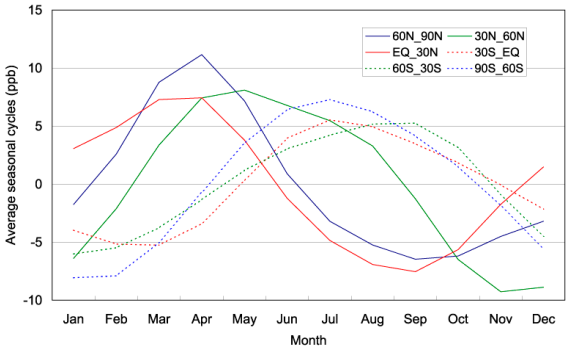

Fig. 7.1 Average seasonal cycles of single-peak type for each 30° latitudinal zone from which the long-term trends were subtracted.

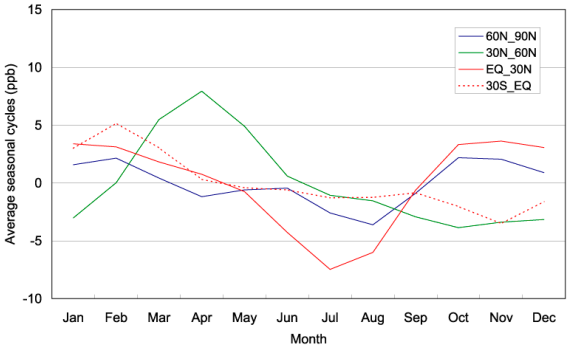

Fig. 7.2 Average seasonal cycles of multi-peak type for each 30° latitudinal zone from which the long-term trends were subtracted.

8.

CARBON MONOXIDE

(CO)

● : CONTINUOUS STATION

△ : FLASK STATION

□ : FLASK MOBILE (SHIP)

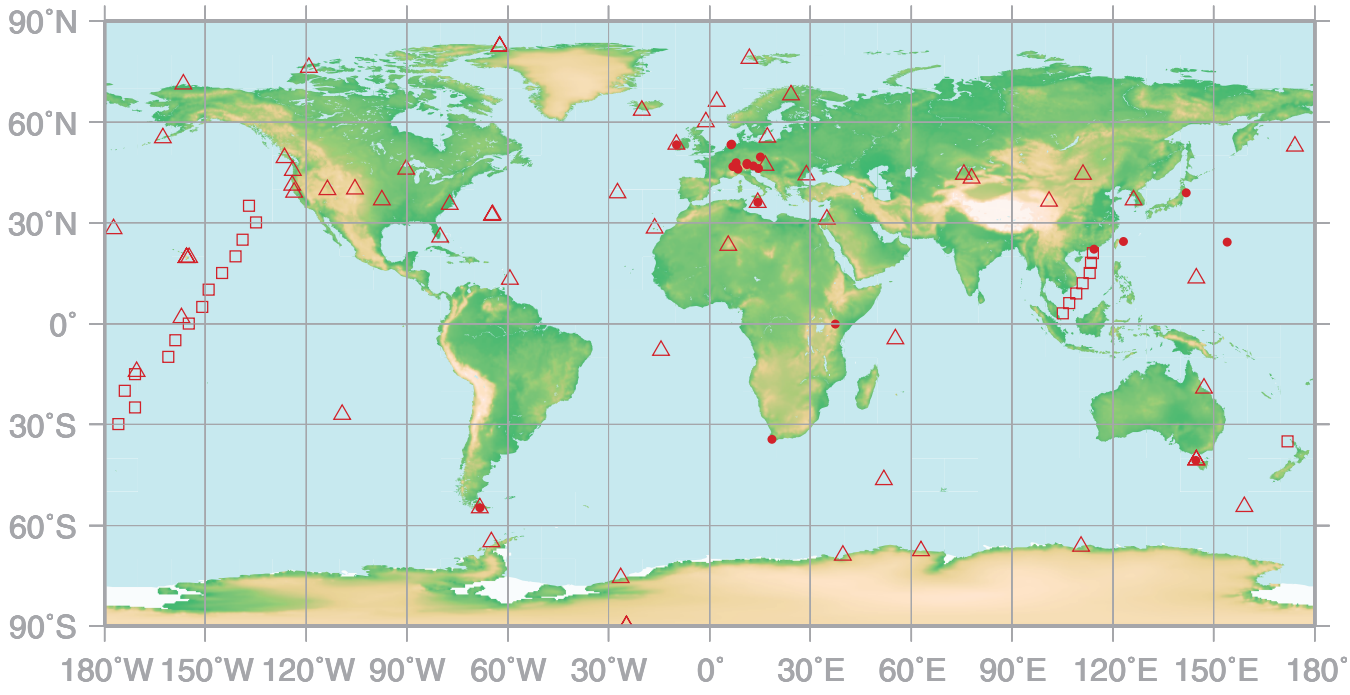

This map shows locations of the site where the monthly mean mole fractions are submitted.

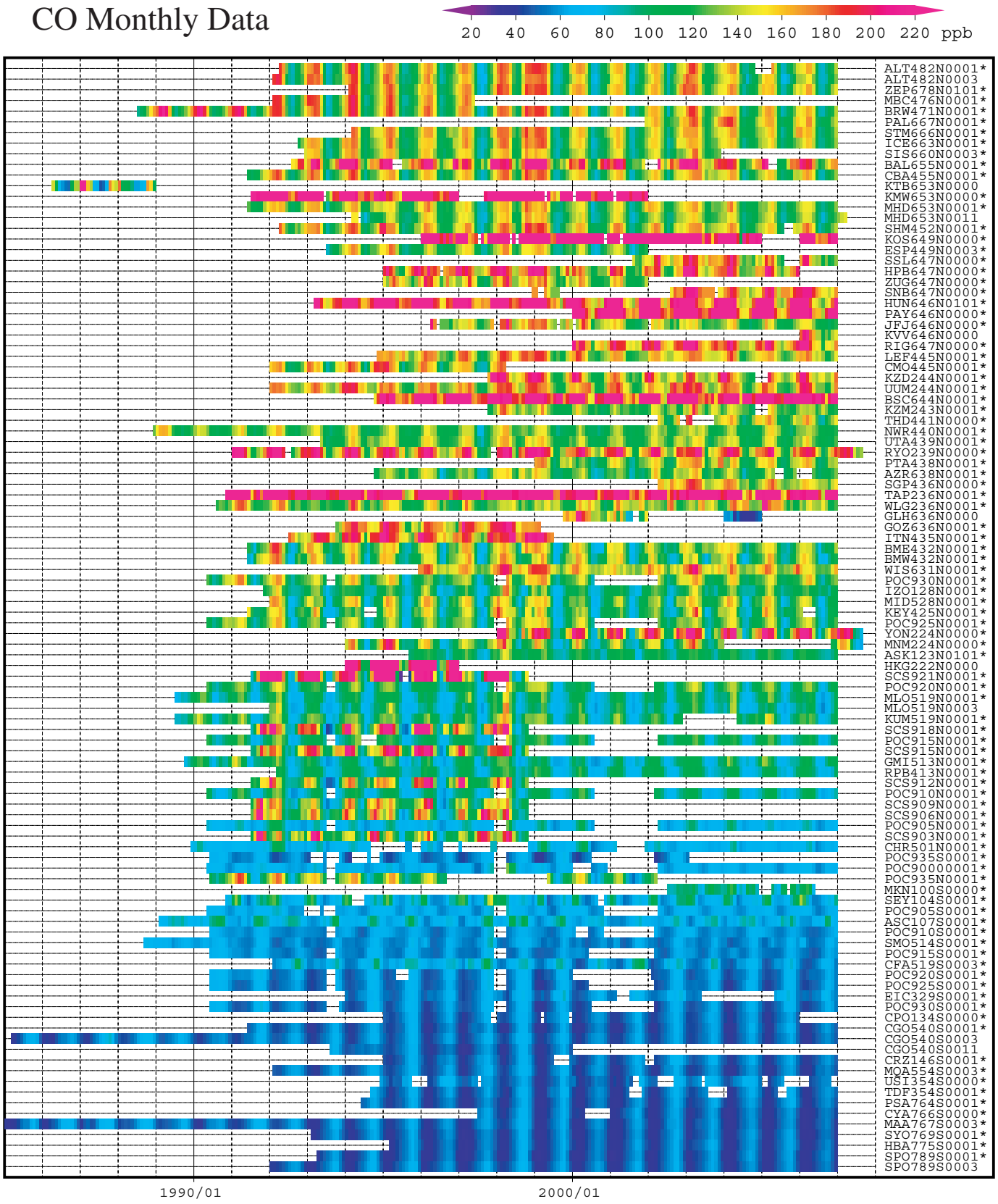

Plate 8.1 Monthly mean mole fractions of CO for all stations reported to the WDCGG. The stations are set from north to south. Filename code with an asterisk shows the station used in the analysis shown in Plate 8.2. (see Chapter 2)

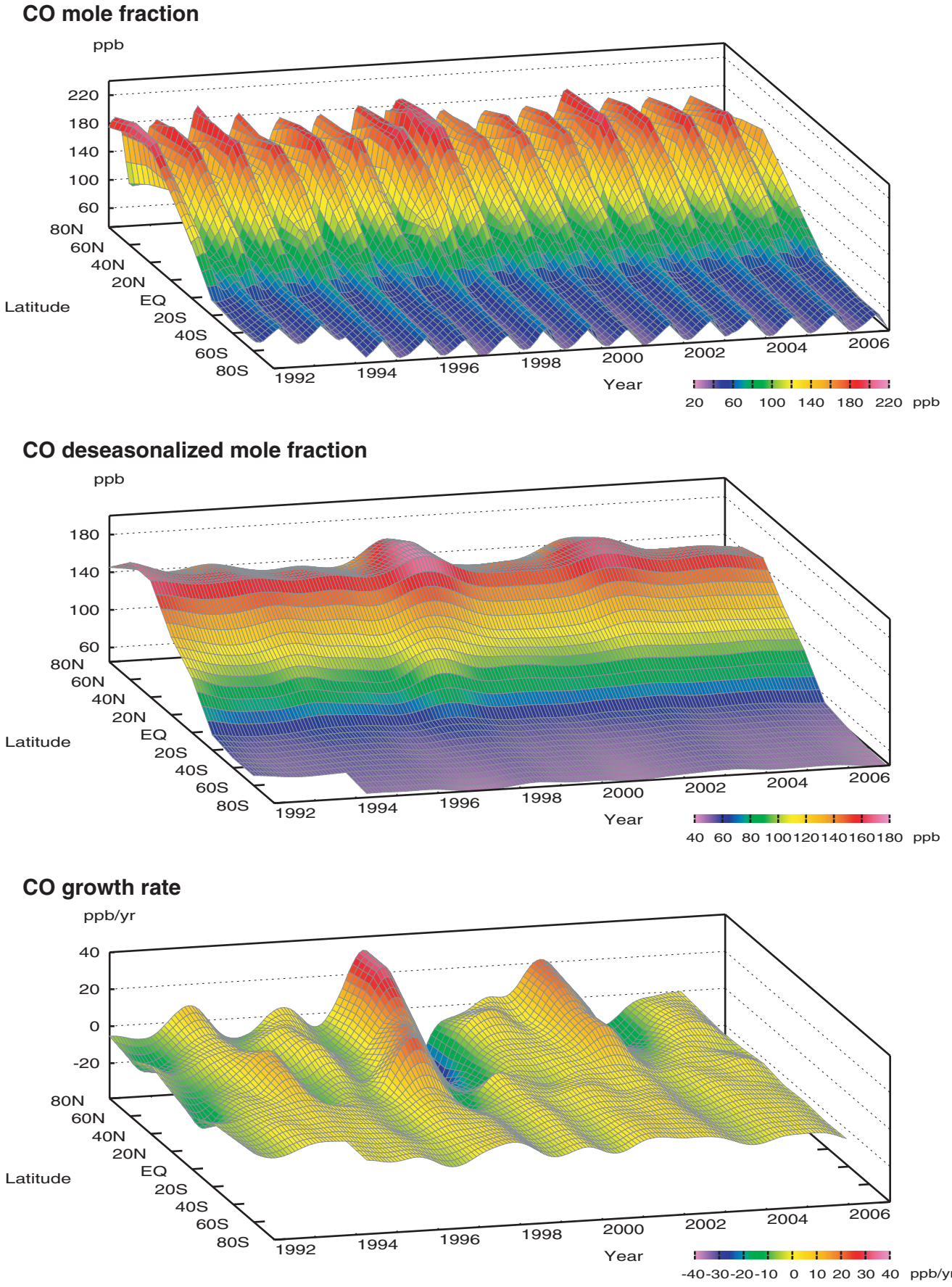

Plate 8.2 Variation of zonally averaged monthly mean CO mole fractions (top), deseasonalized mole fractions (middle), and growth rates (buttom). Zonally averaged mole fractions are calculated for each 20° zone. Deseasonalized mole fractions and growth rates are derived as described in Chapter 2.

8. Carbon Monoxide (CO)

Basic information on CO with regard to environmental issues

Carbon monoxide (CO) is not a significant greenhouse gas as it absorbs little infrared radiation from the Earth. However, it does have an influence on oxidisation in the atmosphere through interaction with hydroxyl radicals (OH), which also react with methane, halocarbons and tropospheric ozone. The eventual indirect influence of current CO emission on radiative forcing has been estimated to be greater than the direct influence of N_2O (Daniel and Solomon, 1998). In addition, CO is identified in IPCC (2001) as an important indirect greenhouse gas.

Sources of atmospheric CO include fossil fuel combustion and biomass burning along with the oxidisation of both natural and anthropogenic methane and non-methane hydrocarbons (NMHC). IPCC (2001) estimated the global total emission of CO as 2,780 Tg per year. Major sinks are primarily reaction with OH and surface deposition. The lifetime of CO in the atmosphere is relatively short (a few months), so that anthropogenic CO emission does not lead to CO accumulation in the atmosphere, unlike CO_2. Furthermore, uneven distribution of the sources causes large spatial and temporal variations in the amounts of CO. Therefore, CO could be used as a tracer of anthropogenic pollution.

Measurements of trapped air in ice cores reveal the CO mole fraction was about 50 ppb during the last two millennia over central Antarctica and then increased to 110 ppb iby 1950 in Greenland (Haan and Raynaud, 1998). The CO mole fraction increased at a rate of 1% per year from 1950, but started to decrease in the late 1980s (WMO, 1999a). Between 1991 and 2001, the global average CO mole fraction decreased at about 0.5 ppb per year, except for temporal enhancements from large biomass burning (Novelli *et al*., 2003). In recent years, CO emission from large forest fires has also been widely observed. Biomass burning including forest fires is considered to account for 30% of the total CO emission in the globe (Holloway *et al*., 2000).

The global CO distribution and the budget have been estimated using satellite observations and inverse methods (e.g. Pétron et al., 2002; Stavrakou and Müller, 2006), but estimated anthropogenic emissions are larger than the inventories from industrial statistics (Bergamaschi *et al*., 2000; Kasihbhatla *et al.*, 2002; Arellano Jr *et al*., 2004).

Annual variation of CO levels in the atmosphere

The map at the beginning of this chapter shows observation sites that have submitted CO data to the WDCGG.

The time series of monthly mean CO data from all the stations that submitted to WDCGG are shown in Plate 8.1. Mole fraction levels are illustrated in different colours. Global and zonal mean mole fractions were calculated using data from selected stations (see caption).

The three-dimensional representations of latitudinal distribution of atmospheric CO mole fractions, deseasonalized mole fractions and growth rate are shown in Plate 8.2.

Please note that the CO data are reported in various units, *i.e.*, ppb, $\mu g/m^3$-25°C, $\mu g/m^3$-20°C and mg/m^3-25°C. All units can be converted to ppb as follows:

$$X_p\,[ppb] = (R * T / M / P_0) * 10 * X_g\,[\mu g/m^3]$$
$$X_p\,[ppb] = (R * T / M / P_0) * 10^4 * X_g\,[mg/m^3]$$

where R is the molar gas constant (8.31451 [J/K/mol]),
T is the absolute temperature reported by an individual station,
M is the molecular weight of CO (28.0101),
P_0 is the standard pressure (1013.25 [hPa]).

Plates 8.1 and 8.2 show that seasonal variation of CO is large in the Northern Hemisphere and small in the Southern, and that deseasonalized mole fraction is highest at the mid–northern latitudes and lowest in the Southern Hemisphere. These results are practically consistent with the global CO distribution derived from a combination of satellite observations and computational models. (Bergamaschi *et al.*, 2000; Holloway *et al*., 2000; Clerbaux *et al*., 2001). The latitudinal gradient of CO is large from the northern middle latitudes to the southern low latitudes, and is small in the Southern Hemisphere. This is due to there being numerous CO sources in the northern middle latitudes and CO being destroyed in the tropics where OH radicals are abundant.

The global monthly mean mole fractions, deseasonalized long-term trends and growth rates are shown in Figure 8.1. Growth rate was high in 1993/1994, 1997/1998 and 2002, and low in 1992 and 1998/1999. The global annual mean mole fraction was about 94 ppb in 2006, although the observation scale depends on the station.

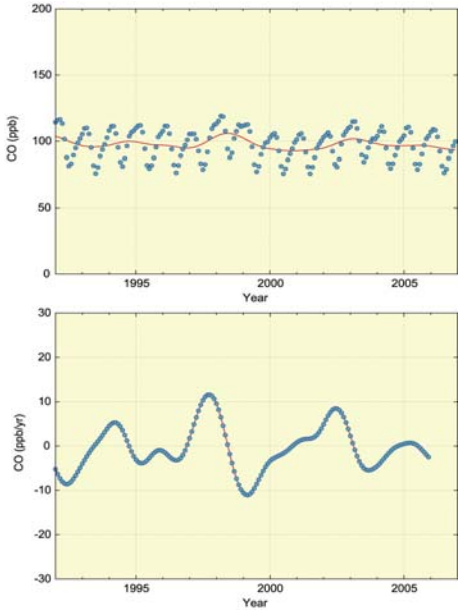

Fig. 8.1 Global monthly mean mole fractions (thick line and dots) and deseasonalized long-term trend (red line) (top) and the growth rate (bottom) of CO from 1992 to 2006.

Figure 8.2 shows the monthly mean mole fractions and the deseasonalized long-term trends of CO for each 30° latitudinal zone. A seasonal variation is seen in both hemispheres. In the Northern Hemisphere, the mole fraction is higher in the winter season. Amplitudes of the seasonal cycle are larger in the Northern Hemisphere than in the Southern Hemisphere.

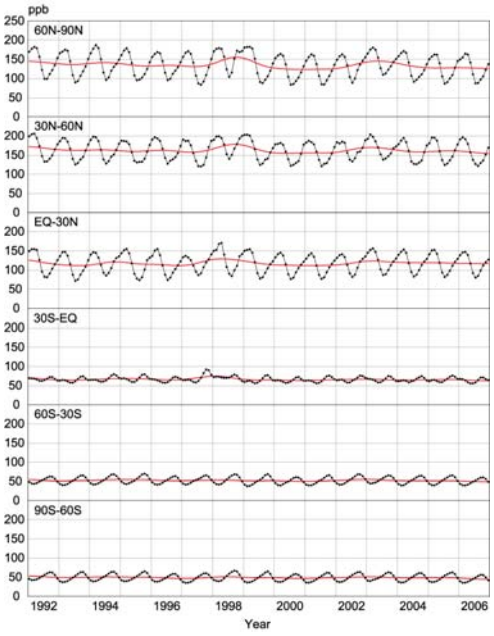

Fig. 8.2 Monthly mean mole fractions (thick lines and dots) and deseasonalized long-term trends (red lines) of CO from 1992 to 2006 for each 30° latitudinal zone.

Figure 8.3 shows the deseasonalized long-term trends and growth rates for each 30° latitudinal zone. CO mole fractions are highest in northern mid latitudinal zone.

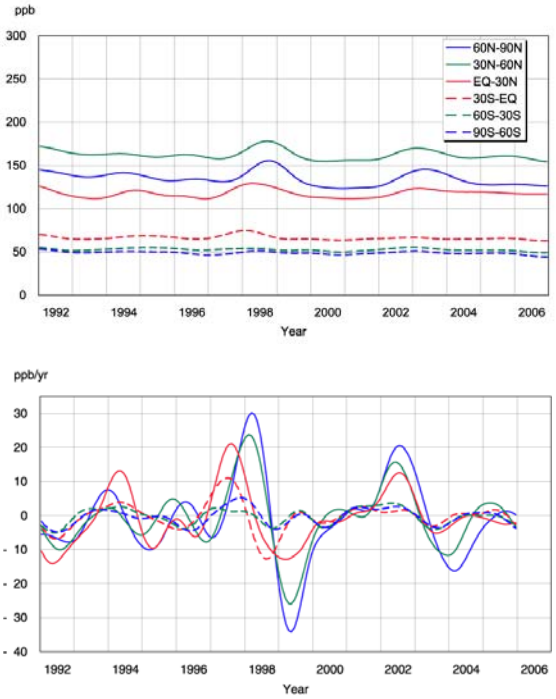

Fig. 8.3 Deseasonalized long-term trends (top) and growth rates (bottom) of CO for each 30° latitudinal zone.

Annual variation of atmospheric flow can influence CO mole fraction as shown by Allen *et al.* (1996). However, a negative growth rate was seen in 1992 at all latitudes. Novelli *et al.* (1998) showed a clear decline in CO mole fractions from late 1991 through mid-1993, with a subsequent recovery from mid-1993 through mid-1994. The decline in CO mole fractions almost coincides with the decrease in growth rate of CH_4 mole fraction, most likely due to variations of their common sinks. Enhanced stratospheric ozone depletion due to the increase in volcanic aerosols following the eruption of Mt. Pinatubo in 1991 may have increased the mole fraction of OH, which reacts with both CO and CH_4 (Dlugokencky *et al.*, 1996).

Increases in CO mole fractions were observed from 1997 to 1998 in northern latitudes and southern low latitudes. These increases were attributed to the large biomass burning around Indonesia in late 1997 and around Siberia between summer and autumn in 1998 (Novelli *et al.*, 1998).

Duncan *et al.* (2003) estimated that 133 Tg of CO was emitted in 1997 from biomass burning in Indonesia and Malaysia, which is almost one forth of their estimation of global biomass burning emission. Observations taken by a Japan Air Line passenger

aircraft showed increased CO mole fraction over the tropical Pacific at an altitude of 10 km, and a model simulation showed that biomass burning in Southeast Asia had brought about this CO enhancement (Matsueda *et al*., 1998; Matsueda *et al*., 2002; Taguchi *et al*., 2002).

A large scale boreal forest fire occurred in Siberia in 1998 (Kasischke *et al*., 1999). The burned area was estimated to be 11,000,000 hectares (ha, 10,000 square metres) by Kajii *et al*. (2002), 13,300,000 ha by Cornard et al. (2002), and 13,100,000 ha by Kasischke and Bruhwiler (2003). From estimates of this forest fire, Yurganov *et al*. (2004) estimated the total emission from all boreal forest fires to be 148 Tg, and the emission from the boreal forest fire in Siberia in 1998 was estimated to be 88~128 Tg by Kasischke and Bruhwiler (2003) and 69 Tg (summer only) by Duncan *et al*. (2003). Boreal forest fires, including those in Siberia, occur from spring to autumn every year, with different magnitudes. The averaged burn area was estimated to be 4.8 million ha by Wotawa *et al*. (2001) and 5.1 million ha by Kajii *et al*. (2002), and the average emission of CO was estimated as 52 Tg per year by Yurganov *et al*. (2004).

CO mole fractions returned to normal levels after 1999, but the growth rates in the Northern Hemisphere increased again substantially in 2002. This increase in CO mole fractions in 2002 might also be attributed to large biomass burning. Large scale boreal forest fires occurred in Siberia and North America from 2002 to 2003. CO emission from these boreal forest fires was estimated to be 142 Tg (Simmonds *et al.*, 2005).

Seasonal cycle of CO in the atmosphere

Figure 8.4 shows the average seasonal cycles for each 30° latitudinal zone from which the long-term trends were subtracted. The seasonal cycle of CO is mainly driven by seasonal variations in OH mole fraction, which acts as a CO sink. Emission and oxidation as CO sources and large-scale transportation of CO are additional factors, although the seasonality of emission and oxidation is relatively weak compared with that of the OH mole fraction. This seasonality and the fact that the lifetime of CO is about a few months produce a sharp decrease in early summer and a relatively gradual increase in autumn. Semi-annual features evident at the southern low latitudes may be attributed to cross-equatorial transportation of CO from the Northern Hemisphere.

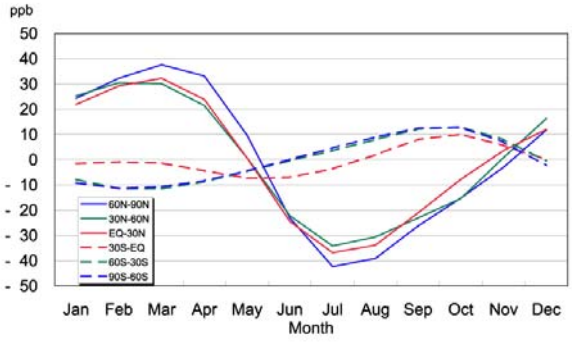

Fig. 8.4 Average seasonal cycles for each 30° latitudinal zone from which the long-term trends were subtracted.

Direct CO emission also brings about intense seasonal variation on some occasions. Novelli *et al.* (1998) showed with a model of a box representing the well-mixed northern layer and a box representing the southern boundary layer that seasonal cycles are strongly affected by changes in emission from biomass burning in both hemispheres. According to model simulations of global CO distribution, regional CO distribution in seasons reflects regional source strength like biomass burning (Bergamaschi *et al*., 2000; Holloway *et al*., 2000). Using observation data for the upper troposphere, Matsueda *et al.* (1998) showed that CO mole fractions in the upper troposphere in southern low latitudes from October to November were increased by tropical biomass burning.

9.

NITROGEN MONOXIDE (NO)

NITROGEN DIOXIDE (NO_2)

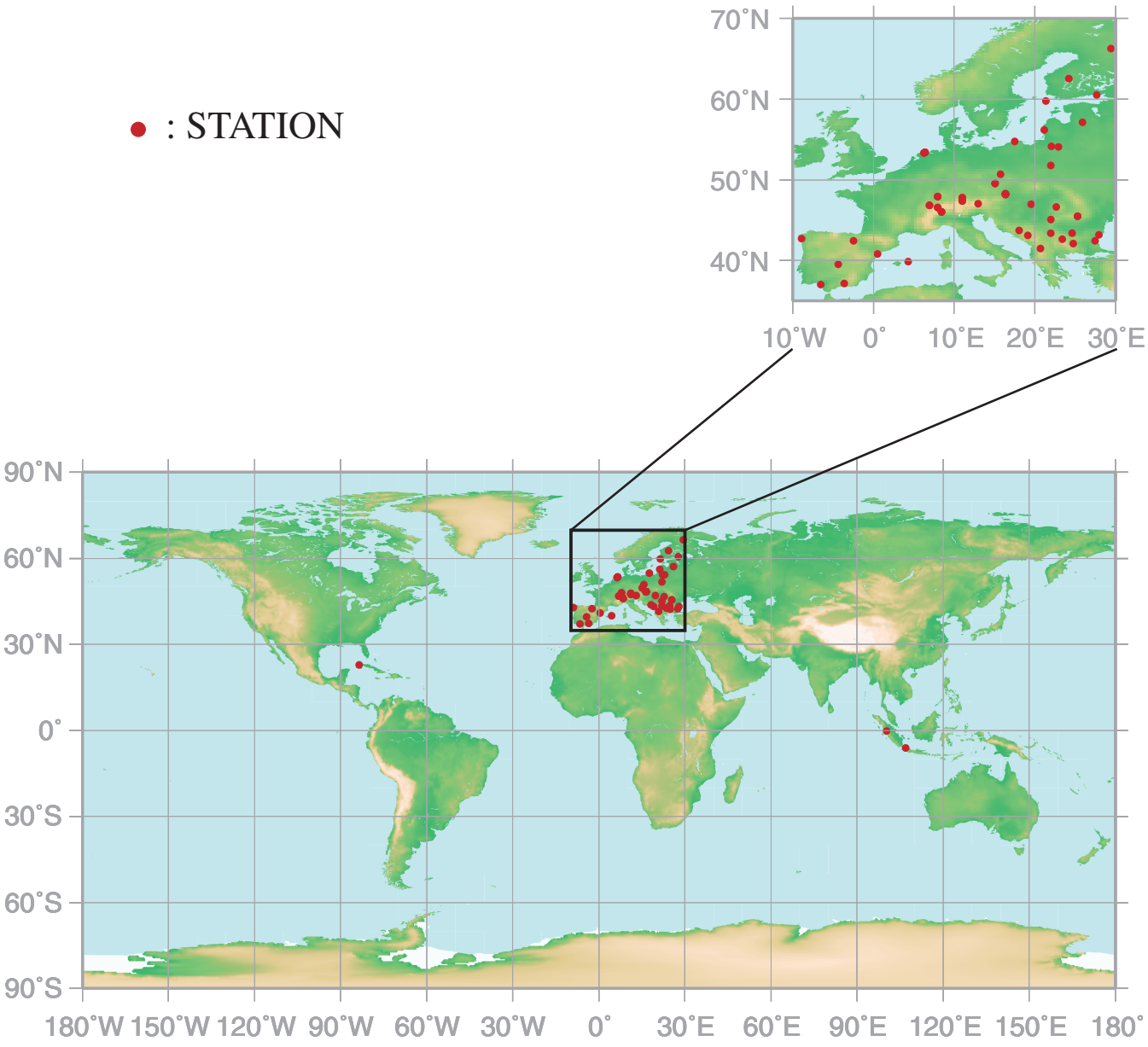

This map shows locations of the site where the monthly mean mole fractions are submitted.

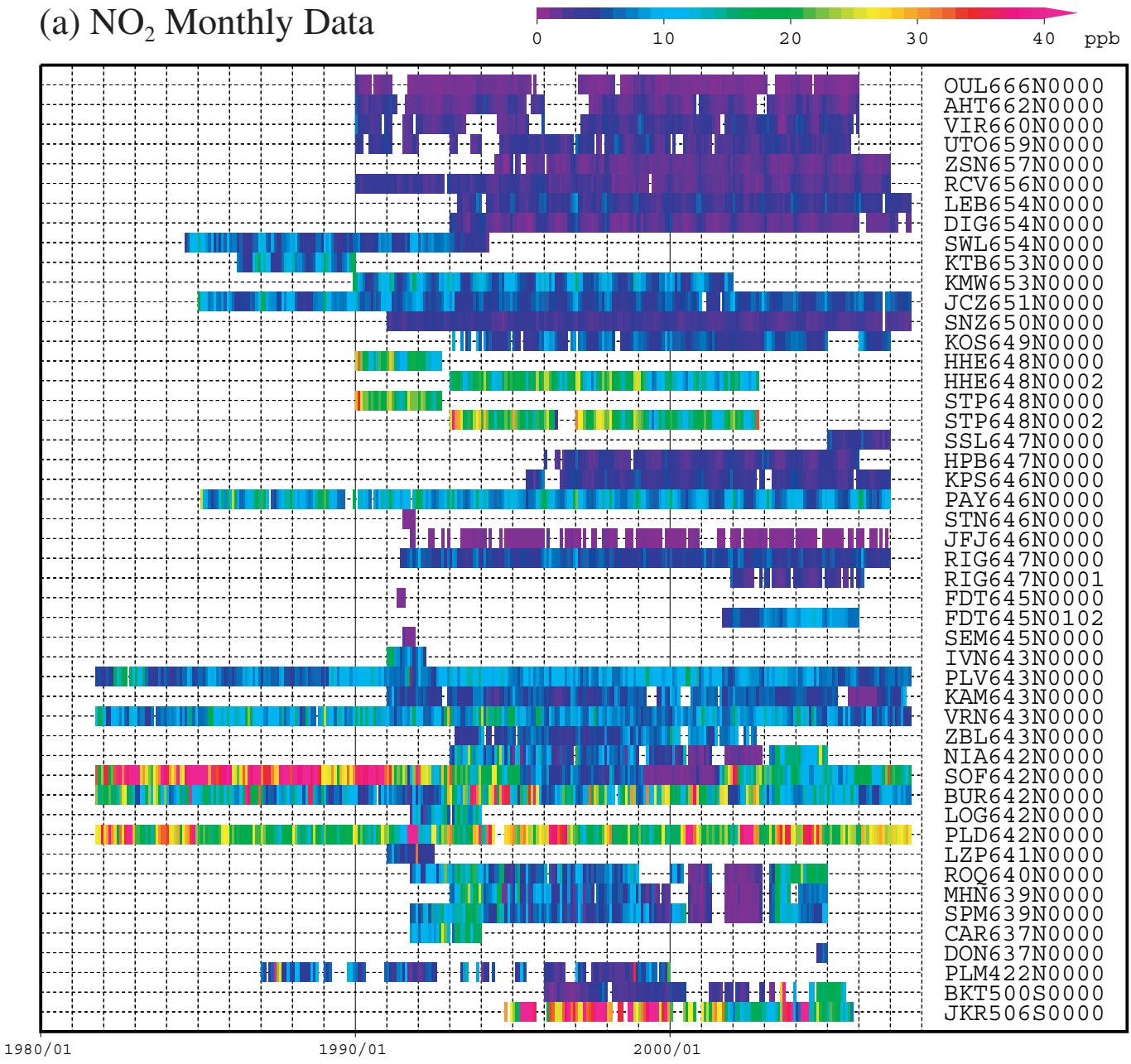

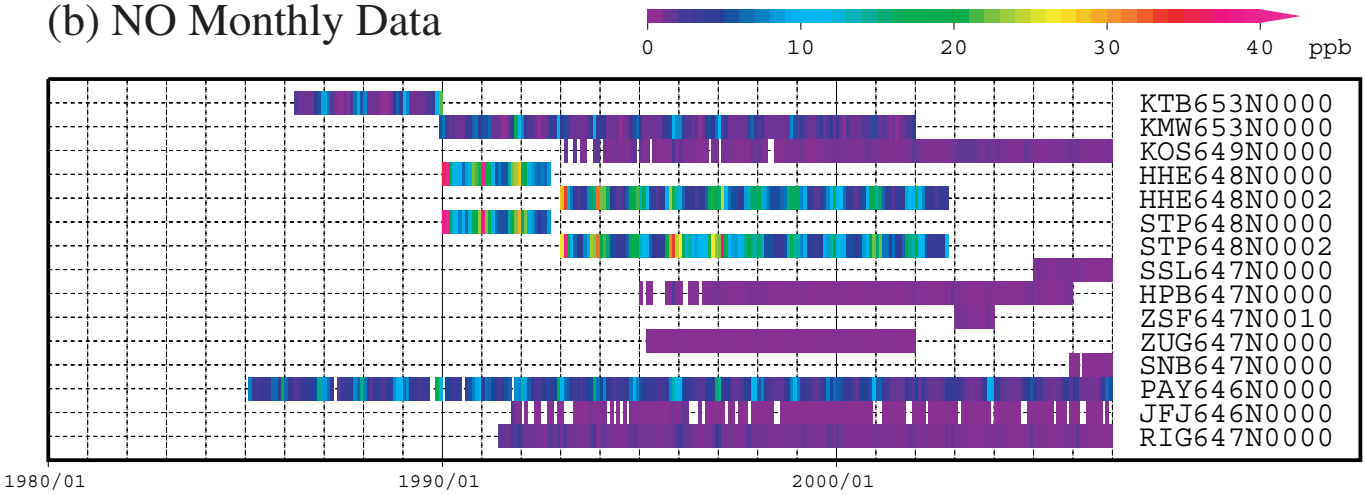

Plate 9.1 Monthly mean (a) NO_2 and (b) NO mole fractions for all sites reported to the WDCGG illustrated in colors that change with the mole fraction. The sites are set from north to south.

9. Nitrogen Monoxide (NO) and Nitrogen Dioxide (NO_2)

Basic information on NO and NO_2 with regard to environmental issues

Nitrogen oxides (NO_x, *i.e.*, NO and NO_2) are not greenhouse gases, but affect hydroxyl radicals (OH), which control many substances in the atmosphere such as methane (CH_4), carbon monoxide (CO) and hydrochlorofluorocarbons (HCFCs). In the presence of NO_x, CO and hydrocarbons are oxidised to produce ozone (O_3) in the troposphere, which is one of major greenhouse gases. Thus, NO_x can influence the Earth's radiative balance and, by generating OH, alter the oxidisation capacity of the atmosphere.

Sources of NO_x include fossil fuel combustion, biomass burning, lightning and soil (IPCC, 2001). The dominant sink of NO_x in the atmosphere is its conversion into nitric acid (HNO_3) and peroxyacetylnitrate (PAN), which are eventually removed by dry or wet deposition. In some cases, NO_x is removed from the atmosphere directly by dry deposition. Anthropogenic emission of NO_x is currently one of the major causes of acid rain and deposition. NO_x mole fractions show large variability in both space and time because of the species' short lifetimes and uneven source distribution.

Annual variation of NO and NO_2 levels in the atmosphere

Observation stations that submitted data for NO_2 and NO to the WDCGG are shown on the map at the beginning of this chapter. Most of the contributing stations are located in Europe.

The time series of monthly mean NO and NO_2 data from all stations submitted to the WDCGG are shown in Plate 9.1. In this plate, mole fraction levels are illustrated in different colours. Please note that the data for NO_x are reported in various units, *i.e.*, ppb, $\mu g/m^3$-25°C, $\mu g/m^3$-20°C, $\mu gN/m^3$-25°C and mg/m^3-25°C.

All units can be converted to ppb as follows:

$$X_p\,[ppb] = (R * T / M / P_0) * 10 * X_g\,[\mu g/m^3]$$
$$X_p\,[ppb] = (R * T / M / P_0) * 10^4 * X_g\,[mg/m^3]$$
$$X_p\,[ppb] = (R * T / M_N / P_0) * 10 * X_g\,[\mu gN/m^3]$$

where R is the molar gas constant (8.31451 [J/K/mol]),
T is the absolute temperature reported by an individual station,
M is the molecular weight of NO (30.00614) or NO_2 (46.00554),
M_N is the atomic weight of N (14.00674), and
P_0 is the standard pressure (1013.25 [hPa]).

As their sources are localised and their lifetimes are short, the distributions of NO and NO_2 are also localised and vary over time. Due to the high temporal variability of NO_2 mole fractions for each observation site, it was difficult to identify a long-term trend. A number of stations located in southern Europe showed higher mole fractions, and some stations reported a winter enhancement of NO_2. An urban site in Southeast Asia showed higher mole fractions.

As there are few observation sites for NO, it is difficult to identify increasing or decreasing trends for NO mole fractions.

10.

SULPHUR DIOXIDE

(SO_2)

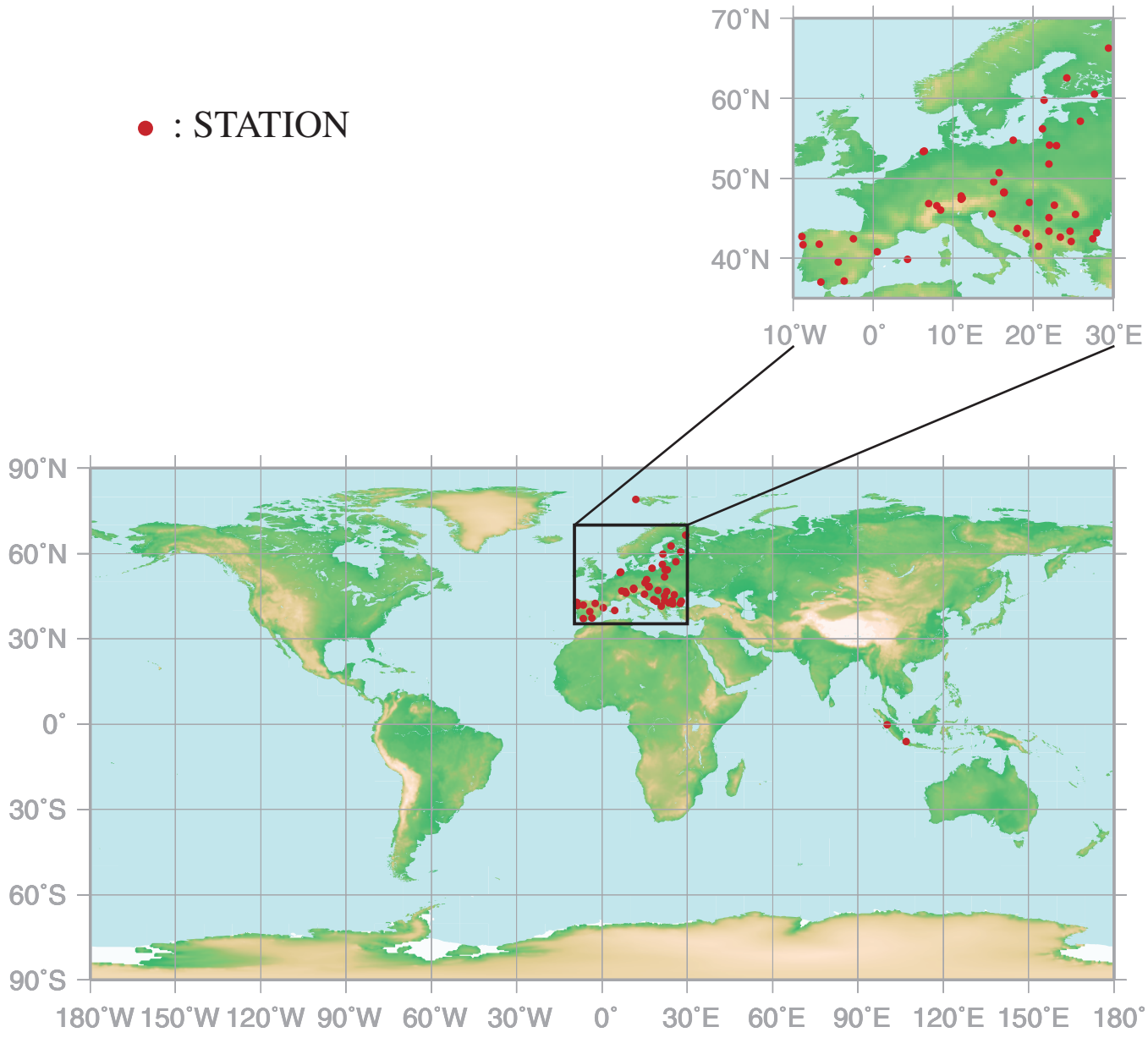

This map shows locations of the site where the monthly mean mole fractions are submitted.

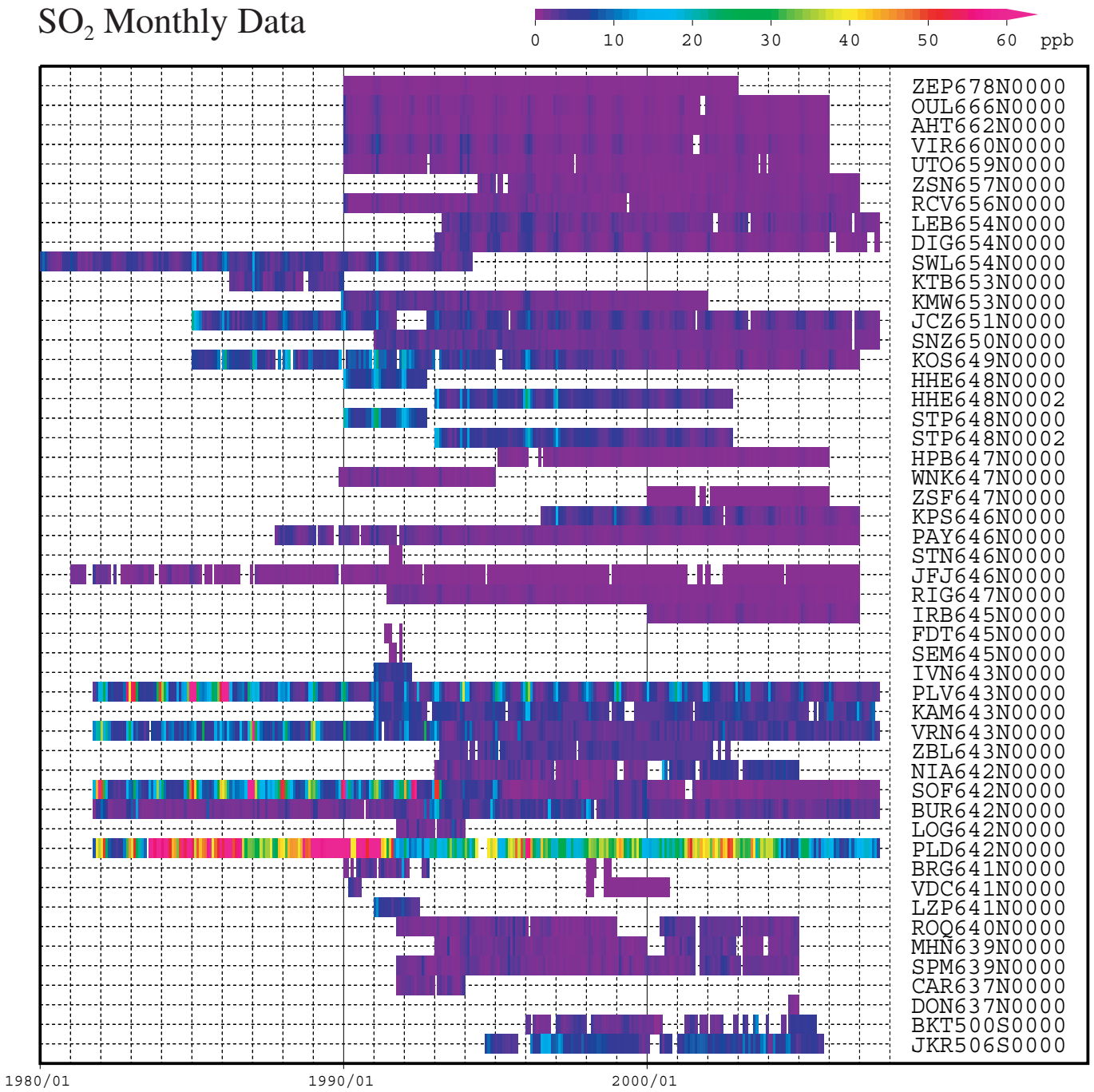

Plate 10.1 Monthly mean SO_2 mole fractions for all sites reported to the WDCGG illustrated in colors that change with the mole fraction. The sites are set from north to south.

10. Sulphur Dioxide (SO_2)

Basic information on SO_2 with regard to environmental issues

Sulphur dioxide (SO_2) is not a greenhouse gas, but a precursor of atmospheric sulphuric acid (H_2SO_4) or sulphate aerosol. SO_2 is oxidised by hydroxyl radicals (OH) to form sulphuric acid, which then produces aerosols through photochemical gas-to-particle conversion. While SO_2 reacts much slower with OH than with NO_2, SO_2 dissolves readily in suspended liquid droplets in the atmosphere. The global sulphur cycle affects atmospheric chemistry including tropospheric ozone (Berglen *et al.*, 2004).

Sources of SO_2 include fossil fuel combustion by industry, biomass burning, volcanic release and the oxidation of dimethylsulphide (DMS) from the oceans (IPCC, 2001). Major SO_2 sinks are oxidation by OH and deposition onto wet surfaces. Anthropogenic SO_2 has caused acid rain and deposition throughout the industrial era. SO_2 mole fractions show large variations in both space and time because of the species' short lifetime and uneven anthropogenic source distribution.

Annual variation of SO_2 levels in the atmosphere

The map at the beginning of this chapter shows observation sites that have submitted SO_2 data to the WDCGG. Most of the contributing stations are located in Europe.

The monthly mean SO_2 data from all stations submitted to the WDCGG are shown in Plate 10.1 with mole fraction levels are illustrated in different colours. Please note that the data for SO_2 are reported in various units, *i.e.*, ppb, $\mu g/m^3$, mg/m^3 and $\mu gS/m^3$.

All units can be converted to ppb as follows:

$X_p\ [ppb] = (R * T / M / P_0) * 10 * X_g\ [\mu g/m^3]$
$X_p\ [ppb] = (R * T / M / P_0) * 10^4 * X_g\ [mg/m^3]$
$X_p\ [ppb] = (R * T / M_S / P_0) * 10 * X_g\ [\mu gS/m^3]$

where R is the molar gas constant (8.31451 [J/K/mol]),
T is the absolute temperature reported by an individual station,
M is the molecular weight of SO_2 (64.0648),
M_S is the atomic weight of S (32.066), and
P_0 is the standard pressure (1013.25 [hPa]).

Certain stations in southern Europe reported higher mole fractions. However, it was difficult to identify any increasing or decreasing trend for SO_2 mole fractions.

REFERENCES

References

Allen, D. J., P. Kasibhatla, A. M. Thompson, R. B. Rood, B. G. Doddridge, K. E. Pickering, R. D. Hudson, and S.-J. Lin, Transport-induced interannual variability of carbon monoxide determined using a chemistry and transport model, *J. Geophys. Res.,* **101**, 28655-28669, 1996.

Angert A., S. Biraud, C. Bonfils, W. Buermann, I. Fung, CO_2 seasonality indicates origins of post-Pinatubo sink, *Geophys. Res. Lett.*, **31**, L11103, doi:10.1029/2004GL019760, 2004.

Arellano Jr., A. F., P. S. Kasibhatla, L. Giglio, G. R. Werf, J. T. Randerson, Top-down esitmates of global CO sources using MOPITT measurements, *Geophys. Res. Lett*., **31**, L01104, doi:10.1029/2004GL018609, 2004.

Bekki, S., K. S. Law, and J. A. Pyle, Effects of ozone depletion on atmospheric CH_4 and CO concentrations, *Nature*, **371**, 595-597, 1994.

Bekki, S., and K. S. Law, Sensitivity of atmospheric CH_4 growth rate to global temperature change observed from 1980 to 1992, *Tellus*, **49B**, 409-416, 1997.

Bergamaschi, P., R. Hein, M. Heimann, and P. J. Crutzen, Inverse modeling of the global CO cycle, 1. Inversion of CO mixing ratios, *J. Geophys. Res.,* **105(D2)**, 1909-1928, 10.1029/1999JD900818, 2000.

Berglen, T. F., T. K. Berntsen, I. S. A. Isaksen, and J. K. Sundet, A global model of the coupled sulfur/oxidant chemistry in the troposphere: The sulfur cycle, *J. Geophys. Res*., **109**, D19310, doi:10.1029/2003JD003948, 2004.

Bousquet, P., P. Ciais, J. B. Miller, E. J. Dlugokencky, D. A. Hauglustaine, C. Prigent, G. R. Van der Werf, P. Peylin, E.-G. Brunke, C. Carouge, R. L. Langenfelds, J. Lathiere, F. Papa, M. Ramonet, M. Schmidt, L. P. Steele, S. C. Tyler and J. White, Contribution of anthropogenic and natural sources to atmospheric methane variability. *Nature*, **443**, 439-443, 2006.

Ciais, P., P. P. Tans, M. Trolier, J. W. C. White, and R. J. Francey, A large northern hemisphere terrestrial CO_2 sink indicated by the $^{13}C/^{12}C$ ratio of atmospheric CO_2, *Science*, **269**, 1098-1102, 1995.

Clerbaux, C, J. Hadji-Lazaro, D. Hauglustaine, G. Megie, B. Khattatov, and J-F. Lamarque, Assimilation of carbon monoxide meaured from satellite in a three-dimensional chemistry-transport model. *J. Geophys. Res.,* **106(D14)**, 15385-15394, 2001.

Cleveland, W. S., S. J. Devlin, Locally weighted regression: an approach to regression analysis by local fitting, *J. Amer. Statist. Assn.*, **83**, 596-610, 1988.Conway, T. J., P. P. Tans, L. S. Waterman, K. W. Thoning, D. R. Kitzis, K. A. Masarie, and N. Zhang, Evidence for interannual variability of the carbon cycle from the National Oceanic and Atmospheric Administration/Climate Monitoring and Diagnostics Laboratory global air sampling network, *J. Geophys. Res*., 99, 22831-22855, 1994.

Conard, S. G., A. I. Sukhinin, B. J. Stocks, D. R. Cahoon, E. P. Davidenko, and G. A. Ivanova, Determining Effects of Area Burned and Fire Severity on Carbon Cycling and Emissions in Siberia. *Climatic Change*, 55, 197-211, 2002.

Daniel, J. S. and S. Solomon, On the climate forcing of carbon monoxide. *J. Geophys. Res*., 103(D11), 13249-13260, 1998.

Denman, K. L., G. Brasseur, A. Chidthaisong, P. Ciais, P. M. Cox, R. E. Dickinson, D. Hauglustaine, C. Heinze, E. Holland, D. Jacob, U. Lohmann, S. Ramachandran, P. L. da Silva Dias, S. C. Wofsy and X. Zhang, 2007: Couplings Between Changes in the Climate System and Biogeochemistry. In: Climate Change 2007: The Physical Science Basis. Contribution of Working Group I to the Fourth Assessment Report of the Intergovernmental Panel on Climate Change [Solomon, S., D. Qin, M. Manning, Z. Chen, M. Marquis, K. B. Averyt, M. Tignor and H. L. Miller (eds.)]. Cambridge University Press, Cambridge, United Kingdom and New York, NY, USA.

Dettinger, M. D. and M. Ghill, Seasonal and interannual variations of atmospheric CO_2 and climate, *Tellus*, **50B**, 1-24, 1998.

Dlugokencky, E. J., L. P. Steele, P. M. Lang, and K. A. Masarie, The grouth rate and distribution of atmospheric methane, *J. Geophys. Res*., **99**, 17021-17043, 1994.

Dlugokencky, E. J., E. G. Dutton, P. C. Novelli, P. P. Tans, K. A. Masarie, K. O. Lantz, and S. Mardronich, Changes in CH4 and CO growth rates after the eruption of Mt. Pinatubo and their link with changes in tropical tropospheric UV flux, *Geophys. Res. Lett*., 23, 2761-2764, 1996.

Dlugokencky, E. J., K. A. Masarie, P. M. Lang, and P. P. Tans, Continuing decline in the growth rate of the atmospheric methane burden, *Nature*, **393**, 447-450, 1998.

Dlugokencky, E. J., B. P. Walter, K. A. Masarie, P. M. Lang and E. S. Kasischke, Measurements of an anomalous global methane increase during 1998, *Geophys. Res. Lett.*, **28**, 499-502, 2001.

Duchon, C. E., Lanczos filtering in one and two dimensions, *J. Appl. Meteor.*, **18**, 1016-1022, 1979.

Duncan, B. N., R. V. Martin, A. C. Staudt, R. Yevich, and J. A. Logan, Interannual and seasonal variability of biomass burning emissions

constrained by satellite observations, *J. Geophys. Res*., **108 (D2)**, 4100, doi:10.1029/2002JD002378, 2003.

Etherridge, D. M., L. P. Steele, R. J. Francey, and R. L. Langenfelds, Atmospheric methane between 1000 A.D. and present: Evidence of anthropogenic emissions and climatic variability, *J. Geophys. Res.*, **103**, 15979-15993, 1998.

Fiore, A. M., L. W. Horowitz, E. J. Dlugokencky, and J. J. West , Impact of meteorology and emissions on methane trends, 1990–2004, *Geophys. Res. Lett*., **33**, L12809, doi:10.1029/2006GL026199, 2006.

Francey, R. J., P. P. Tans, C. E. Allison, I. G. Enting, J. W. C. White, and M. Trolier, Changes in oceanic and terrestrial carbon uptake since 1982, *Nature*, **373**, 326-330, 1995.

Gu, L., D. D. Baldocchi, S. C. Wofsy, J. W. Munger, J. J. Michalsky, S. P. Urbanski, and T. A. Bonden, Response of a deciduous forest to the Mount Pinatubo eruption enhanced photosysthesis, *Science*, **299**, 2035-2038, 2003.

Haan, D. and D. Raynaud, Ice core record of CO variations during the last two millennia: atmospheric implications and chemical interactions within the Greenland ice, *Tellus*, **50B**, 253-262, 1998.

Hansen, J., A.Lacis, R. Ruedy, and M. Sato, Potential Clim. Impact of Mount-Pinatubo Eruption, *Geophys. Res. Lett.,* **19(2)**, 215-218, 1992.

Holloway, T., H. Levy II, and P. Kasibhatla, Global distribution of carbon monoxide. *J. Geophys. Res.,* **105(D10)**, 12123-12148, 2000.

IPCC, Climate Change 2001: The Science Basis, Contribution of Working Group I to the Third Assessment Report of the Intergovernmental Panel on Climate Change, Cambridge University Press, Cambridge, United Kingdom and New York, NY, USA, 881pp, 2001.

IPCC, 2007:Climate Change 2007: The Physical Science Basis. Contribution of Working Group I to the Fourth Assessment Report of the Intergovernmental Panel on Climate Change [Solomon, S., D. Qin, M.Manning, Z.Chen, M.Marquis, K.B.Averyt, M.Tignor and H.L.Miller(eds.)]. Cambridge University Press, Cambridge, United Kingdom and New York, NY, USA.

IPCC/TEAP, 2005: IPCC/TEAP Special Report on Safeguarding the Ozone Layer and the Global Climate System: Issues Related to Hydrofluorocarbons and Perfluorocarbons, Summary for Policymakers and Technical Summary, WMO and UNEP, 88pp.

Kajii, Y., S. Kato, D. G. Streets, N. Y. Tsai, A. Shvidenko, S. Nilsson, I. McCallum, N. P. Minko, N. Abushenko, D. Altyntsev, and T. V. Khodzer, Boreal forest fires in Siberia in 1998: Estimation of area burned and emissions of pollutants by advanced very high resolution radiometer satellite data. *J. Geophys. Res*., **107(D24)**, 4745-4752, 2002.

Kasibhatla, P., A. Arellano, J. A. Logan, P. I. Palmer, and P. Novelli, Top-down estimate of a large source of atmospheric carbon monoxide associated with fuel combustion in Asia. *Geophys. Res. Lett.,* 29(19), 1900, doi:10.1029/2002GL015581, 2002.

Kasischke, E. S., K. Bergen, R. Fennimore, F. Sotelo, G. Stephens, A. Janetos, and H. H. Shugart, Satellite imagery gives a clear picture of Russia's boreal forest fires, *EOS Trans*. AGU, **80**, 141-147, 1999.

Kasischke, E. S., and L. P. Bruhwiler, Emission of carbon dioxide, carbon monoxide, and methane from boreal forest fires in 1998, *J. Geophys. Res*., **108(D1)**, 8146, doi:10.1029/2001JD000461, 2003.

Keeling, C. D., R. B. Bacastow, A. F. Carter, S. C. Piper, T. P. Whorf, M. Heimann, W. G. Mook, and H. Roeloffzen, A three-dimensional model of atmospheric CO_2 transport based on observed winds: 1. Analysis of observational data, in aspects of climate variability in the Pacific and the Western Americas, edited by D. H. Peterson, *Geophysical Monograph* **55**, 165-236, American Geophysical Union, Washington, D.C, 1989.

Keeling, C. D., T. P. Whorf, M. Wahlen, and J. van der Plicht, Interannual extremes in the rate of rise of atmospheric carbon dioxide since 1980, *Nature*, **375**, 666-670, 1995.

Keppler, F., John T. G. Hamilton, M. Braß, and T. Röckmann, Methane emissions from terrestrial plants under aerobic conditions, *Nature*, **439**, 187-191, 2006.

Lambert, G., P. Monfray, B. Ardouin, G. Bonsang,, A.Gaudry, V. Kazan and G. Polian, Year-to-year changes in atmospheric CO_2, *Tells*, **47B**, 35-55,1995.

Lelieveld, J., P. J. Crutzen, and F. J. Dentener: Changing concentration, lifetime and climate forcing of atmospheric methane, *Tellus*, **50B**, 128-150, 1998.

Lowe, D. C., M. R. Manning, G. W. Brailsford, and A. M. Bromley, The 1991-1992 atmospheric methane anomaly: Southern hemisphere ^{13}C decrease and growth rate fluctuations, *Geophys. Res. Lett.*, **24**, 857-860, 1997.

Marenco, A, and F. Said: Meridional and vertical ozone distribution in the background troposphere from Scientific aircraft measurements during the STRATOZ III experiment. *Atmos. Env.,* **23**, 201-214, 1989.

Matsueda, H., H. Inoue, Y. Sawa, Y. Tsutsumi, and M. Ishii, Carbon monoxide in the upper troposphere over the western Pacific between 1993 and 1996, *J. Geophys. Res.*, **103**, 19093-19110, 1998.

Matsueda, H., S. Taguchi, H.Y. Inoue, and M. Ishii, A large impact of tropical biomass burning on CO and CO_2 in the upper troposphere. *Science in China (Series C)*, **45**, 116-125, 2002.

Morimoto, S., T. Nakazawa, K. Higuchi, and S. Aoki, Latitudinal distribution of atmospheric CO_2 sources nad sinks inferred by $\delta^{13}C$ measurements from 1985 to 1991. *J. Geophys. Res*., **105(D19)**, 24,315-24,326, 2000.

Morimoto, S., S. Aoki, T. Nakazawa, and T. Yamanouchi, Temporal variations of the carbon isotopic ratio of atmospheric methane observed at Ny Alesund, Svalbard from 1996 to 2004, *Geophys. Res. Lett*., **33**, L01807, doi:10.1029/2005GL024648, 2006.

Nakazawa, T., K. Miyashita, S. Aoki, and M. Tanaka, Temporal and spatial variations of upper tropospheric and lower stratospheric carbon dioxide, *Tellus*, **43B**, 106-117, 1991.

Nakazawa, T., S. Morimoto, S. Aoki and M. Tanaka, Time and space variations of the carbon isotopic ratio of tropospheric carbon dioxide over Japan, *Tellus*, **45B**, 258-274, 1993.

Nakazawa, T., S. Morimoto, S. Aoki and M. Tanaka, Temporal and spatial variations of the carbon isotopic ratio of atmospheric carbon dioxide in the western Pacific region, *J. Geophys. Res.*, **102**, 1271-1285, 1997a.

Nakazawa, T., S. Murayama, M. Toi, M. Ishizawa, K. Otonashi, S. Aoki and S. Yamamoto, Temporal variations of CO_2 concentration and its carbon and oxygen isotopic ratios in a temperate forest in the central part of the main island of Japan, *Tellus*, **49B**, 364-381, 1997b.

Nemry, B., L. Francois, P. Warnant, F. Robinet, and J.C. Gerard, The seasonality of the CO_2 exchange between the atmosphere and the land biosphere: A study with a global mechanistic vegetation model, *J. Geophys. Res.*, **101**, 7111-7125, 1996.

Novelli, P. C., K. A. Masarie, and P. M. Lang, Distributions and recent changes of carbon monoxide in the lower troposphere, *J. Geophys. Res.*, **103**, 19015-19033, 1998.

Novelli, P. C., K. A. Masarie, P. M. Lang, B. D. Hall, R. C. Myers, and J. W. Elkins, Reanalysis of tropospheric CO trends: Effects of the 1997-1998 wildfires. *J. Geophys. Res.,* **108(D15)**, 4464, doi:10.1029/2002JD003031, 2003.

Oltmans et al., Long-term changes in tropospheric ozone, *Atmos. Env*., **40**, 3156-3173, 2006.

Onogi, J. K., Tsutsui, H. Koide, M. Sakamoto, S. Kobayashi, H. Hatsushika, T. Matsumoto, N. Yamazaki, H. Kamahori, K. Takahashi, S. Kadokura, K. Wada, K. Kato, R. Oyama, T. Ose, N. Mannoji, and R. Taira, The JRA-25 Reanalysis. *Journal of the Meteorological Society of Japan*, **85,** No.3, 369-432, 2007.

Pétron, G., C. Granier, B. Khattatov, J. Lamarque, V. Yudin, J. Muller, and J. Gille, Inverse modeling of carbon monoxide surface emissions using Climate Monitoring and Diagnostics Laboratory network observations, *J. Geophys. Res.,* **107(D24)**, 4761, doi:10.1029/2001JD001305, 2002.

Prinn, R. G., J. Huang, R. F. Weiss, D. M. Cunnold, P. J. Fraser, P. G. Simmonds, A. McCulloch, C. Harth, P. Salameh, S. O'Doherty, R. H. J. Wang, L. Porter and B. R. Miller, Evidence for substantial variations of atmospheric hydroxyl radicals in the past two decades, *Science*, **292**, 1882-1888, 2001.

Rayner, P. J., I. G. Enting, R. J. Francey and R. Langenfelds, Reconstructing the recent carbon cycle from atmospheric CO_2,$\delta^{13}C$ and O_2/N_2 observations, *Tellus*, **51B**, 213-232, 1999.

Ramonet, M. and P. Monfray, CO_2 baseline concept in 3-D atmospheric transport models, *Tellus*, **48B**, 502-520, 1996.

Shindell, D., G. Faluvegi, A. Lacis, J. Hansen, R. Ruedy, and E. Aguilar, Role of tropospheric ozone increases in 20th-century climate change, *J. Geophys. Res.,* **111**, D08302, doi:10.1029/2005JD006348, 2006.

Simmonds, P. G., A. J. Manning, R. G. Derwent, P. Ciais, M. Ramonet, V. Kazan, and D. Ryall, A burning question. Can recent growth rate anomalies in the greenhouse gases be attributed to large scale biomass burning events? *Atmos. Env*., **39**, 2513-2517, 2005.

Solomon, S., D. Qin, M. Manning, R.B. Alley, T. Berntsen, N.L. Bindoff, Z. Chen, A. Chidthaisong, J.M. Gregory, G.C. Hegerl, M. Heimann, B. Hewitson, B.J. Hoskins, F. Joos, J. Jouzel, V. Kattsov, U. Lohmann, T. Matsuno, M. Molina, N. Nicholls, J. Overpeck, G. Raga, V. Ramaswamy, J. Ren, M. Rusticucci, R. Somerville, T.F. Stocker, P. Whetton, R.A. Wood and D. Wratt, 2007: Technical Summary. In: Climate Change 2007: The Physical Science Basis. Contribution of Working Group I to the Fourth Assessment Report of the Intergovernmental Panel on Climate Change [Solomon, S., D. Qin, M. Manning, Z. Chen, M. Marquis, K.B. Averyt, M. Tignor and H.L. Miller (eds.)]. Cambridge University Press, Cambridge, United Kingdom and New York, NY, USA.

Staehelin, J., J. Thudium, R.Buehler, A. Voltz-Thomas, and W. Graber, Trends in surface ozone concentrations at Arosa (Switzerland), *Atmos. Env*., **28**, 75-87, 1994.

Stavrakou, T., and J.-F. Müller , Grid-based versus big region approach for inverting CO emissions using Measurement of Pollution in the Troposphere (MOPITT) data, *J. Geophys. Res*., **111**, D15304, doi:10.1029/2005JD006896, 2006.

Stenchikov, G., A.Robock, V. Ramaswamy, M. D. Schwarzkopf, K. Hamilton, and S. Ramachandran,

Arctic Oscillation response to the 1991 Mount Pinatubo eruption: Effects of volcanic aerosols and ozone depletion, *J. Geophys. Res.*, **107(D24)**, 4803, doi:10.1029/2002JD002090., 2002.

Taguchi, S., H. Matsueda, H. Y. Inoue, and Y. Sawa, Long-range transport of carbon monoxide from tropical ground to upper troposphere: a case study for South East Asia in October 1997. *Tellus*, **54B**, 22-40, 2002.

Tanaka, M., T. Nakazawa, S. Aoki, Seasonal and meridional variations of atmospheric carbon dioxide in the lower troposphere of the northern and southern hemispheres, *Tellus*, **39B**, 29-41, 1987.

Tsutsumi, Y, Y. Makino, and J. B. Jensen: Vertical and latitudinal distributions of tropospheric ozone over the western Pacific: Case studies from the PACE aircraft missions. *J. Geophys. Res.*, 108(D8), 4251, doi:10.1029/2001JD001374, 2003.

Thoning, K. W., P. P. Tans, and W. D. Komhyr, Atmospheric carbon dioxide at Mauna Loa observatory, 2. Analysis of the NOAA GMCC data, 1974-1985, *J. Geophys. Res.*, **94**, 8549-8565, 1989.

van der Werf,G. R., J. T. Randerson, G. J. Collatz, L. Giglio, P. S. Kasibhatla, A. F. Arellano, Jr., S. C. Olsen, and E. S. Kasischke, Continental-scale partitioning of fire emissions during the 1997 to 2001 El Nino/La Nina period, *Science*, **303**, 73-76, 2004.

Wittenberg, U., M. Heimann, G. Esser, A.D. Mcguire, and W. Sauf, On the influence of biomass burning on the seasonal CO_2 signal as observed at monitoring stations, *Global Biogeochem. Cycles*, **12**, 531-544, 1998.

WMO, Scientific assessment of ozone depletion: 1998. WMO global ozone research and monitoring project - Report No. 44, World Meteorological Organization, Geneva, 1999a.

WMO, WMO statement on the status of the global climate in 1998, WMO- No.896, World Meteorological Organization, Geneva, 1999b.

WMO, World Data Centre for Greenhouse Gases (WDCGG) Data Summary, WDCGG No. 22, 84pp, 2000.

WMO, Global Amospheric Watch (GAW) Strategic Plan: 2008-2015, GAW Report No. 172, WMO TD No. 1384, 2007a.

WMO, World Data Centre for Greenhouse Gases Data Submission and Disseminatin Guide, GAW Report No. 174, WMO TD No. 1416, 2007b

Wotawa, G., P. C. Novelli, M. Trainer, and C. Granier, Inter-annual variability of summertime CO concentrations in the Northern Hemisphere explained by boreal forest fires in North America and Russia. *Geophys. Res. Lett.*, **28**, 4575-4578, 2001.

Yurganov, L. N., et al., A quantitative assessment of the 1998 carbon monoxide emission anomaly in the Northern Hemisphere based on total column and surface concentration measurements. *J. Geophys. Res.*, **109**, D15305, doi:10.1029/2004JD004559, 2004.

APPENDICES

Calibration and Standard Scales

1. Calibration System in the GAW programme

Under the Global Atmosphere Watch (GAW) programme, World Calibration Centres (WCCs) are responsible for maintaining calibration standards for certain species, establishing instrument calibrations and providing training to the stations. A Reference Standard is designated for each species to be used for all GAW measurements of that species at Central Calibration Laboratories. Table 1 lists the organizations that serve as WCCs and CCLs for GAW [*WMO*, 2001, 2004].

Table 1. Overview of the GAW Central Calibration Laboratories (GAW-CCL, Reference Standard) and World Calibration Centres for greenhouse and other related gases. The World Calibration Centres have assumed global responsibilities, except where indicated (Am, Americas; E/A, Europe and Africa; A/O, Asia and the South-West Pacific)

Species	Central Calibration Laboratory (Reference Standard)	World Calibration Centre
Carbon Dioxide (CO_2)	NOAA/GMD	NOAA/GMD
Methane (CH_4)	NOAA/GMD	EMPA (Am, E/A) JMA (A/O)
Nitrous Oxide (N_2O)	NOAA/GMD	IFU
Chlorofluorocarbons (CFCs)		
Surface Ozone (O_3)	NIST	EMPA
Carbon Monoxide (CO)	NOAA/GMD	EMPA
Volatile Organic Compounds (VOCs)		IFU
Sulphur Dioxide (SO_2)		
Nitrogen Oxides (NO_x)		

2. Carbon Dioxide (CO_2)

In 1995, the National Oceanic and Atmospheric Administration Earth System Research Laboratory, Global Monitoring Division(NOAA/GMD, former CMDL) in Boulder, Colorado, USA took over the role of Central Calibration Laboratory (CCL) from the Scripps Institution of Oceanography (SIO) in San Diego, California, USA. Since then, NOAA/GMD has been designated by WMO as the CCL responsible for maintenance of the GAW Reference Standard for CO_2. As the World Calibration Centre (WCC) for CO_2, NOAA/GMD maintains a high-precision manometric system for absolute calibration of CO_2 as the reference used for GAW measurements throughout the world [*Zhao et al.*, 1997]. It is recommended that the standards of the GAW measurement laboratories be calibrated every two years at the CCL (WMO, 2003).

Under the WMO calibration system, there have been several calibration scales for CO_2 data, *e.g.*, SIO-based X74, X85, X87, X93 and X2002 scales and the NOAA/GMD-based WMO Mole Fraction Scale partially based on the past SIO scales. The NOAA/GMD and SIO are working to resolve the possible small differences between their scales. The CCL adopted the WMO X2005 scale, reflecting historical manometric calibrations of the WMO CCL set of cylinders and the possible small differences between SIO and NOAA/GMD calibrations.

To assess the differences in standard scales among CO_2 measuring laboratories, NOAA/GMD organizes intercomparisons or Round Robin experiments endorsed by WMO every few years. Many laboratories participated in the experiments organized in 1991-1992, 1995-1997, 1999-2000, and 2002-2006. Table 2 shows the results of the experiments performed in 1996-1997 in which the mole fractions measured by various laboratories are compared with the mole fractions measured by NOAA/GMD [*Peterson et al.*, 1999]. In addition, many laboratories compare their standards bilaterally or multilaterally among themselves.

Table 3 lists laboratories and sites used in the present issue of *Data Summary* with standard scales of reported data and history of participation in the WMO intercomparison experiments.

Table 2. Round robin results for carbon dioxidemole fraction. Differences between the mole fractions measured by various laboratories and the mole fraction measured by NOAA (Laboratory minus NOAA, ppm).

Laboratory	Analysis Date	Mole fraction Difference (ppm)		
		Low 340-350 ppm	Medium 350-360 ppm	High 370-380 ppm
NIWA	Feb-96	0.02	0.1	0.2
CSIRO	May-96	-0.07	-0.02	-0.02
AES	Jun-97	-0.04	0	-0.02
CMA	Dec-95	-0.07	-0.01	-0.02
Tohoku Univ.	Jun-96	-0.01	0.04	0.02
AIST(NIRE)	Jul-96	-0.11	-0.04	-0.06
NIES	Aug-96	-0.02	0.09	0.12
MRI	Dec-96	0.04	0.07	0.14
JMA	Jan-97	0.07	0.31	0.3
SNU	Mar-97	0.24	0.13	0.29
CFR	Jan-96	0.1	0.08	0.16
IMS	Mar-96	0.04	0.06	0.07
ENEA	Apr-96	-0.29	-0.06	0.19
UBA	Jul-96	0	-0.02	0.11
HMS	Dec-96	-1.22	-1.04	-0.8

Table 3. Status of standard scales and calibration/intercomparison for carbon dioxide at laboratories.

Laboratory	WDCGG Filename Code	Calibration Scale	WMO Intercomparison
Aichi	MKW234N0000	WMO	
AIST(NIRE)	TKY236N0000	NIRE	96/97, 99/00, 02/06
BoM&CSIRO	CGO540S0010,CGO540S0000	WMO	
CAMS	WLG236N0000	WMO	96/97, 99/00, 02/06
CESI	PRS645N0000	WMO	99/00, 02/06
CSIRO	ALT482N0003,CFA519S0003,CGO540S0003,CYA766S0000, ESP449N0003,MAA767S0003,MLO519N0003,MQA554S0003, SIS660N0003,SPO789S0003	WMO	91/92, 96/97, 99/00, 02/06
EC	ALT482N0000,CSJ451N0000,SBL443N0000	WMO	91/92, 96/97, 99/00, 02/06
ENEA	LMP635N0000	WMO	91/92, 96/97, 99/00, 02/06
FMI	PAL667N0000	WMO	02/06
GERC	GSN233N0101		
HMS	KPS646N0000,HUN646N0000	WMO	91/92, 96/97, 99/00, 02/06
IAFMS	CMN644N0000	WMO	91/92, 96/97, 02/06
IGP	HUA312S0000	WMO	
IMK-IFU	WNK647N0000,ZUG647N0014	WMO	99/00

INM	IZA128N0000	WMO	91/92, 96/97, 99/00
INMH	FDT645N0102		
IOEP	DIG654N0000		
ICES	JBN762S0000	WMO	
ITM	ZEP678N0000	WMO	96/97, 99/00
JMA	MNM224N0000,RYO239N0000,YON224N0000	WMO	91/92, 96/97, 99/00, 02/06
KMA	AMY236N0000		02/06
KSNU	ISK242N0000		
LSCE	AMS137S0000,MHD653N0002	WMO	91/92, 96/97, 99/00, 02/06
METRI	KSN233N0000	WMO	96/97
MGO	BER255N0000,KOT276N0000,KYZ240N0000,STC652N0000, TER669N0000	WMO	
MMS	DMV504N0000	WMO	
MRI	TKB236N0102	MRI	91/92, 96/97, 99/00, 02/06
NIES	COI243N0000,HAT224N0000	NIES	96/97, 99/00, 02/06
NIPR&Tohoku Univ.	SYO769S0000		Tohoku Univ.:91/92, 96/97, 99/00, 02/06
NIWA	BAR541S0000	WMO	91/92, 96/97, 99/00, 02/06
NOAA/GMD	BRW471N0000,MLO519N0000,SMO514S0000,SPO789S0000, NOAA/GMD flask network*	WMO	91/92, 96/97, 99/00, 02/06
Osaka Univ.	STA234N0000		
RIVM	KMW653N0000	NIST	
Saitama	URW235N0000,KIS236N0000,DDR236N0000	WMO	
SAWS	CPO134S0000	WMO	99/00, 02/06
Shizuoka Univ.	HMM234N0000		
UBA	BRT648N0000,DEU649N0000,LGB652N0000,NGL653N0000 SNB647N0000,SSL647N0000,SSL647N0001,WES654N0000, ZGT654N0000,ZSF647N0010,ZUG647N0000	WMO	91/92, 96/97, 99/00, 02/06

* NOAA/GMD flask network:
ALT482N0001,AMS137S0101,ASC107S0001,ASK123N0101,AVI417N0001,AZR638N0001,BAL655N0001,BKT500S0001,BME432N0001, BMW432N0001,BRW471N0001,BSC644N0001,CBA455N0001,CGO540S0001,CHR501N0001,CMO445N0001,CRZ146S0001,EIC329S0001, GMI513N0001,GOZ636N0001,HBA775S0001,HUN646N0101,ICE663N0001,ITN435N0001,IZO128N0001,KCO204N0001,KEY425N0001, KUM519N0001,KZD244N0001,KZM243N0001,LEF445N0001,MBC476N0001,MHD653N0001,MID528N0001,MKN100S0001,MLO519N0001, NMB123S0001,NWR440N0001,OPW448N0001,PAL667N0001,POC90000001,POC905N0001,POC905S0001,POC910N0001,POC910S0001, POC915N0001,POC915S0001,POC920N0001,POC920S0001,POC925N0001,POC925S0001,POC930N0001,POC930S0001,POC935S0001, PSA764S0001,PTA438N0001,RPB413N0001,SCS903N0001,SCS906N0001,SCS909N0001,SCS912N0001,SCS915N0001,SCS918N0001, SCS921N0001,SEY104S0001,SGP436N0001,SHM452N0001,SMO514S0001,SPO789S0001,STC654N0001,STM666N0001,SUM672N0001, SYO769S0001,TAP236N0001,TDF354S0001,TRH441N0001,UTA439N0001,UUM244N0001,WIS631N0001,WLG236N0001,ZEP678N0001

3. Methane (CH_4)

The GAW programmes have established two WCCs forCH_4: the Swiss Federal Laboratory for Materials Testing and Research (EMPA), Dübendorf, Switzerland and the Japan Meteorological Agency (JMA), Tokyo, Japan [*WMO*, 2001]. In addition, the Central Calibration Centre for methane has been established in NOAA /GMD [*WMO*, 2004; *Dlugokencky, et. al.*, 2005].

The NOAA04 scale has been designated as the Reference Standards of the GAW programme. This scale results in CH_4 mole fractions that are a factor of 1.0124 greater than the NOAA previous scale. [*Dlugokencky et al.*, 2005]

Table 4 summarizes the methane standard scales used by laboratories contributing to the WDCGG and lists tentative multiplying conversion factors applied for analysis in this issue of *Data Summary*. The standard is the NOAA04 scale and conversion factors

are calculated from the results of intercomparisons of the mole fractions with other laboratories bilaterally or multilaterally performed before the establishment of GAW Standards. The conversion factors will be abolished when a station employs the NOAA04 scale.

The former CMDL scale is lower than an absolute gravimetric scale [*Aoki et al.*, 1992] by ~1.5% [*Dlugokencky et al.*, 1994] and lower than the AES (MSC) scale by a factor of 1.0151 [Worthy et al., 1998]. The CSIRO scale can be converted to the Tohoku University standard by multiplying by 1.0119 [*Cunnold et al.*, 2002]. So we adopt the conversion factors 1.0124/1.0151=0.997 and 1.0119*1.0124/1.0151= 1.0092 to intercompare with the new WMO scale, NOAA04.

Table 4. Status of methane standard scales at laboratories with conversion factors used in this issue of Data Summary.

Laboratory	WDCGG Filename Code	Calibration Scale	Conversion Factor
AGAGE	CGO540S0011,CGO540S0013,CMO445N0011, MHD653N0011,MHD653N0013,RPB413N0000, RPB413N0011,SMO514S0014,SMO514S0016, THD441N0000	Tohoku Univ.	0.9973
CESI	PRS645N0000	NOAA/CMDL	1.0124
CHMI	KOS649N0000	CHMI	0.9973
CSIRO	ALT482N0003,CFA519S0003,CGO540S0003, CYA766S0000,ESP449N0003,MAA767S0003, MLO519N0003,MQA554S0003,SIS660N0003, SPO789S0003	CSIRO94	1.0092
ENEA	LMP635N0000	NOAA/CMDL	1.0124
INM	IZA128N0000	NOAA/CMDL	1.0124
JMA	MNM224N0000,RYO239N0000,YON224N0000	NOAA04	1
KMA	AMY236N0000		
KSNU	ISK242N0000		
METRI	GSN233N0000		
MGO	TER669N0000	NOAA04	1
MRI	TKB236N0000	MRI	0.9973
NIES	COI243N0000,HAT224N0000	NIES	0.9973
NOAA/GMD	BRW471N0000,MLO519N0000, NOAA/GMD flask network*	NOAA04	1
	KPA432N0001,LEF445N0001,MCM777S0001 NZL543S0001,POC935S0001,SGI354S0001,SIO432N0001	NOAA/CMDL	1.0124
RIVM	KMW653N0000	NIST	0.9973
SAWS	CPO134S0000	NOAA04	1
UBA	DEU649N0000,NGL653N0000,SSL647N0000, ZGT654N0000,ZSF647N0010,ZUG647N0000	NOAA/CMDL	1.0124

* NOAA/GMD flask network:
ALT482N0001,AMS137S0101,ASC107S0101,ASK123N0101,AVI417N0001,AZR638N0001,BAL655N0001,BKT500S0001,BME432N0001, BMW432N0001,BRW471N0001,BSC644N0001,CBA455N0001,CGO540S0001,CHR501N0001,CMO445N0001,CRZ146S0001,EIC329S0001, GMI513N0001,GOZ636N0001,HBA775S0001,HUN646N0101,ICE663N0001,ITN435N0001,IZO128N0001,KEY425N0001,KUM519N0001, KZD244N0001,KZM243N0001,MBC476N0001,MHD653N0001,MID528N0001,MLO519N0001,NWR440N0001,OPW448N0001,POC90000001, POC905N0001,POC905S0001,POC910N0001,POC910S0001,POC915N0001,POC915S0001,POC920N0001,POC920S0001,POC925N0001, POC925S0001,POC930N0001,POC930S0001,PSA764S0001,PTA438N0001,RPB413N0001,SCS903N0001,SCS906N0001,SCS909N0001, SCS912N0001,SCS915N0001,SCS918N0001,SCS921N0001,SEY104S0001,SGP436N0000,SHM452N0001,SMO514S0001,SPO789S0001, STM666N0001,SYO769S0001,TAP236N0001,UTA439N0001,UUM244N0001,WIS631N0001,WLG236N0001,ZEP678N0101

4. Nitrous Oxide (N_2O)

The Halocarbons and other Atmospheric Trace Species (HATS) Group of NOAA/GMD maintains a set of standards for N_2O [*Hall et al.*, 2001]. The NOAA-2006 N_2O scale [*Hall et al.*, 2007] has been designated as the Reference Standards of the GAW programme. The HATS Group analyses the standards of laboratories, including the Meteorological Service of Canada (MSC) and the Australian Commonwealth Scientific and Industrial Research Organisation (CSIRO). The Fraunhofer Institut für Atmosphärische Umweltforschung (IFU) in Garmisch-Partenkirchen, Germany, serves as the GAW WCC.

The NOAA CMDL N_2O calibration scale agrees to within 0.3% of that predicted using NIST Standard Reference Materials (at 300 and 330 ppb). According to results of the Nitrous Oxide and Halocarbons Intercalibration Experiment (NOHALICE) implemented under the International Global Atmospheric Chemistry (IGAC) programme, the difference between the scales of AGAGE (SIO-98) and NOAA/CMDL is 1% or less [*Prinn et al.*, 2000].

Table 5. Status of N_2O standard scales at laboratories.

Submitter	WDCGG Filename Code	Calibration Scale
AGAGE	ADR652N0010,CGO540S0011,CGO540S0012,CGO540S0013, CMO445N0010,CMO445N0011,MHD653N0011,MHD653N00013, RPB413N0000,RPB413N0010,RPB413N0011,SMO514S0014, SMO514S0015,SMO514S0016,THD441N0000	SIO 1998
CSIRO	ALT482N0003,CFA519S0003,CGO540S0003,CYA766S0000, EPC449N0003,MAA767S0003,MLO519N0003,MQA554S0003, SIS660N0003,SPO789S0003	CSIRO
ENEA	LMP635N0000	CMDL 2000
GERC	GSN233N0101	
JMA	RYO239N0000	NOAA2006
KMA	AMY236N0000	
METRI	GSN233N0000	
MRI	MMB243N0000	MRI
Nagoya University	NGY235N0000	
NIES	HAT224N0000	NIES
NILU	ZEP678N0000	
NOAA/GMD	ALT482N0002,BRW471N0002,BRW471N0010,BRW471N0011, CGO540S0002,KUM519N0002,MLO519N0002,MLO519N0010, MLO519N0011,NWR440N0102,NWR440N0110,NWR440N0111, SMO514S0002,SMO514S0010,SMO514S0011,SPO789S0002, SPO789S0010,SPO789S0011	CMDL 2000
SAWS	CPO134S0000	CMDL 2000
UBA	SSL647N0000	SIO 1998

5. Surface Ozone (O_3)

The National Institute of Standards and Technology (NIST) has developed and deployed Standard Reference Photometers (SRPs) in the USA and other countries. The GAW has designated the SRP #2 maintained at NIST as the Reference Standard for the GAW programme making NIST the CCL for O_3. The Swiss Federal Laboratory for Materials Testing and Research (EMPA) maintains NIST SRP #15 as the reference and is GAW WCC for surface ozone [*Hoferetal.,* 1998]. The traceability and uncertainty of O_3 within the GAW network were reported by Klausen *et al.,* (2003). Regional Calibration Centres have been established at the Czech Hydrometeorological Institute (CHMI) in Prague, Czech Republic, and Servicio Meteorológico Nacional (SMN) in Buenos Aires, Argentina [*WMO,* 2001]. The former maintains the SRP #17 directly purchased from NIST.

Table 6. Status of surface ozone standard scales at laboratories

Laboratory	WDCGG Filename Code	Calibration Scale	Audit EMPA-WCC
AQRB	ALG447N0000,BRA450N0000,CHA446N0000, EGB444N0000,EST451N0000,ELA449N0000, KEJ444N0000,SAT448N0000		
AWI	NMY770S0000		
BMG	BKT500S0000	WMO (NIST & EMPA)	99,01,04,07
BoM/CSIRO	CGO540S0000	WMO (NIST & EMPA)	02
CHMI	KOS649N0000	WMO (NIST & EMPA)	
DEFRA	EDM655N0000		
DWD	HPB647N0000	WMO (NIST & EMPA)	97,06
EARS	IRB645N0000,KVV646N0000,KVK646N0000, ZRN646N0000	WMO (NIST & EMPA)	
EMPA	JFJ646N0000,MKN100S0000,PAY646N0000, RIG647N0000	WMO (NIST & EMPA)	Jungfraujoch:99,06
FMI	AHT662N0000,OUL666N0000,PAL667N0000, UTO659N0000,VIR660N0000		Pallas-Sammaltunturi: 97,03
HMS	KPS646N0000		
INM	DON637N0000,MHN639N0000,NIA642N0000, ROQ640N0000,SPM639N0000	NPL(U. K.)	
	IZA128N0000	WMO (NIST & EMPA)	96,98,00,04
INMH	FDT645N0102		
IM	ANG638N0000,BEJ638N0000,CAS639N0000, FUN132N0000,LIS638N0000,MVH638N0000, PEN640N0000		
IOEP	DIG654N0000	WMO (NIST & EMPA)	
ISAC	CMN644N0000		
IVL	VDL664N0000	Stockholm Univ.(Sweden)	
JMA	MNM224N0000,RYO239N0000,SYO769S0002, YON224N0000	WMO (NIST & EMPA)	Ryori:05
	TKB236N1003		
KSNU	ISK242N0000		
LEGMA	RCV656N0000	WMO (NIST & EMPA)	
MMS	TAR504N0000		
NILU	ZEP678N0000	WMO (NIST & EMPA)	97,01,05

NIWA	BAR541S0000	WMO (NIST & EMPA)	
NOAA/GMD	BMW432N0004,BRW471N0004,ICE663N0004, LAU545S0004, MCM777S0104,MLO519N40, NWR440N0202,NWR440N0404,RPB413N0004, SMO514S0004,SPO789S0004,SUM672N0004, THD441N0004	NOAA/GMD	Mauna Loa:03
NUI	MHD653N0000	WMO (NIST & EMPA)	96,98,02,05
ONM	ASK123N0000		03
PolyU	HKG222N0000		
RIVM	KMW653N0000		
Roshydromet	DAK654N0000, SHP659N0000		
SAWS	CPO134S0000	WMO (NIST & EMPA)	97,98,02,06
SMN	USI354S0000	WMO (NIST & EMPA)	98,03
UBA	BRT648N0000,DEU649N0000,LGB652N0000, NGL653N0000,SNB647N0000,SSL647N0000, WES654N0000,ZGT654N0000,ZSF647N0010, ZUG647N0000	WMO (NIST & EMPA)	Zugspitze:96,97,01 Sonnblick:98
UM	GLH636N0000		

6. Carbon Monoxide (CO)

The Swiss Federal Laboratory for Materials Testing and Research (EMPA) serves as the WCC under GAW based on its secondary standards calibrated against the standard at NOAA/GMD designated as the Reference Standard for GAW.

Table 7. Status of carbon monoxide standard scales at laboratories

Laboratory	WDCGG Filename Code	Calibration Scale	Audit EMPA-WCC
AGAGE	CGR540S0011,MCH653N0011	SIO 1998	
CHMI	KOS649N0000	CHMI	
CSIRO	ALT482N0003,CFA519S0003,CGO540S0003, CYA766S0000, ESP449N0003,MAA767S0003, MLO519N0003,MQA554S0003,SIS660N0003, SPO789S0003	WMO (NOAA/GMD & EMPA)	Cape Grim:02
DWD	HPB647N0000	WMO (NOAA/GMD & EMPA)	97,06
EARS	KVV646N0000		
EMPA	JFJ646N0000,MKN100S0000,PAY646N0000, RIG647N0000	WMO (NOAA/GMD & EMPA)	Jungfraujoch: 99,06
JMA	RYO239N0000, MNM224N0000, YON224N0000	JMA	Ryori:05
NOAA/GMD	NOAA/GMD flask network*	WMO (NOAA/GMD & EMPA)	Mauna Loa:03
PolyU	HKG222N0000		
RIVM	KMW653N0000,KTB653N0000	National	

SAWS	CPO134S0000	WMO (NOAA/GMD & EMPA)	98,02,06
SMN	USI354S0000	WMO (NOAA/GMD & EMPA)	98,03
UBA	SNB647N0000,SSL647N0000,ZUG647N0000	WMO (NOAA/GMD & EMPA)	Zugspitze:01 Sonnblick:98
UM	GLH636N0000		

NOAA/GMD flask network:
ALT482N0001,ASC107S0001,ASK123N0101,AZR638N0001,BAL655N0001,BME432N0001,BMW432N0001,BRW471N0001,BSC644N0001, CBA455N0001,CGO540S0001,CHR501N0001,CMO445N0001,CRZ146S0001,EIC329S0001,GMI513N0001,GOZ636N0001,HBA775S0001, HUN646N0101,ICE663N0001,ITN435N0001,IZO128N0001,KEY425N0001,KUM519N0001,KZD244N0001,KZM243N0001,LEF445N0001, MBC476N0001,MHD653N0001,MID528N0001,MLO519N0001,NWR440N0001,PAL667N0001,POC90000001,POC905N0001,POC905S0001, POC910N0001,POC910S0001,POC915N0001,POC915S0001,POC920N0001,POC920S0001,POC925N0001,POC925S0001,POC930N0001, POC930S0001,POC935N0001,POC935S0001,PSA764S0001,PTA438N0001,RPB413N0001,SCS903N0001,SCS906N0001,SCS909N0001, SCS912N0001,SCS915N0001,SCS918N0001,SCS921N0001,SEY104S0001, SGP436N0000,SHM452N0001,SMO514S0001,SPO789S0001, STM666N0001,SYO769S0001,TAP236N0001,TDF354S0001, THD441N0000,UTA439N0001,UUM244N0001,WIS631N0001,WLG236N0001, ZEP678N0101

Acronyms and Abbreviations:

AES:	Atmospheric Environment Service (presently MSC)
AGAGE:	Advanced Global Atmospheric Gases Experiment
Aichi:	Aichi Prefecture, Japan
AIST:	National Institute of Advanced Industrial Science and Technology, Japan
AQRB: (Canada)	Environment Canada, Meteorological Service of Canada, Air Quality Research Branch
AWI:	Alfred Wegener Institute, Germany
BMG:	Bureau of Meteorology and Geophysics, Indonesia
BoM:	Commonwealth Bureau of Meteorology, Australia
CAMS:	Chinese Academy of Meteorological Sciences, China
CESI:	Italian Electrical Experimental Center, Italy
CFR:	Laboratoire des Sciences du Climat et de l'Environnement, CEA-CNRS, France
CHMI:	Czech Hydrometeorological Institute, Prague, Czech Republic
CMA:	Chinese Academy of Meteorological Sciences, China Meteorological Administration
CMDL:	Climate Monitoring and Diagnostics Laboratory, NOAA, USA (presently NOAA/GMD)
CSIRO:	Commonwealth Scientific and Industrial Research Organisation, Australia
DEFRA:	Department for Environment, Food and Rural Affairs, London, United Kingdom
DWD:	Deutscher Wetterdienst, Germany
EARS:	Environmental Agency of the Republic of Slovenia
EC:	Environment Canada, Canada
EMPA:	Swiss Federal Laboratories for Materials Research and Testing, Dübendorf, Switzerland
ENEA:	Italian National Agency for New Technology, Energy and the Environment, Italy
FMI:	Finnish Meteorological Institute
GERC:	Global Environment Research Center of NIER, Republic of Korea
HMS:	Hungarian Meteorological Service, Hungary
IAFMS:	Italian Air Force Meteorological Service, Italy
ICES:	International Center for Earth Sciences c/o CNR,Italy
IGP:	Instituto Geofísico del Perú
IM:	Instituto de Meteorologia, Portugal
IMK-IFU:	Fraunhofer Institut für Atmosphärische Umweltforschung, Garmich-Partenkirchen, Germany
INM:	Instituto Nacional de Meteorología, Spain
INMET:	Instituto Nacional de Meteorologia, Brazil
INMH:	National Meteorological Administration, Romania
IOEP:	Institute of Environmental Protection, Warsaw
ISAC:	Istituto di Scienze dell'Atmosfera e del Clima, Consiglio Nazionale delle Ricerche, Italy
ITM:	Department of Applied Environmental Science, Stockholm University, Sweden
IVL:	Swedish Environmental Research Institute, Göteborg, Sweden
JMA:	Japan Meteorological Agency, Tokyo, Japan
JMA/AO:	Aerological Observatory, Japan Meteorological Agency, Tsukuba, Japan

KMA:	Korea Meteorological Administration, Republic of Korea
KMD:	Kenya Meteorological Department, Kenya
KSNU:	Kyrgyz State National University, Kyrgyzstan
LEGMA:	Latvian Environment, Geology and Meteorology Agency, Latvia
LSCE:	Laboratoire des Sciences du Climat et de l'Environnement, CEA-CNRS, France
METRI:	Meteorological Research Institute, KMA, Republic of Korea
MGO:	Main Geophysical Observatory, Russian Federation
MISU:	Department of Meteorology, Stockholm University, Sweden
MMS:	Malaysian Meteorological Department
MRI:	Meteorological Research Institute, Japan Meteorological Agency, Japan
MSC:	Meteorological Service of Canada (formerly AES)
NIES:	National Institute for Environmental Studies, Japan
NILU:	Norwegian Institute for Air Research, Norway
NIMH:	Institutul National de Meteorologie, Hidrologie si Gospodarirea Apelor, Romania
NIPR:	National Institute of Polar Research, Japan
NIRE:	National Institute for Resources and Environment, Japan
NIST:	National Institute of Standards and Technology, Gaithersburg MD, USA
NIWA:	National Institute of Water and Atmospheric Research, New Zealand
NOAA/GMD:	Earth System Research Laboratory, Global Monitoring Division, NOAA, USA (formerly CMDL)
NUI:	National University of Ireland, Galway, Ireland
ONM:	Office National de la Météorologie, Algeria
PolyU:	Hong Kong Polytechnik University, Hong Kong, China
RIVM:	National Institute of Public Health and the Environment, Bilthoven, Netherlands
Roshydromet	Russian Hydrometeorological Service
Saitama:	Saitama Prefecture, Japan
SAWS:	South African Weather Service, South Africa
Shizuoka:	Shizuoka University, Japan
SIO:	Scripps Institution of Oceanography, USA
SMN:	Servicio Meteorológico Nacional, Argentina
SNU:	Seoul National University, Republic of Korea
Tohoku Univ.:	Tohoku University, Japan
UBA:	Umweltbundesamt (Federal Environmental Agency), Germany
UBA Austria:	Umweltbundesamt (Federal Environmental Agency), Austria
UHEI-IUP:	Institut für Umweltphysik, Universität Heidelberg, Germany
UM:	University of Malta
ZAMG:	Central Institute of Meteorology and Geodynamics, Austria

References

Aoki, S., T. Nakazawa, S. Murayama and S. Kawaguchi, Measurements of atmospheric methane at the Japanese Antarctic station, Syowa, *Tellus, Ser. B,* **44**, 273-281, 1992.

CMDL, Climate Monitoring and Diagnostics Laboratory Summary Report No.26 2000-2001, 2002.

Cunnold, D. M., L. P. Steele, P. J. Fraser, P. G. Simmonds, R. G. Prinn, R. F. Weiss, L. W. Porter, S. O'Doherty, R. L. Langenfelds, P. B. Krummel, H. J. Wang, L. Emmons, X. X. Tie, and E. J. Dlugokencky, In situ measurements of atmospheric methane at GAGE/AGAGE sites during 1985-2000 and resulting source inferences, *J. Geophys, Res,* **107**（**D14**）, 10.1029/2001JD001226, 2002.

Dlugokencky, E. J., L. P. Steele, P. M. Lang, and K. A. Masarie, The growth rate and distribution of atmospheric methane, *J. Geophys. Res.,* **99**, 17021-17043, 1994.

Dlugokencky, E. J., R. C. Myers, P. M. Lang, K. A. Masarie, A. M. Crotwell, K. W. Thoning, B. D. Hall, J. W. Elkins, and L. P. Steele, Conversion of NOAA atmospheirc dry air CH4 mole fractions to a gravimetrically prepared standard scale, *J. Geophys. Res.,***110**, D18306, doi: 10.1029/2005JD006035, 2005.

Hall, B. D. (ed.), J. W. Elkins, J. H. Butler, S. A. Montzka, T. M. Thompson, L. Del Negro, G. S. Dutton, D. F. Hurst, D. B. King, E. S. Kline, L. Lock, D. Mactaggart, D. Mondeel, F. L. Moore, J. D. Nance, E. A. Ray, and P. A. Romashkin,

Halocarbons and Other Atmospheric Gases, Section 5 in Climate Monitoring and Diagnostics Laboratory, Summary Report N. 25, 1998-1999, R. S. Schnell, D. B. King, R. M. Rosson (eds.), NOAA-CMDL, Boulder, CO., USA, 2001.

Hall, B. D., G. S. Dutton, and J. W. Elkins , The NOAA nitrous oxide standard scale for atmospheric observations, *J. Geophys. Res.*, 112, D09305, doi:10.1029/2006JD007954, 2007.

Hofer, P., B. Buchmann and A. Herzog, Traceability, Uncertainty and Assessment Criteria of Surface Ozone Measurements, *EMPA-WCC Report 98/5*, 20 pp, 1998.

Klausen, J., C. Zellweger, B. Buchmann, and P. Hofer, Uncertainty and bias of surface ozone measurements at selected Global Atmosphere Watch sites, *J. Geophys. Res.,* **108(D19)**, 4622, doi:10.1029/2003JD003710, 2003.

Peterson, J., P. Tans, and D. Kitzis, "CO_2 Round-Robin Reference Gas Intercomparison" in Report of the Ninth WMO Meeting of Experts on Carbon Dioxide Concentration and Related Tracer Measurement Techniques, Aspendale, Vic. Australia, 1 - 4 September 1997, edited by R. Francey, WMO/GAW Report No. 132, 1999.

WMO, Strategy for the Implementation of the Global Atmosphere Watch Programme (2001-2007), WMO/GAW Report No. 142, 62pp, 2001.

WMO, Report of the Eleventh WMO/IAEA Meeting of Experts on Carbon Dioxide Concentration and Related Tracer Measurement Techniques, Global Atmosphere Watch Report Series No.148, 2003.

WMO, Addendum for the Period 2005-2007 To the Strategy for the Implementation of the Global Atmosphere Watch Programme (2001-2007), WMO/GAW Report No. 142, WMO/GAW Report No. 156, 2004.

Worthy, D. E. J., I. Levin, N. B. A. Trivett, A. J. Kuhlmann, J. F. Hopper and M. K. Ernst, Seven years of continuous methane observations at a remote boreal site in Ontario, Canada, *J. Geophys. Res.,* **103***,* 15995-16007, 1998.

Zhao, C. L., P. P. Tans, and K. W. Thoning, A high precision manometric system for absolute calibrations of CO_2 in dry air, *J. Geophys. Res.,* **102**, 5885-5894, 1997.

LIST OF OBSERVATION STATIONS

Station	Country/Territory	Index Number	Location Latitude (° ')	Location Longitude (° ')	Altitude (m)	Parameter
REGION I (Africa)						
Amsterdam Island	FRANCE	AMS137S00	37 47 S	77 31 E	65	CO_2
Amsterdam Island	FRANCE	AMS137S01	37 57 S	77 31 E	150	CH_4, CO_2
Ascension Island	UNITED KINGDOM	ASC107S00	7 55 S	14 25 W	54	$^{13}CO_2$, $C_{18}O_2$, CH_4, CO, CO_2, H_2
Assekrem	ALGERIA	ASK123N00	23 16 N	5 37 E	2710	O_3
Assekrem	ALGERIA	ASK123N01	23 10 N	5 25 E	2728	$^{13}CO_2$, $C_{18}O_2$, CH_4, CO, CO_2, H_2
Cape Point	SOUTH AFRICA	CPO134S00	34 21 S	18 28 E	230	CH_4, CO, CO_2, N_2O, O_3
Crozet	FRANCE	CRZ146S00	46 27 S	51 51 E	120	$^{13}CO_2$, $C_{18}O_2$, CH_4, CO, CO_2, H_2
Funchal	PORTUGAL	FUN132N00	32 38 N	16 52 W	58	O_3
Gobabeb	NAMIBIA	NMB123S00	23 34 S	15 1 E	461	$^{13}CO_2$, $C_{18}O_2$, CH_4, CO_2
Izaña	SPAIN	IZA128N00	28 18 N	16 30 W	2367	CH_4, CO_2, O_3
Mahe Island	SEYCHELLES	SEY104S00	4 40 S	55 10 E	7	$^{13}CO_2$, $C_{18}O_2$, CH_4, CO, CO_2, H_2
Mt. Kenya	KENYA	MKN100S00	0 3 S	37 17 E	3678	CO, O_3
Mt. Kenya	KENYA	MKN100S00	0 3 S	37 17 E	3678	$^{13}CO_2$, $C_{18}O_2$, CH_4, CO_2
Tenerife	SPAIN	IZO128N00	28 18 N	16 28 W	2360	$^{13}CO_2$, $C_{18}O_2$, CH_4, CO, CO_2, H_2
REGION II (Asia)						
Anmyeon-do	KOREA, REPUBLIC OF	AMY236N00	36 31 N	126 19 E	47	CFCs, CH_4, CO_2, N_2O
Bering Island	RUSSIAN FEDERATION	BER255N00	55 12 N	165 58 E	13	CO_2
Cape Ochi-ishi	JAPAN	COI243N00	43 8 N	145 30 E	45	CH_4, CO_2
Gosan	KOREA, REPUBLIC OF	GSN233N00	33 16 N	126 10 E	72	CFCs, CH_4, CO_2, N_2O
Gosan	KOREA, REPUBLIC OF	GSN233N01	33 8 N	126 7 E	72	CFCs, CH_4, CO_2, N_2O
Hamamatsu	JAPAN	HMM234N00	34 43 N	137 43 E	35	CO_2
Hateruma	JAPAN	HAT224N00	24 3 N	123 47 E	10	CH_4, CO_2, N_2O
Hok Tsui	HONG KONG	HKG222N00	22 13 N	114 15 E	60	CO, O_3
Issyk-Kul	KYRGYZSTAN	ISK242N00	42 37 N	76 58 E	1640	CH_4, CO_2, O_3
Kaashidhoo	MALDIVES	KCO204N00	4 58 N	73 28 E	1	$^{13}CO_2$, CH_4, CO_2
Kisai	JAPAN	KIS236N00	36 4 N	139 33 E	13	CO_2
Kotelny Island	RUSSIAN FEDERATION	KOT276N00	76 0 N	137 52 E	5	CO_2
Kyzylcha	UZBEKISTAN	KYZ240N00	40 52 N	66 9 E	340	CO_2
Memanbetsu	JAPAN	MMB243N00	43 55 N	144 11 E	32.9	N_2O
Mikawa-Ichinomiya	JAPAN	MKW234N00	34 51 N	137 25 E	50	CO_2
Minamitorishima	JAPAN	MNM224N00	24 16 N	153 58 E	8	CH_4, CO, CO_2, O_3
Mt. Dodaira	JAPAN	DDR236N00	36 0 N	139 10 E	840	CO_2
Mt. Waliguan	CHINA	WLG236N00	36 16 N	100 54 E	3810	$^{13}CO_2$, $C_{18}O_2$, CH_4, CO, CO_2, H_2
Mt. Waliguan	CHINA	WLG236N00	36 16 N	100 54 E	3810	CO_2
Nagoya	JAPAN	NGY235N00	35 8 N	136 58 E	35	N_2O
Plateau Assy	KAZAKHSTAN	KZM243N00	43 15 N	77 52 E	2519	$^{13}CO_2$, $C_{18}O_2$, CH_4, CO, CO_2, H_2
Ryori	JAPAN	RYO239N00	39 1 N	141 49 E	260	CCl_4, CFCs, CH_3CCl_3, CH_4, CO, CO_2, N_2O, O_3
Sary Taukum	KAZAKHSTAN	KZD244N00	44 27 N	75 34 E	412	$^{13}CO_2$, $C_{18}O_2$, CH_4, CO, CO_2, H_2
Ship between Ishigaki Island and Hateruma Island	JAPAN	SIH224N00	24 7 N	123 49 E	5	CO_2
Suita	JAPAN	STA234N00	34 49 N	135 31 E	63	CO_2
Tae-ahn Peninsula	KOREA, REPUBLIC OF	TAP236N00	36 43 N	126 7 E	20	$^{13}CO_2$, $C_{18}O_2$, CH_4, CO, CO_2, H_2

LIST OF OBSERVATION STATIONS (continued)

Station	Country/Territory	Index Number	Location Latitude (° ')	Location Longitude (° ')	Altitude (m)	Parameter
Takayama	JAPAN	TKY236N00	36 7 N	137 25 E	1420	CO_2
Tsukuba	JAPAN	TKB236N00	36 2 N	140 7 E	26	CH_4
Tsukuba	JAPAN	TKB236N01	36 2 N	140 7 E	26	CO_2
Tsukuba	JAPAN	TKB236N10	36 2 N	140 7 E	25	O_3
Ulaan Uul	MONGOLIA	UUM244N00	44 27 N	111 4 E	914	$^{13}CO_2$, $C_{18}O_2$, CH_4, CO, CO_2, H_2
Urawa	JAPAN	URW235N00	35 52 N	139 35 E	10	CO_2
Yonagunijima	JAPAN	YON224N00	24 28 N	123 1 E	30	CH_4, CO, CO_2, O_3
REGION III (South America)						
Arembepe	BRAZIL	ABP312S00	12 46 S	38 10 W	0	O_3
Bird Island	UNITED KINGDOM	SGI354S00	54 0 S	38 2 W	30	CH_4, CO_2
Easter Island	CHILE	EIC329S00	27 7 S	109 27 W	50	$^{13}CO_2$, $C_{18}O_2$, CH_4, CO, CO_2, H_2
Huancayo	PERU	HUA312S00	12 4 S	75 31 W	3313	CO_2
Tierra del Fuego	ARGENTINA	TDF354S00	54 52 S	68 28 W	20	$^{13}CO_2$, $C_{18}O_2$, CFCs, CH_3CCl_3, CH_4, CO, CO_2, H_2, HCFCs, HFCs
Ushuaia	ARGENTINA	USI354S00	54 51 S	68 19 W	18	CO, O_3
REGION IV (North and Central America)						
Alert	CANADA	ALT482N00	82 27 N	62 31 W	210	CH_4, CO, CO_2, N_2O, SF_6
Alert	CANADA	ALT482N00	82 27 N	62 31 W	210	$^{13}CO_2$, $C_{18}O_2$, C_2Cl_4, CCl_4, CFCs, CH_2Cl_2, CH_3CCl_3, CH_4, CO, CO_2, H_2, HCFCs, HFCs, N_2O, SF_6
Alert	CANADA	ALT482N00	82 27 N	62 31 W	210	CH_4, CO, CO_2, H_2, N_2O
Algoma	CANADA	ALG447N00	47 1 N	84 22 W	411	O_3
Barrow	UNITED STATES	BRW471N00	71 19 N	156 35 W	11	$^{13}CH_4$, $^{13}CO_2$, $C_{18}O_2$, C_2Cl_4, CCl_4, CFCs, CH_2Cl_2, CH_3CCl_3, CH_4, CO, CO_2, H_2, HCFCs, HFCs, N_2O, O_3, SF_6
Bratt's Lake	CANADA	BRA450N00	50 12 N	104 12 W	588	O_3
Candle Lake	CANADA	CDL454N00	53 52 N	104 39 W	489	CH_4, CO, CO_2
Cape Meares	UNITED STATES	CMO445N00	45 28 N	123 58 W	30	$^{13}CO_2$, $C_{18}O_2$, CH_4, CO, CO_2, H_2
Cape Meares	UNITED STATES	CMO445N00	45 28 N	123 58 W	30	CCl_4, CFCs, CH_3CCl_3, CH_4, N_2O
Cape St. James	CANADA	CSJ451N00	51 55 N	131 1 W	89	CO_2
Chalk River	CANADA	CHA446N00	46 4 N	77 24 W	184	O_3
Chapais	CANADA	CPS449N00	49 49 N	74 58 W	381	O_3
Cold Bay	UNITED STATES	CBA455N00	55 12 N	162 43 W	25	$^{13}CO_2$, $C_{18}O_2$, CH_4, CO, CO_2, H_2
Egbert	CANADA	EGB444N00	44 13 N	79 46 W	253	O_3
Estevan Point	CANADA	ESP449N00	49 22 N	126 32 W	39	CH_4, CO, CO_2, H_2, N_2O
Estevan Point	CANADA	ESP449N00	49 22 N	126 32 W	39	CH_4, CO_2, N_2O, SF_6
Esther	CANADA	EST451N00	51 40 N	110 12 W	707	O_3
Experimental Lakes Area	CANADA	ELA449N00	49 40 N	93 43 W	369	O_3
Frasedale	CANADA	FSD449N00	49 52 N	81 34 W	210	CH_4, CO, CO_2
Grifton	UNITED STATES	ITN435N00	35 21 N	77 22 W	505	$^{13}CO_2$, $C_{18}O_2$, CCl_4, CFCs, CH_4, CO, CO_2, H_2, N_2O, SF_6
Harvard Forest	UNITED STATES	HFM442N00	42 53 N	72 17 W	340	CCl_4, CFCs, CH_3CCl_3, HCFCs, HFCs, N_2O, SF_6
Kejimkujik	CANADA	KEJ444N00	44 25 N	65 12 W	127	O_3
Key Biscayne	UNITED STATES	KEY425N00	25 40 N	80 12 W	3	$^{13}CO_2$, $C_{18}O_2$, CH_4, CO, CO_2, H_2
Kitt Peak	UNITED STATES	KPA432N00	31 58 N	111 35 W	2083	CH_4

LIST OF OBSERVATION STATIONS (continued)

Station	Country/Territory	Index Number	Location Latitude (° ')	Location Longitude (° ')	Altitude (m)	Parameter
La Jolla	UNITED STATES	SIO432N00	32 49 N	117 16 W	14	CH_4
La Palma	CUBA	PLM422N00	22 45 N	83 31 W	47	NO_2
Longwoods	CANADA	LON442N00	42 52 N	81 28 W	239	O_3
Moody	UNITED STATES	WKT431N00	31 19 N	97 19 W	708	CH_4
Mould Bay	CANADA	MBC476N00	76 15 N	119 19 W	58	$^{13}CO_2$, $C_{18}O_2$, CH_4, CO, CO_2, H_2
Niwot Ridge	UNITED STATES	NWR440N00	40 1 N	105 34 W	3526	$^{13}CH_4$, $^{13}CO_2$, $C_{18}O_2$, CH_4, CO, CO_2, H_2
Niwot Ridge	UNITED STATES	NWR440N01	40 2 N	105 34 W	3475	C_2Cl_4, CCl_4, CFCs, CH_2Cl_2, CH_3CCl_3, HCFCs, HFCs, N_2O, SF_6
Niwot Ridge	UNITED STATES	NWR440N02	40 1 N	105 31 W	3022	O_3
Niwot Ridge (Saddle)	UNITED STATES	NWR440N04	40 2 N	105 34 W	3538	O_3
Niwot Ridge C-1	UNITED STATES	NWR440N03	40 0 N	105 35 W	3475	HFCs
Olympic Peninsula	UNITED STATES	OPW448N00	48 15 N	124 25 W	488	CH_4, CO_2, H_2
Park Falls	UNITED STATES	LEF445N00	45 55 N	90 16 W	868	$^{13}CO_2$, $C_{18}O_2$, CFCs, CH_3CCl_3, CH_4, CO, CO_2, H_2, HCFCs, HFCs, N_2O, SF_6
Point Arena	UNITED STATES	PTA438N00	38 57 N	123 43 W	17	$^{13}CO_2$, $C_{18}O_2$, CH_4, CO, CO_2
Ragged Point	BARBADOS	RPB413N00	13 10 N	59 25 W	45	$^{13}CO_2$, $C_{18}O_2$, CH_4, CO, CO_2, H_2, O_3
Ragged Point	BARBADOS	RPB413N00	13 10 N	59 25 W	45	$CBrClF_2$, $CBrF_3$, CCl_4, CFCs, CH_2Cl_2, CH_3Br, CH_3CCl_3, CH_3Cl, CH_4, $CHCl_3$, HCFCs, HFCs, N_2O, SF_6
Sable Island	CANADA	SBL443N00	43 55 N	60 1 W	5	CH_4, CO, CO_2, N_2O, SF_6
Saturna	CANADA	SAT448N00	48 46 N	123 7 W	178	O_3
Shemya Island	UNITED STATES	SHM452N00	52 43 N	174 4 E	40	$^{13}CO_2$, $C_{18}O_2$, CH_4, CO, CO_2, H_2
Southern Great Plains	UNITED STATES	SGP436N00	36 46 N	97 30 W	314	$^{13}CO_2$, $C_{18}O_2$, CH_4, CO, CO_2
St. Croix	UNITED STATES	AVI417N00	17 45 N	64 45 W	3	CH_4, CO_2
St. David's Head	UNITED KINGDOM	BME432N00	32 22 N	64 39 W	30	$^{13}CO_2$, $C_{18}O_2$, CH_4, CO, CO_2, H_2
Sutton	CANADA	SUT445N00	45 4 N	72 40 W	243	O_3
Trinidad Head	UNITED STATES	THD441N00	41 2 N	124 9 W	120	$^{13}CO_2$, $C_{18}O_2$, CCl_4, CFCs, CH_3CCl_3, CH_4, $CHCl_3$, CO, CO_2, HCFCs, HFCs, N_2O, O_3, SF_6
Trinidad Head	UNITED STATES	THD441N00	41 2 N	124 9 W	120	CFCs, CH_3CCl_3, CH_4, $CHCl_3$, N_2O, $CBrClF_2$, $CBrF_3$, CCl_4, CH_2Cl_2, CH_3Br, CH_3Cl, HCFCs, HFCs, SF_6
Tudor Hill	UNITED KINGDOM	BMW432N00	32 16 N	64 52 W	30	$^{13}CO_2$, $C_{18}O_2$, CH_4, CO, CO_2, H_2, O_3
Wendover	UNITED STATES	UTA439N00	39 52 N	113 43 W	1320	$^{13}CO_2$, $C_{18}O_2$, CH_4, CO, CO_2, H_2
REGION V (South-West Pacific)						
Baring Head	NEW ZEALAND	BAR541S00	41 25 S	174 52 E	85	$^{13}CH_4$, CH_4, CO, CO_2, N_2O, O_3
Bukit Koto Tabang	INDONESIA	BKT500S00	0 12 S	100 19 E	864.5	$^{13}CO_2$, $C_{18}O_2$, CH_4, CO_2
Bukit Koto Tabang	INDONESIA	BKT500S00	0 12 S	100 19 E	864.5	NO_2, O_3, SO_2
Cape Ferguson	AUSTRALIA	CFA519S00	19 16 S	147 3 E	2	CH_4, CO, CO_2, H_2, N_2O
Cape Grim	AUSTRALIA	CGO540S00	40 40 S	144 40 E	94	CO_2, O_3
Cape Grim	AUSTRALIA	CGO540S00	40 40 S	144 40 E	94	CCl_4, $CBrClF_2$, $CBrF_3$, CFCs, CH_2Cl_2, CH_3Br, CH_3CCl_3, CH_3Cl, CH_4, $CHCl_3$, CO, H_2, HCFCs, HFCs, N_2O, SF_6
Cape Grim	AUSTRALIA	CGO540S00	40 40 S	144 40 E	94	CH_4, CO, CO_2, H_2, N_2O, O_3

LIST OF OBSERVATION STATIONS (continued)

Station	Country/Territory	Index Number	Location Latitude (° ')	Location Longitude (° ')	Altitude (m)	Parameter
Cape Grim	AUSTRALIA	CGO540S00	40 40 S	144 40 E	94	$^{13}CH_4$, $^{13}CO_2$, $C_{18}O_2$, C_2Cl_4, CCl_4, CFCs, CH_2Cl_2, CH_3CCl_3, CH_4, CO, CO_2, H_2, HCFCs, HFCs, N_2O, SF_6
Cape Kumukahi	UNITED STATES	KUM519N00	19 31 N	154 49 W	3	$^{13}CO_2$, $C_{18}O_2$, C_2Cl_4, CCl_4, CFCs, CH_2Cl_2, CH_3CCl_3, CH_4, CO, CO_2, H_2, HCFCs, HFCs, N_2O, SF_6
Christmas Island	KIRIBATI	CHR501N00	1 42 N	157 10 W	3	$^{13}CO_2$, $C_{18}O_2$, CH_4, CO, CO_2, H_2
Danum Valley GAW Baseline Station	MALAYSIA	DMV504N00	4 58 N	117 49 E	426	CO_2
Guam	UNITED STATES	GMI513N00	13 25 N	144 46 E	2	$^{13}CO_2$, $C_{18}O_2$, CH_4, CO, CO_2, H_2
Jakarta	INDONESIA	JKR506S00	6 10 S	106 49 E	7	NO_2, SO_2
Kaitorete Spit	NEW ZEALAND	NZL543S00	43 49 S	172 37 E	3	CH_4
Lauder	NEW ZEALAND	LAU545S00	45 1 S	169 40 E	370	O_3
Macquarie Island	AUSTRALIA	MQA554S00	54 28 S	158 58 E	12	CH_4, CO, CO_2, H_2, N_2O
Mauna Loa	UNITED STATES	MLO519N00	19 32 N	155 34 W	3397	CH_4, CO, CO_2, H_2, N_2O
Mauna Loa	UNITED STATES	MLO519N00	19 32 N	155 34 W	3397	$^{13}CH_4$, $^{13}CO_2$, $C_{18}O_2$, C_2Cl_4, CCl_4, CFCs, CH_2Cl_2, CH_3CCl_3, CH_4, CO, CO_2, H_2, HCFCs, HFCs, N_2O, O_3, SF_6
Sand Island	UNITED STATES	MID528N00	28 11 N	177 22 W	7.7	$^{13}CO_2$, $C_{18}O_2$, CH_4, CO, CO_2, H_2
Tanah Rata	MALAYSIA	TAR504N00	4 28 N	101 22 E	1545	O_3
Tutuila (Cape Matatula)	AMERICAN SAMOA	SMO514S00	14 14 S	170 34 W	42	$^{13}CH_4$, $^{13}CO_2$, $C_{18}O_2$, C_2Cl_4, CCl_4, CFCs, CH_2Cl_2, CH_3CCl_3, CH_4, CO, CO_2, H_2, HCFCs, HFCs, N_2O, O_3, SF_6
Tutuila (Cape Matatula)	AMERICAN SAMOA	SMO514S00	14 14 S	170 34 W	42	$CBrClF_2$, $CBrF_3$, CCl_4, CFCs, CH_2Cl_2, CH_3Br, CH_3CCl_3, CH_3Cl, CH_4, $CHCl_3$, HCFCs, HFCs, N_2O, SF_6
REGION VI (Europe)						
Adrigole	IRELAND	ADR652N00	51 40 N	9 43 W	50	CCl_4, CFCs, CH_3CCl_3, N_2O
Angra do Heroismo	PORTUGAL	ANG638N00	38 40 N	27 13 W	74	O_3
Baltic Sea	POLAND	BAL655N00	55 21 N	17 13 E	28	$^{13}CO_2$, $C_{18}O_2$, CH_4, CO, CO_2, H_2
Beja	PORTUGAL	BEJ638N00	38 1 N	7 52 W	246	O_3
Black Sea	ROMANIA	BSC644N00	44 10 N	28 40 E	3	$^{13}CO_2$, $C_{18}O_2$, CH_4, CO, CO_2, H_2
Braganca	PORTUGAL	BRG641N00	41 47 N	6 43 W	690	SO_2
Brotjacklriegel	GERMANY	BRT648N00	48 49 N	13 13 E	1016	VOCs
Brotjacklriegel	GERMANY	BRT648N00	48 49 N	13 13 E	1016	CO_2, O_3
Burgas	BULGARIA	BUR642N00	42 28 N	27 28 E	16	NO_2, SO_2
Campisabalos	SPAIN	CAM641N00	41 16 N	3 8 W	1360	VOCs
Castelo Branco	PORTUGAL	CAS639N00	39 49 N	7 28 W	386	O_3
Danki	RUSSIAN FEDERATION	DAK654N00	54 53 N	37 47 E	140	O_3
Deuselbach	GERMANY	DEU649N00	49 46 N	7 2 E	480	CH_4, CO_2, O_3
Donon	FRANCE	DNN649N00	48 30 N	7 7 E	775	VOCs
Doñana	SPAIN	DON637N00	37 2 N	6 32 W	5	NO_2, O_3, SO_2
Dwejra Point	MALTA	GOZ636N00	36 2 N	14 10 E	30	$^{13}CO_2$, $C_{18}O_2$, CH_4, CO, CO_2, H_2
Eskdalemuir	UNITED KINGDOM	EDM655N00	55 19 N	3 12 W	242	O_3
Fundata	ROMANIA	FDT645N00	45 28 N	25 18 E	1371	NO_2, SO_2
Fundata	ROMANIA	FDT645N01	45 28 N	25 18 E	1383.5	CO_2, NO_2, O_3

LIST OF OBSERVATION STATIONS (continued)

Station	Country/Territory	Index Number	Location Latitude (° ')	Location Longitude (° ')	Altitude (m)	Parameter
Giordan Lighthouse	MALTA	GLH636N00	36 4 N	14 13 E	167	CO, O_3
Hegyhatsal	HUNGARY	HUN646N00	46 57 N	16 38 E	248	CO_2
Hegyhatsal	HUNGARY	HUN646N01	46 57 N	16 38 E	248	$^{13}CO_2$, $C_{18}O_2$, CH_4, CO, CO_2, H_2
Heimaey	ICELAND	ICE663N00	63 23 N	20 16 W	100	$^{13}CO_2$, $C_{18}O_2$, CH_4, CO, CO_2, H_2, O_3
Hohe Warte	AUSTRIA	HHE648N00	48 15 N	16 22 E	202	NO, NO_2, SO_2
Hohe Warte	AUSTRIA	HHE648N00	48 15 N	16 22 E	202	NO, NO_2, SO_2
Hohenpeissenberg	GERMANY	HPB647N00	47 47 N	11 1 E	985	$_{222}$Rn, CO, H_2O_2, NO, NO_2, NOx, NOy, O_3, PAN, ROOH, SO_2, VOCs
Iskrba	SLOVENIA	IRB645N00	45 34 N	14 52 E	520	O_3, SO_2
Ivan Sedlo	BOSNIA AND HERZEGOVINA	IVN643N00	43 46 N	18 1 E	970	NO_2, SO_2
Jarczew	POLAND	JCZ651N00	51 49 N	21 58 E	180	NO_2, SO_2
Jungfraujoch	SWITZERLAND	JFJ646N00	46 32 N	7 58 E	3578	CO, NO, NO_2, NOx, O_3, SO_2
K-puszta	HUNGARY	KPS646N00	46 58 N	19 33 E	125	CO_2, NO_2, O_3, SO_2
Kamenicki Vis	SERBIA	KAM643N00	43 23 N	21 56 E	813	NO_2, SO_2
Kloosterburen	NETHERLANDS	KTB653N00	53 23 N	6 25 E	0	CO, NO, NO_2, NOx, SO_2
Kollumerwaard	NETHERLANDS	KMW653N00	53 19 N	6 16 E	0	CH_4, CO, CO_2, NO, NO_2, NOx, O_3, SO_2
Kosetice	CZECH REPUBLIC	KOS649N00	49 34 N	15 4 E	534	VOCs
Kosetice	CZECH REPUBLIC	KOS649N00	49 34 N	15 4 E	534	CH_4, CO, NO, NO_2, O_3, SO_2
Kovk	SLOVENIA	KVK646N00	46 7 N	15 5 E	600	O_3
Krvavec	SLOVENIA	KVV646N00	46 17 N	14 31 E	1720	CO, O_3
La Cartuja	SPAIN	CAR637N00	37 12 N	3 36 W	720	NO_2, SO_2
La Tardiere	FRANCE	LAT647N00	46 38 N	0 45 W	133	VOCs
Lampedusa	ITALY	LMP635N00	35 31 N	12 37 E	45	CFCs, CH_4, CO_2, HCFCs, HFCs, N_2O, SF_6
Lazaropole	MACEDONIA, THE FORMER YUGOSLAV REPUBLIC OF	LZP641N00	41 31 N	20 41 E	1320	NO_2, SO_2
Leba	POLAND	LEB654N00	54 45 N	17 31 E	2	NO_2, SO_2
Lisboa / Gago Coutinho	PORTUGAL	LIS638N00	38 46 N	9 7 W	105	O_3
Logroño	SPAIN	LOG642N00	42 27 N	2 30 W	370	NO_2, SO_2
Mace Head	IRELAND	MHD653N00	53 19 N	9 54 W	25	$^{13}CO_2$, $C_{18}O_2$, CCl_4, CFCs, CH_3CCl_3, CH_4, CO, CO_2, H_2, HCFCs, HFCs, N_2O, SF_6
Mace Head	IRELAND	MHD653N00	53 19 N	9 54 W	25	CCl_4, $CBrClF_2$, $CBrF_3$, CFCs, CH_2Cl_2, CH_3Br, CH_3CCl_3, CH_3Cl, CH_4, $CHCl_3$, CO, H_2, HCFCs, HFCs, N_2O, SF_6
Mace Head	IRELAND	MHD653N00	53 19 N	9 54 W	25	CO_2
Mace Head	IRELAND	MHD653N00	53 19 N	9 54 W	25	O_3
Mahón	SPAIN	MHN639N00	39 52 N	4 19 E	78	NO_2, O_3, SO_2
Monte Cimone	ITALY	CMN644N00	44 10 N	10 41 E	2165	CO_2
Monte Cimone	ITALY	CMN644N00	44 10 N	10 41 E	2165	O_3
Monte Velho	PORTUGAL	MVH638N00	38 4 N	8 48 W	43	O_3
Neuglobsow	GERMANY	NGL653N00	53 10 N	13 1 E	65	CH_4, CO, CO_2, O_3
Noia	SPAIN	NIA642N00	42 43 N	8 55 W	685	NO_2, O_3, SO_2
Ny-Alesund	NORWAY	ZEP678N01	78 54 N	11 52 E	475	$^{13}CO_2$, $C_{18}O_2$, CH_4, CO, CO_2, H_2
Ocean Station "C"	UNITED STATES	STC654N00	54 0 N	35 0 W	6	CO_2
Ocean Station "M"	NORWAY	STM666N00	66 0 N	2 0 E	5	$^{13}CO_2$, $C_{18}O_2$, CH_4, CO, CO_2, H_2
Ocean Station Charlie	RUSSIAN FEDERATION	STC652N00	52 45 N	35 30 W	5	CO_2

LIST OF OBSERVATION STATIONS (continued)

Station	Country/Territory	Index Number	Location Latitude (° ')	Location Longitude (° ')	Altitude (m)	Parameter
Oulanka	FINLAND	OUL666N00	66 19 N	29 23 E	310	NO_2, O_3, SO_2
Pallas-Sammaltunturi	FINLAND	PAL667N00	67 58 N	24 7 E	560	CO_2, O_3
Pallas-Sammaltunturi	FINLAND	PAL667N00	67 58 N	24 7 E	560	$^{13}CO_2$, $C_{18}O_2$, CH_4, CO, CO_2
Pallas-Sammaltunturi	FINLAND	PAL667N01	68 0 N	24 8 E	340	VOCs
Payerne	SWITZERLAND	PAY646N00	46 49 N	6 57 E	490	CO, NO, NO_2, NOx, O_3, SO_2
Penhas Douradas	PORTUGAL	PEN640N00	40 25 N	7 32 W	1380	O_3
Peyrusse Vieille	FRANCE	PVI644N00	43 37 N	0 10 E	200	VOCs
Plateau Rosa	ITALY	PRS645N00	45 55 N	7 42 E	3480	CH_4, CO_2, O_3
Pleven	BULGARIA	PLV643N00	43 25 N	24 36 E	64	NO_2, SO_2
Plovdiv	BULGARIA	PLD642N00	42 7 N	24 45 E	179	NO_2, SO_2
Puszcza Borecka/Diabla Gora	POLAND	DIG654N00	54 8 N	22 4 E	157	CO_2, NO_2, O_3, SO_2
Rigi	SWITZERLAND	RIG647N00	46 4 N	8 26 E	1031	CO, NO, NO_2, NOx, O_3, SO_2, VOCs
Roquetes	SPAIN	ROQ640N00	40 49 N	0 28 E	50	NO_2, O_3, SO_2
Rucava	LATVIA	RCV656N00	56 10 N	21 10 E	18	NO_2, O_3, SO_2
San Pablo de los Montes	SPAIN	SPM639N00	39 32 N	4 20 W	917	NO_2, O_3, SO_2
Schauinsland	GERMANY	SSL647N00	47 55 N	7 55 E	1205	CH_4, CO, CO_2, N_2O, NO, NO_2, O_3, SF_6
Schmuecke	GERMANY	SCH651N00	50 38 N	10 46 E	937	VOCs
Sede Boker	ISRAEL	WIS631N00	31 7 N	34 52 E	400	$^{13}CO_2$, $C_{18}O_2$, CH_4, CO, CO_2, H_2
Semenic	ROMANIA	SEM645N00	45 7 N	21 58 E	1432	NO_2, SO_2
Shepelevo	RUSSIAN FEDERATION	SHP659N00	59 58 N	29 7 E	4	O_3
Shetland	UNITED KINGDOM	SIS660N00	60 4 N	1 15 W	30	CH_4, CO, CO_2, H_2, N_2O
Site J	DENMARK	GRL666N00	66 30 N	46 12 W	2030	CH_4
Sniezka	POLAND	SNZ650N00	50 43 N	15 43 E	1603	NO_2, SO_2
Sofia	BULGARIA	SOF642N00	42 38 N	23 22 E	586	NO_2, SO_2
Sonnblick	AUSTRIA	SNB647N00	47 2 N	12 56 E	3106	CO, CO_2, NO, NOy, O_3
Starina	SLOVAKIA	STA649N00	49 2 N	22 16 E	345	VOCs
Stephansplatz	AUSTRIA	STP648N00	48 13 N	16 22 E	171	NO, NO_2, SO_2
Stephansplatz	AUSTRIA	STP648N00	48 13 N	16 22 E	171	NO, NO_2, SO_2
Stîna de Vale	ROMANIA	STN646N00	46 40 N	22 37 E	1116	NO_2, SO_2
Summit	GREENLAND	SUM672N00	72 34 N	38 28 W	3238	$^{13}CO_2$, $C_{18}O_2$, CCl_4, CFCs, CH_3CCl_3, CH_4, CO_2, HCFCs, HFCs, O_3
Suwalki	POLAND	SWL654N00	54 7 N	22 56 E	184	NO_2, SO_2
Terceira Island	PORTUGAL	AZR638N00	38 46 N	27 22 W	40	$^{13}CO_2$, $C_{18}O_2$, CH_4, CO, CO_2, H_2
Teriberka	RUSSIAN FEDERATION	TER669N00	69 12 N	35 6 E	40	CH_4, CO_2
Utö	FINLAND	UTO659N00	59 46 N	21 22 E	7	VOCs
Utö	FINLAND	UTO659N00	59 46 N	21 22 E	7	NO_2, O_3, SO_2
Varna	BULGARIA	VRN643N00	43 12 N	27 55 E	41	NO_2, SO_2
Viana do Castelo	PORTUGAL	VDC641N00	41 42 N	8 48 W	16	SO_2
Vindeln	SWEDEN	VDL664N00	64 15 N	19 46 E	271	O_3
Virolahti	FINLAND	VIR660N00	60 31 N	27 40 E	4	NO_2, O_3, SO_2
Waldhof	GERMANY	LGB652N00	52 47 N	10 46 E	74	VOCs
Waldhof	GERMANY	LGB652N00	52 47 N	10 46 E	74	CO_2, O_3
Wank Peak	GERMANY	WNK647N00	47 31 N	11 9 E	1780	CO_2, NOx, SO_2
Westerland	GERMANY	WES654N00	54 55 N	8 19 E	12	CO_2, O_3
Zabljak	MONTENEGRO	ZBL643N00	43 8 N	19 7 E	1450	NO_2, SO_2
Zavodnje	SLOVENIA	ZRN646N00	46 25 N	15 0 E	770	O_3
Zeppelinfjellet	NORWAY	ZEP678N00	78 54 N	11 52 E	475	CCl_4, CFCs, CH_3CCl_3, N_2O, O_3, SO_2

LIST OF OBSERVATION STATIONS (continued)

Station	Country/Territory	Index Number	Location Latitude (° ')	Location Longitude (° ')	Altitude (m)	Parameter
Zeppelinfjellet	NORWAY	ZEP678N00	78 54 N	11 52 E	475	CO_2
Zingst	GERMANY	ZGT654N00	54 25 N	12 43 E	1	CH_4, CO_2, O_3
Zingst	GERMANY	ZGT654N00	54 25 N	12 43 E	1	VOCs
Zoseni	LATVIA	ZSN657N00	57 7 N	25 55 E	183	NO_2, SO_2
Zugspitze	GERMANY	ZUG647N00	47 25 N	10 58 E	2960	CO_2
Zugspitze	GERMANY	ZUG647N00	47 25 N	10 58 E	2960	CH_4, CO, CO_2, NO, NOx, NOy, O_3
Zugspitze / Schneefernerhaus	GERMANY	ZSF647N00	47 25 N	10 58 E	2656	SO_2
Zugspitze / Schneefernerhaus	GERMANY	ZSF647N00	47 25 N	10 58 E	2656	CH_4, CO, CO_2, N_2O, NO, NO_2, NOy, O_3, SF_6
Ähtäri	FINLAND	AHT662N00	62 34 N	24 11 E	180	NO_2, O_3, SO_2
ANTARCTICA						
Arrival Heights	ANTARCTICA	ARH778S00	77 47 S	166 40 E	184	$^{13}CH_4$, CH_4, CO, N_2O
Casey Station	ANTARCTICA	CYA766S00	66 16 S	110 31 E		CH_4, CO, CO_2, H_2, N_2O
Halley Bay	ANTARCTICA	HBA775S00	75 34 S	26 30 W	33	$^{13}CO_2$, $C_{18}O_2$, CH_4, CO, CO_2, H_2
Jubany	ANTARCTICA	JBN762S00	62 13 S	58 40 W	15	CO_2
Mawson	ANTARCTICA	MAA767S00	67 37 S	62 52 E	32	CH_4, CO, CO_2, H_2, N_2O
McMurdo / Arrival Heights	ANTARCTICA	MCM777S01	77 47 S	166 46 E	50	O_3
McMurdo Station	ANTARCTICA	MCM777S00	77 49 S	166 34 E	11	CH_4
Mizuho	ANTARCTICA	MZH770S00	70 42 S	44 17 E	2230	CH_4
Neumayer	ANTARCTICA	NMY770S00	70 39 S	8 15 W	42	O_3
Palmer Station	ANTARCTICA	PSA764S00	64 55 S	64 0 W	10	$^{13}CO_2$, $C_{18}O_2$, CCl_4, CFCs, CH_3CCl_3, CH_4, CO, CO_2, H_2, HCFCs, HFCs, N_2O, SF_6
South Pole	ANTARCTICA	SPO789S00	89 58 S	24 48 W	2810	CH_4, CO, CO_2, H_2, N_2O
South Pole	ANTARCTICA	SPO789S00	89 58 S	24 48 W	2810	$^{13}CH_4$, $^{13}CO_2$, $C_{18}O_2$, C_2Cl_4, CCl_4, CFCs, CH_2Cl_2, CH_3CCl_3, CH_4, CO, CO_2, H_2, HCFCs, HFCs, N_2O, O_3, SF_6
Syowa Station	ANTARCTICA	SYO769S00	69 0 S	39 34 E	21	$^{13}CO_2$, $C_{18}O_2$, CH_4, CO, CO_2, H_2
Syowa Station	ANTARCTICA	SYO769S00	69 0 S	39 34 E	21	CO_2
Syowa Station	ANTARCTICA	SYO769S00	69 0 S	39 34 E	21	O_3
MOBILE STATION						
Aircraft (over Bass Strait and Cape Grim)	AUSTRALIA	AIA999900				CH_4, CO, CO_2, H_2, N_2O
Akademik Korolev, R/V	UNITED STATES	AKD999900				CH_4
Alligator liberty, M/V	JAPAN	ALG999900				CO_2
Atlantic Ocean	UNITED STATES	AOC9XXX00			10	CH_4, CO_2
BACPAC 99	UNITED STATES	BAC999900				CCl_4, CFCs, CH_3Br, CH_3CCl_3, CH_3Cl, HCFCs
BLAST1	UNITED STATES	BLA999900				CCl_4, CFCs, CH_3Br, CH_3CCl_3, CH_3Cl, HCFCs
BLAST2	UNITED STATES	BLA999901				CCl_4, CFCs, CH_3Br, CH_3CCl_3, CH_3Cl, HCFCs
BLAST3	UNITED STATES	BLA999902				CCl_4, CFCs, CH_3Br, CH_3CCl_3, CH_3Cl, HCFCs
CLIVAR 01	UNITED STATES	CLI999900				CCl_4, CFCs, CH_3Br, CH_3CCl_3, CH_3Cl, HCFCs

LIST OF OBSERVATION STATIONS (continued)

Station	Country/Territory	Index Number	Location Latitude (° ')	Location Longitude (° ')	Altitude (m)	Parameter
Discoverer 1983 & 1984, R/V	UNITED STATES	DIS999900				CH_4
Discoverer 1985, R/V	UNITED STATES	DSC999900				CH_4
Environmental observation and monitoring project	JAPAN	EOM999900				CH_4, CO_2
Gas Change Experiment	UNITED STATES	GAS999900				CCl_4, CFCs, CH_3Br, CH_3CCl_3, CH_3Cl, HCFCs
HATS Ocean Projects	UNITED STATES	HOP999900				HFCs
INSTAC-I (International Strato/Tropospheric Air Chemistry Project)	JAPAN	INS999900				$^{13}CO_2$, CH_4, CO_2
John Biscoe, R/V	UNITED STATES	JBS999900				CH_4
Keifu Maru, R/V	JAPAN	KEF999900				CO_2
Kofu Maru, R/V	JAPAN	KOF999900				CO_2
Korolev, R/V	UNITED STATES	KOR999900				CH_4
Long Lines Expedition, R/V	UNITED STATES	LLE999900				CH_4
MRI Research, 1978-1986, R/V	JAPAN	MRI999900				CH_4
MRI Research, Hakuho Maru, R/V	JAPAN	HKH999900				CO_2
MRI Research, Kaiyo Maru, R/V	JAPAN	KIY999900				CO_2
MRI Research, Mirai, R/V	JAPAN	MMR999900				CO_2
MRI Research, Natushima, R/V	JAPAN	NTU999900				CO_2
MRI Research, Ryofu Maru, R/V	JAPAN	RFM999900				CO_2
MRI Research, Wellington Maru, R/V	JAPAN	WLT999900				CO_2
Mexico Naval H-02, R/V	UNITED STATES	MXN999900				CH_4
NOPACCS - Hakurei Maru -	JAPAN	HAK999900				TIC
Oceanographer, R/V	UNITED STATES	OCE999900				CH_4
PHASE I-04	UNITED STATES	PHA999900				CCl_4, CFCs, CH_3Br, CH_3CCl_3, CH_3Cl, HCFCs
Pacific Ocean	UNITED STATES	POC9XXX00			10	$^{13}CO_2$, $C_{18}O_2$, CH_4, CO, CO_2, H_2
Polar Star, R/V	UNITED STATES	PLS999900				CH_4
Ryofu Maru, R/V	JAPAN	RYF999900				CFCs, CH_4, CO_2, N_2O, TIC
South China Sea	UNITED STATES	SCS9XXX00			15	$^{13}CO_2$, $C_{18}O_2$, CH_4, CO, CO_2, H_2
Soyo Maru, R/V	JAPAN	SOY999900				CO_2
Surveyor, R/V	UNITED STATES	SUR999900				CH_4
The Observation of Atmospheric Methane Over Japan	JAPAN	OAM999900				CH_4
The Observation of Atmospheric Sulfur Hexafluoride Over Japan	JAPAN	OAS999900				SF_6
WEST COSMIC - Hakurei Maru No.2 -	JAPAN	HAK999901				TIC
Western Pacific	UNITED STATES	WPC9XXX00			10	CH_4, CO_2

LIST OF CONTRIBUTORS

Station Country/Territory	Name	Address
REGION I (Africa)		
Izaña (Spain)	Angel J. Gomez-Pelaez Carlos Marrero	Observatorio Atmosferico de Izana,Instituto Nacional de Meteorologia (Spain) C/ La Marina, 20, Planta 6. Apartado 880. 38071 Santa Cruz de Tenerife
Cape Point (South Africa)	Ernst-Günther Brunke	South African Weather Service (Climate Division) SAWS, c/o CSIR (Environmentek), P.O. Box 320,Stellenbosch 7599
Mt. Kenya (Kenya)	Josiah Kariuki Murageh Jörg Klausen Stephan Henne	KMD, Kenyan Meteorological Department Kenya Meteorological Department Dagoretti Corner P.O. Box 30259 00100 Nairobi
Funchal (Portugal)	Maria Amelia V.Lopes Clotilde P.N.Goncalves	Instituto de Meteorologia Rua C-Aeroporto de Lisboa1749-077 Lisboa Portugal
Amsterdam Island (France)	Michel Ramonet	LSCE (Laboratoire des Sciences du Climat et de l'Environnement) UMR CEA-CNRS LSCE - CEA Saclay - Orme des Merisiers - Bat.709 91191 Gif-sur-Yvette, France
Assekrem (Algeria)	Mimouni Mohamed	Office National de la Meteorologie POBox 31 Tamanrasset 11000, Algeria
REGION II (Asia)		
Nagoya (Japan)	A. Matsunami	Research Center for Advanced Energy Conversion, Nagoya University Furo-cho, Chikusaku, Nagoya 464-8603
Cape Ochi-ishi Hateruma (Japan)	Hitoshi MUKAI	Center for Global Environmental Research, National Institute for Environmental Studies 16-2, Onogawa, Tsukuba-shi, Ibaraki 305-8506, Japan
Gosan (Korea, Republic Of)	Jaebum Lee Okjung Ju Sang-Kyun Kim	Researcher of Global Environment Research Center Environmental Research Complex, Gyeongseo-dong, Seo-gu, Incheon, 404-708
Anmyeon-do (Korea, Republic Of)	Jeong-Sik Kim Byoung-Cheol Kim	National Institute of Meteorological Researc, Korea Global Atmosphere Watch Center, Korea Meteorology Administration 1764-6, Seungen-Ri, Anmyeon-Eup, Taean-Kun, ChungNam, 357-961, Republic of Korea
Hok Tsui (Hong Kong)	Ka Se Lam	Department of Civil and Structural Engineering,Hong Kong Polytechnic University Hung Hom, Kowloon, Hong Kong

LIST OF CONTRIBUTORS (continued)

Station Country/Territory	Name	Address
Minamitorishima Ryori Yonagunijima (Japan)	Kazuhiro TSUBOI	Atmospheric Environment Division, Global Environment and Marine Department,Japan Meteorological Agency (JMA) 1-3-4 Otemachi, Chiyoda-ku, Tokyo 100-8122, Japan
Mikawa-Ichinomiya (Japan)	Koji Ohno	Aichi Air Environment Division 1-2 Sannomaru-3chome, Naka-ku, Nagoya, Aichi 460-8501, Japan
Memanbetsu Tsukuba (Japan)	Michio Hirota	Kobe Marine Observatory 1-4-3 Wakinohamakaigandori, Chuo-ku, Kobe 651-0073 Japan
Hamamatsu (Japan)	Mitsuo TODA	Shizuoka University 3-5-1 Jyohoku, Hamamatsu 432-8561, Japan
Bering Island Kotelny Island (Russian Federation) Kyzylcha (Uzbekistan)	Nina Paramonova	Main Geophysical Observatory (MGO) Karbyshev Street 7, St. Petersburg, 194021, Russian Federation
Takayama (Japan)	Shohei Murayama	Research Institute for Environmental Management Technology, National Institute of Advanced Industrial Science and Technology (AIST) AIST Tsukuba West, 16-1 Onogawa, Tsukuba, Ibaraki 305-8569, Japan
Gosan (Korea, Republic Of)	So-young Bang	Applied Meteorology Research Laboratory,Meteorological Research Institute (METRI),Korea Meteorological Administration (KMA) 460-18, Shindaebang-dong, Dongjak-gu, Seoul 156-720, Rep. of Korea
Ship between Ishigaki Island and Hateruma Island (Japan)	Takakiyo Nakazawa Shuji Aoki	Center for Atmospheric and Oceanic Studies, Graduate School of Science, Tohoku University Aoba, Sendai 980-8578, Japan
Mt. Waliguan (China)	Tang Jie	Chinese Academy of Meteorological Sciences 46 Zhongguancun Nandajie, Haidian, Beijing 100081, P.R. of China
Suita (Japan)	Tomohiro Oda	Division of Sustainable Energy and Environmental Engineering, Graduate School of Engineering, Osaka Universiy, Japan Green Engieering Lab Division of Sustainable Energy and Environmental Engineering 2-1 Yamadaoka, Suita, Osaka 565-0871 Japan

LIST OF CONTRIBUTORS (continued)

Station Country/Territory	Name	Address
Tsukuba (Japan)	Tosiro Kimura	Lower Aerological Observations Division, Aerological Observatory, Japan Meteorological Agency (JMA) Lower Aerological Observations Division, Aerological Observatory1-2 Nagamine, Tsukuba, Ibaraki, 305-0052, Japan
Issyk-Kul (Kyrgyzstan)	V. Sinyakov	Laboratory of Geophysics, Institute of Fundamental sciences at the Kyrgyz National University Manas Street 101, Bishkek, 720033, Kyrgyz Republic
Mt. Dodaira Kisai Urawa (Japan)	Yosuke MUTO	Center for Environmental Science in Saitama 914 Kamitanadare, Kisai-machi, Kita-Saitama-gun, Saitama 347-0115, Japan
Tsukuba (Japan)	Yousuke Sawa	Geochemical Research Department, Meteorological Research Institute 1-1, Nagamine, Tsukuba, Ibaraki 305-0052, Japan
REGION III (South America)		
Arembepe (Brazil)	Joelmo Oliveira	
Huancayo (Peru)	Mutsumi Ishitsuka	Observatorio de Huancayo, Instituto Geofisico del Peru Apartado 46, Huancayo, Peru
Ushuaia (Argentina)	Sergio Luppo	Servicio Meteorol'ogico Nacional - Gobierno de Tierra del Fuego Estaci'on VAG Ushuaia Direcci'on de Ciencia y Tecnologia, Gobierno de Tierra del Fuego Fagnano 486, Planta Alta 9410 Ushuaia, Tierra del Fuego, Argentina
REGION IV (North and Central America)		
Alert Candle Lake Cape St. James Estevan Point Frasedale Sable Island (Canada)	Doug Worthy	Environment Canada (EC) 4905 Dufferin Street, Toronto, Ontario, Canada, M3H 5T4

LIST OF CONTRIBUTORS (continued)

Station Country/Territory	Name	Address
Algoma Bratt's Lake Chalk River Chapais Egbert Experimental Lakes Area Esther Kejimkujik Longwoods Saturna Sutton (Canada)	Mike Shaw	Environment CanadaMeteorological Service of CanadaAir Quality Research Branch 4905 Dufferin StreetToronto, Ontario CANADA M3H 5T4
La Palma (Cuba)	Osvaldo Cuesta Santos	Institute of Meteorology, Atmospheric Environment Research Center Aptdo. 17032, Postal Code 11700, Havana 17, Cuba
REGION V (South-West Pacific)		
Baring Head (New Zealand)	Antony Gomez Sylvia Nichol Gordon Brailsford	National Institute of Water & Atmospheric Research Ltd. 301 Evans Bay Parade, Greta PointPrivate Bag 14-901, Kilbirnie, Wellington
Cape Grim (Australia)	Bruce Forgan Ian Galbally	Commonwealth Bureau of Meteorology 700 Collins St, Docklands GPO Box 1289K, Melbourne, Victoria 3001
Bukit Koto Tabang (Indonesia)	Hery Harjanto Nurhayati	Global GAW Bukit Kototabang Palupuh, District Agam, West Sumatera, IndonesiaPO BOX 11 Bukittinggi 26100
Danum Valley GAW Baseline Station Tanah Rata (Malaysia)	Lim Sze Fook	Environmental Studies DivisionMalaysian Meteorological Department Jalan Sultan46667 Petaling Jaya, Selangor, Malaysia
Jakarta (Indonesia)	Nurhayati	Bureau of Meteorology and Geophysics Jalan Angkasa 1 No.2 Jakarta 10720, Indonesia
REGION VI (Europe)		
Plateau Rosa (Italy)	Andrea Lanza Daniela Heltai Domenico Cipriano	CESI RICERCA via Rubattino 54, 20134 Milan
Puszcza Borecka/Diabla Gora (Poland)	Anna Degorska	Institute of Environmental Protection Kolektorska 4 01-692 Warsaw

LIST OF CONTRIBUTORS (continued)

Station Country/Territory	Name	Address
Kollumerwaard Kloosterburen (Netherlands)	Arien Stolk	RIVM - Laboratory for Environmental Measurements (LVM) P.O. Box 1, 3720 BA Bilthoven
Hohe Warte Stephansplatz (Austria)	August Kaiser	Department for Environmental MeteorologyCentral Institute for Meteorology and Geodynamics Postfach 342, Hohe Warte 38, A-1191 Wien
Iskrba Kovk Krvavec Zavodnje (Slovenia)	Brigita Jesenovec	Ministry of Environment and Spatial Planning - Environmental Agency of the Republic of Slovenia (EARS) Vojkova 1/b, Sl-1000 Ljubljana
Jungfraujoch (Switzerland)	Brigitte Buchmann	Swiss Federal Laboratories for Materials Testing and Research (Empa)Air Pollution / Environmental Technology Uberlandstrasse 129CH-8600 Dubendorf
Payerne Rigi (Switzerland)	Brigitte Buchmann Thomas Seitz	Swiss Federal Laboratories for Materials Testing and Research (Empa)Air Pollution / Environmental Technology Uberlandstrasse 129CH-8600 Dubendorf
Fundata Semenic Stîna de Vale (Romania)	Daniela ZISU	National Research and Development Institute for Environmental Protection Splaiul Independentei nr. 294, sector 6, 77703 Bucuresti
Kamenicki Vis (Serbia)	Dragan Djordjevic	Republic Hydrometeorological Service of Serbia P.O. Box 37, Kneza Viseslava 6611030 Belgrade
Burgas Plovdiv Pleven Sofia Varna (Bulgaria)	Ekaterina Batchvarova	National Institute of Meteorology and Hydrology 66 Tzarigradsko chaussee, 1784 Sofia
Jarczew Leba Sniezka Suwalki (Poland)	Eugeniusz Brejnak	Institute of Meteorology and Water Management;Laboratory for Research and Monitoring of Air Pollution 61 Podlesna Street, 01-673 Warszawa
Fundata (Romania)	Florin Nicodim	National Meteorological Administration Sos. Bucuresti-Ploiesti nr. 97, 71552 Bucharest

LIST OF CONTRIBUTORS (continued)

Station Country/Territory	Name	Address
Lampedusa (Italy)	Florinda Artuso Salvatore Piacentino Alcide di Sarra	Italian National Agency for New Technology, Energy and the Environment (ENEA) ENEA CLIM-OSS, Via Anguillarese 301, 00060 S.Maria di Galeria, Rome, Italy.ENEA-Station for Climate Observations, Capo Grecale, 92010 Lampedusa (AG), Italy
Site J (Denmark)	Gen Hashida Shinji Morimoto Shuji Aoki	National Institute of Polar Research Kaga 1-9-10, Itabashi-ku, Tokyo 173-8515
Mace Head (Ireland)	Gerard Spain	National University of Ireland, Galway (NUI) Mace Head Research StationCarna, Co. Galway
Hohe Warte Stephansplatz (Austria)	Guenther Schermann	Municipal Department 22 - Environmental ProtectionAir quality subdepartment, City of Vienna Ebendorferstrasse 4, A-1082 Vienna, Austria
Vindeln (Sweden)	Hakan Blomgren	IVL Swedish Environmental Research Institute P.O.Box 5302S-400 14 Goteborg, Sweden
Wank Peak Zugspitze (Germany)	Hans-Eckhart Scheel	Fraunhofer-Institute for Atmospheric Environmental Research, since 1.1.2002:Forschungszentrum Karlsruhe, IMK-IFU D-82467 Garmisch-Partenkirchen, Germany
Rucava Zoseni (Latvia)	Iraida Lyulko	Observation Network Department, Latvian Environment, Geology and Meteorology Agency, Ministry of Environmental 165 Maskavas str. LV-1019, Riga, Latvia
Danki Shepelevo (Russian Federation)	Irina Brouskina	
La Cartuja Doñana Logroño Mah'on Noia Roquetes San Pablo de los Montes (Spain)	J.M. Saenz	Servicio de Desarrollos Medioambientales, Instituto Nacional de Meteorologia,Ministerio de Medio Ambiente Leonardo Prieto Castro, 8, 28071 Madrid, Spain
Zeppelinfjellet (Norway)	Johan Strom	Department of Applied Environmental Science (ITM), Stockholm University SE-106 91 Stockholm, Sweden
Pallas-Sammaltunturi (Finland)	Juha Hatakka Timo Salmi	Finnish Meteorological Institute P.O.Box 503,FI-00101 Helsinki, Finland

LIST OF CONTRIBUTORS (continued)

Station Country/Territory	Name	Address
Brotjacklriegel Deuselbach Waldhof Neuglobsow Schauinsland Westerland Zingst Zugspitze / Schneefernerhaus Zugspitze (Germany)	Karin Uhse	Umweltbundesamt (UBA, Federal Environmental Agency) Air Monitoring Network Paul-Ehrlich-Strasse 29 D-63225 Langen, Germany
Hegyhatsal K-puszta (Hungary)	Laszlo Haszpra	Hungarian Meteorological Service P.O. Box 39H-1675 Budapest, Hungary
Braganca Viana do Castelo (Portugal)	Maria Amelia V.Lopes	Instituto de Meteorologia Rua C-Aeroporto de Lisboa1749-077 Lisboa Portugal
Angra do Heroismo Beja Castelo Branco Lisboa / Gago Coutinho Monte Velho Penhas Douradas (Portugal)	Maria Amelia V.Lopes Clotilde P.N.Goncalves	Instituto de Meteorologia Rua C-Aeroporto de Lisboa1749-077 Lisboa Portugal
Sonnblick (Austria)	Marina Fröhlich Wolfgang Spangl Elisabeth Friedbacher	Federal Environment Agency Austria Spittelauer Lände 5, A-1090 Wien, Austria
Ivan Sedlo (Bosnia and Herzegovina)	Martin Tais	Meteoroloski zavod Bosne i Hercegovine Bardakcije 12, 71000 Sarajevo, Bosnia and Herzegovina
Mace Head (Ireland)	Michel Ramonet	LSCE (Laboratoire des Sciences du Climat et de l'Environnement) UMR CEA-CNRS LSCE - CEA Saclay - Orme des Merisiers - Bat.709 91191 Gif-sur-Yvette, France
Kosetice (Czech Republic)	Milan Vana	Czech Hydrometeorological Institute, Kosetice Observatory Na Sabatce 17, 143 06 Praha 4 - Komorany, Czech Republic
Ocean Station Charlie Teriberka (Russian Federation)	Nina Paramonova	Main Geophysical Observatory (MGO) Karbyshev Street 7, St. Petersburg, 194021, Russian Federation
Zeppelinfjellet (Norway)	Ove Hermansen	Norwegian Institute for Air Research (NILU) P. O. Box 100 Instituttveien 18, N-2027 Kjeller, Norway

LIST OF CONTRIBUTORS (continued)

Station Country/Territory	Name	Address
Monte Cimone (Italy)	Paolo Bonasoni	National Research Council, Institute of Atmospheric Sciences and Climate (CNR-ISAC) Via Gobetti 10140129 Bologna, Italy
Eskdalemuir (United Kingdom)	Peter Kuria	Air and Environment Quality Division, DEFRA 4/F15, Ashdown House123 Victoria StreetLondon, SW1E 3DE, United Kingdom
Giordan Lighthouse (Malta)	Raymond Ellul	Atmospheric Research Unit / Physics Department /University of Malta Msida MSD 06, Malta
Monte Cimone (Italy)	Riccardo Santaguida	Italian Air Force Meteorological Service C.A.M.M. Mt. CIMONE,Via delle Ville 40, 41029-Sestola (MO), Italy
Hohenpeissenberg Zugspitze / Schneefernerhaus (Germany)	Stefan Gilge Christian Plass-Duelmer	Deutscher Wetterdienst (DWD, German Meteorological Service)Meteorologisches Observatorium Hohenpeissenberg Albin-Schwaiger-Weg 10D-82383 Hohenpeissenberg, Germany
Lazaropole (Macedonia, The Former Yugoslav Republic Of)	Suzana Alcinova Monevska	Hydrometeorological Service Skupi bb, 1000 Skopie,The former Yugoslav Republic of Macedonia
Kosetice (Czech Republic)	Sverre Solberg	Norwegian Institute for Air Research P.O.Box 100NO-2027 Kjeller
Pallas-Sammaltunturi Utö (Finland)		
Donon La Tardiere Peyrusse Vieille (France)		
Brotjacklriegel Waldhof Schmuecke Zingst (Germany)		
Starina (Slovakia)		
Campisabalos (Spain)		

LIST OF CONTRIBUTORS (continued)

Station Country/Territory	Name	Address
Ähtäri Oulanka Utö Virolahti (Finland)	Timo Salmi	Finnish Meteorological Institute Erik Palmenin aukio 1, P.O.Box 503, FIN-00101 Helsinki, Finland
ANTARCTICA		
Arrival Heights (New Zealand)	Antony Gomez Sylvia Nichol Gordon Brailsford	National Institute of Water & Atmospheric Research Ltd. 301 Evans Bay Parade, Greta PointPrivate Bag 14-901, Kilbirnie, Wellington
Jubany (Italy)	Luigi Ciattaglia	ICES (Int.l Center for Earth Sciences) c/o CNR-Istituto di Acustica- Area della Ricerca di Roma Tor Vergata,via Fosso del Cavaliere, 10000133 Rome, Italy
Neumayer (Germany)	Rolf Weller	Alfred Wegener Institute Am Handelshafen 12,27570 Bremerhaven, Germany
Mizuho (Japan)	Takakiyo Nakazawa	Center for Atmospheric and Oceanic Studies, Graduate School of Science, Tohoku University Aoba, Sendai 980-8578, Japan
Syowa Station (Japan)	Takakiyo Nakazawa Gen Hashida Shinji Morimoto	Center for Atmospheric and Oceanic Studies, Graduate School of Science, Tohoku University Aoba, Sendai 980-8578, Japan
Syowa Station (Japan)	Yasuo Shudou	Office of Antarctic Observations,Japan Meteorological Agency (JMA) 1-3-4 Otemachi, Chiyoda-ku, Tokyo 100-8122, Japan
MOBILE STATION		
NOPACCS - Hakurei Maru - WEST COSMIC - Hakurei Maru No.2 - (Japan)	General Environmental Texhnos	The General Environmental Technos Co., Ltd. (Old:Kansai Environmental Engineering Center, Co., Ltd.) 1-3-5, Azuchi machi, Chuo-ku, Osaka 541-0052
Environmental observation and monitoring project INSTAC-I (International Strato/Tropospheric Air Chemistry Project) (Japan)	Hidekazu Matsueda	Geochemical Research Department, Meteorological Research Institute Nagamine 1-1, Tsukuba, Ibaraki 305-0052, Japan

LIST OF CONTRIBUTORS (continued)

Station Country/Territory	Name	Address
MRI Research, Mirai, R/V (Japan)	Hisayuki Yoshikawa-Inoue	Laboratory of Marine and Atmospheric GeochemistryGraduate School of Environmental Earth ScienceHokkaido University N10W5, Kita-ku, Sapporo 060-0810, Japan
MRI Research, Hakuho Maru, R/V MRI Research, Kaiyo Maru, R/V MRI Research, 1978-1986, R/V MRI Research, Natushima, R/V MRI Research, Ryofu Maru, R/V MRI Research, Wellington Maru, R/V (Japan)	Masao Ishii	Geochemical Research Department, Meteorological Research Institute Nagamine 1-1, Tsukuba, Ibaraki 305-0052, Japan
The Observation of Atmospheric Methane Over Japan The Observation of Atmospheric Sulfur Hexafluoride Over Japan (Japan)	Michio Hirota	Kobe Marine Observatory 1-4-3 Wakinohamakaigandori, Chuo-ku, Kobe 651-0073 Japan
Alligator liberty, M/V Keifu Maru, R/V Kofu Maru, R/V Ryofu Maru, R/V (Japan)	Takashi Miyao	Pollutants Chemical Analysis Center, Marine Division, Climate and Marine Department, Japan Meteorological Agency (JMA) 1-3-4 Otemachi, Chiyoda-ku, Tokyo 100-8122, Japan
Soyo Maru, R/V (Japan)	Tsuneo Ono	Hokkaido National Fisheries Research Institute 116 Katsurakoi, Kushiro 085-0802, Japan

LIST OF CONTRIBUTORS (continued)

Station Country/Territory	Name	Address
NOAA/CMDL Flask Network		
Assekrem (Algeria)	Bruce Vaughn** James White** ($^{13}CH_4$, $^{13}CO_2$ and $C_{18}O_2$)	(*)NOAA/ESRL Global Monitoring Division 325 Broadway R/GMD1 Boulder, CO 80305-3328, U.S.A
Tutuila (Cape Matatula) (American Samoa)	Edward J. Dlugokencky* (CH_4)	(**)Institute of Arctic and Alpine Research (INSTAAR) Campus box 450, University of Colorado, Boulder, CO 80309-0450, U.S.A.
Halley Bay McMurdo Station McMurdo / Arrival Heights Palmer Station South Pole Syowa Station (Antarctica)	Paul C. Novelli* (CO and H_2) Thomas J. Conway* (CO_2)	
Tierra del Fuego (Argentina)		
Cape Grim (Australia)		
Ragged Point (Barbados)		
Alert Mould Bay (Canada)		
Easter Island (Chile)		
Mt. Waliguan (China)		
Pallas-Sammaltunturi (Finland)		
Amsterdam Island Crozet (France)		
Summit (Greenland)		
Hegyhatsal (Hungary)		
Heimaey (Iceland)		
Bukit Koto Tabang (Indonesia)		

LIST OF CONTRIBUTORS (continued)

Station Country/Territory	Name	Address
Mace Head (Ireland)		
Sede Boker (Israel)		
Sary Taukum Plateau Assy (Kazakhstan)		
Mt. Kenya (Kenya)		
Christmas Island (Kiribati)		
Tae-ahn Peninsula (Korea, Republic Of)		
Kaashidhoo (Maldives)		
Dwejra Point (Malta)		
Ulaan Uul (Mongolia)		
Gobabeb (Namibia)		
Lauder Kaitorete Spit (New Zealand)		
Ocean Station "M" Ny-Alesund (Norway)		
Baltic Sea (Poland)		
Terceira Island (Portugal)		
Black Sea (Romania)		
Mahe Island (Seychelles)		

LIST OF CONTRIBUTORS (continued)

Station Country/Territory	Name	Address
Tenerife (Spain)		
Ascension Island St. David's Head Tudor Hill Bird Island (United Kingdom)		
Akademik Korolev, R/V Atlantic Ocean St. Croix Barrow Cold Bay Cape Meares Discoverer 1983 & 1984, R/V Drake Passage Discoverer 1985, R/V Guam Grifton John Biscoe, R/V Key Biscayne Korolev, R/V Kitt Peak Cape Kumukahi Park Falls Long Lines Expedition, R/V Sand Island Mauna Loa Mexico Naval H-02, R/V Niwot Ridge Niwot Ridge Niwot Ridge (Saddle) Oceanographer, R/V Olympic Peninsula Pacific-Atlantic Ocean Polar Star, R/V Pacific Ocean Point Arena South China Sea Southern Great Plains Shemya Island La Jolla Ocean Station "C" Surveyor, R/V Trinidad Head Wendover Moody Western Pacific (United States)		

LIST OF CONTRIBUTORS (continued)

Station Country/Territory	Name	Address
NOAA/CMDL/HATS Network		
Tutuila (Cape Matatula) (American Samoa) Palmer Station South Pole (Antarctica) Tierra del Fuego (Argentina) Cape Grim (Australia) Alert (Canada) Summit (Greenland) Mace Head (Ireland) BACPAC 99 BLAST1 BLAST2 BLAST3 Barrow CLIVAR 01 Gas Change Experiment Harvard Forest HATS Ocean Projects Grifton Cape Kumukahi Park Falls Mauna Loa Niwot Ridge Niwot Ridge C-1 PHASE I-04 Trinidad Head (United States)	Geoffrey S. Dutton James W. Elkins Stephen A. Montzka	Halocarbons and Other Atmosphere Trace Species Group (HATS)/NOAA/ESRL Global Monitoring Division 325 Broadway R/GMD1 Boulder, CO 80305-3328, U.S.A
NOAA/CMDL Surface Ozone Network		
Tutuila (Cape Matatula) (American Samoa)	Sam Oltmans	NOAA/ESRL Global Monitoring Division 325 Broadway R/GMD1 Boulder, CO 80305-3328, U.S.A

LIST OF CONTRIBUTORS (continued)

Station Country/Territory	Name	Address
McMurdo / Arrival Heights South Pole (Antarctica)		
Ragged Point (Barbados)		
Summit (Greenland)		
Heimaey (Iceland)		
Lauder (New Zealand)		
Tudor Hill (United Kingdom)		
Barrow Mauna Loa Niwot Ridge Niwot Ridge (Saddle) Trinidad Head (United States)		

LIST OF CONTRIBUTORS (continued)

Station Country/Territory	Name	Address
CSIRO Flask Network		
Casey Station Mawson South Pole (Antarctica) Aircraft (over Bass Strait and Cape Grim) Cape Ferguson Cape Grim Macquarie Island (Australia) Alert Estevan Point (Canada) Shetland (United Kingdom) Mauna Loa (United States)	Ray Langenfelds Paul Krummel	Commonwealth Scientific and Industrial Research Organisation (CSIRO) CSIRO Marine and Atmospheric Research 107-121 Station Street Aspendale, Victoria 3195, Australia Postal address: PMB 1, Aspendale, Victoria 3195, Australia
ALE/GAGE/AGAGE Network		
Tutuila (Cape Matatula) (American Samoa) Cape Grim (Australia) Ragged Point (Barbados) Adrigole Mace Head (Ireland) Cape Meares Trinidad Head (United States)	Ray Wang Derek Cunnold	School of Earth and Atmospheric Sciences, Georgia Institute of Technology 311 Ferst Drive School of Earth and Atmospheric Sciences Georgia Institute of Technology Atlanta, GA 30332-0340

GLOSSARY

AGENCIES AND PROGRAMMES:

AES	Atmospheric Environment Service (Canada, presently MSC)
AGAGE	Advanced Global Atmospheric Gases Experiment
Aichi	Aichi Prefecture (Japan)
AIST	National Institute of Advanced Industrial Science and Technology (Japan)
AQRB	Environment CanadaMeteorological Service of CanadaAir Quality Research Branch (Canada)
ALE	Atmospheric Lifetime Experiment
AWI	Alfred Wegener Institute (Germany)
BMG	Bureau of Meteorology and Geophysics (Indonesia)
BoM	Commonwealth Bureau of Meteorology (Australia)
CAMS	Chinese Academy of Meteorological Sciences (China)
CESI	Italian Electrical Experimental Center (Italy)
CFR	Centre des Faibles Radioactivites (France)
CHMI	Czech Hydrometeorological Institute (Czech Republic)
CMA	China Meteorological Administration (China)
CMDL	Climate Monitoring and Diagnostics Laboratory (USA/NOAA, presently ESRL/GMD)
CNRS	Centre National de la Recherche Scientifique (France)
CSIRO	Commonwealth Scientific and Industrial Research Organisation (Australia)
DEFRA	Department for Environment, Food and Rural Affairs, London, United Kingdom
DNA-IAA	Direccion Nacional del Antartico-Instituto Antartico Argentino (Argentina)
DWD	Deutscher Wetterdienst (German Meteorological Service, Germany)
EARS	Environmental Agency of the Republic of Slovenia
EC	Environment Canada (Canada)
EMPA	Swiss Federal Laboratories for Material Testing and Research (Switzerland)
ENEA	Italian National Agency for New Technology, Energy and the Environment (Italy)
FMI	Finnish Meteorological Institute
GAGE	Global Atmospheric Gases Experiment
GAW	Global Atmosphere Watch (WMO)
GERC	Global Environment Research Center of NIER (Republic of Korea)
HATS	Halocarbons and other Atmospheric Trace Species
HMS	Hungarian Meteorological Service (Hungary)
IAFMS	Italian Air Force Meteorological Service, Italy
ICES	International Center for Earth Sciences c/o CNR. (Italy)
IGP	Instituto Geofísico del Perú (Peru)
IM	Instituto de Meteorologia (Portugal)
IMK-IFU	Fraunhofer Institut für Atmosphärische Umweltforschung, Garmich-Partenkirchen, Germany
INM	Instituto Nacional de Meteorología (Spain)
INMET	Instituto Nacional de Meteorologia (Brazil)
INMH	National Meteorological Administration (Romania)
IOEP	Institute of Environmental Protection (Warsaw)
ISAC	Istituto di Scienze dell'Atmosfera e del Clima, Consiglio Nazionale delle Ricerche, Italy
ITM	Department of Applied Environmental Science, Stockholm University,

	Sweden
IVL	Swedish Environmental Research Institute, Göteborg, Sweden
JMA	Japan Meteorological Agency (Japan)
KMA	Korea Meteorological Administration (Republic of Korea)
KMD	Kenya Meteorological Department (Kenya)
KSNU	Kyrgyz State National University (Kyrgyzstan)
LEGMA	Latvian Environment, Geology and Meteorology Agency, Latvia
LSCE	Laboratoire des Sciences du Climat et de l'Environnement (France)
METRI	Meteorological Research Institute (Republic of Korea /KMA)
MGO	Main Geophysical Observatory (Russian Federation)
MMS	Malaysian Meteorological Department,
MISU	Department of Meteorology, Stockholm University (Sweden)
MRI	Meteorological Research Institute (Japan/JMA)
MSC	Meteorological Service of Canada (Canada, formerly AES)
NCEP	National Centers for Environmental Prediction (USA/NOAA)
NIES	National Institute for Environmental Studies (Japan)
NILU	Norwegian Institute for Air Research (Norway)
NIMH	Institutul National de Meteorologie, Hidrologie si Gospodarirea Apelor (Romania)
NIPR	National Institute of Polar Research (Japan)
NIRE	National Institute for Resources and Environment (Japan)
NIST	National Institute of Standards and Technology (USA)
NIWA	National Institute of Water & Atmospheric Research (New Zealand)
NOAA/GMD:	Earth System Research Laboratory, Global Monitoring Division, NOAA, USA (formerly CMDL)
NUI	National University of Ireland, Galway (Ireland)
ONM	Office National de la Météorologie (Algeria)
Osaka Univ.	Osaka University (Japan)
PolyU	Hong Kong Polytechnik University, Hong Kong (China)
RIVM	National Institute for Health and Environment (Netherlands)
Roshydromet	Russian Hydrometeorological Service
Saitama	Saitama Prefecture (Japan)
SAWS	South African Weather Service (South Africa)
Shizuoka	Shizuoka University (Japan)
SIO	Scripps Institution of Oceanography, University of California at San Diego (USA)
SMN	Servicio Meteorológico Nacional (Argentina)
SNU	Seoul National University, Republic of Korea
Tohoku Univ.	Tohoku University (Japan)
UBA	Umweltbundesamt (Germany)
UBA Austria	Umweltbundesamt (Federal Environmental Agency), Austria
UHEI-IUP	Institut für Umweltphysik, Universität Heidelberg (Germany)
UM	University of Malta
WDCGG	World Data Centre for Greenhouse Gases, operated by JMA, Japan (WMO)
WMO	World Meteorological Organization
ZAMG	Central Institute of Meteorology and Geodynamics (Austria)

ATMOSPHERIC SPECIES:

CCl_4	tetrachloromethane (carbon tetrachloride)
CFC-11	chlorofluorocarbon-11 (trichlorofluoromethane, CCl_3F)

CFC-12	chlorofluorocarbon-12 (dichlorodifluoromethane, CCl_2F_2)
CFC-113	chlorofluorocarbon-113 (1,1,2-trichlorotrifluoroethane, CCl_2FCClF_2)
CFCs	chlorofluorocarbons
HCFC-141b	hydrochlorofluorocarbon-141b (1,1-dichloro-1-fluoroethane, CH_3CCl_2F)
HCFC-142b	hydrochlorofluorocarbon-142b (1,1-difluoro-1-chloroethane, CH_3CClF_2)
HCFC-22	hydrochlorofluorocarbon-22 (chlorodifluoromethane, $CHClF_2$)
HCFCs	hydrochlorofluorocarbons
CH_4	methane
CH_3CCl_3	trichloroethane (methyl chloroform)
CO	carbon monoxide
CO_2	carbon dioxide
N_2O	nitrous oxide
NO	nitrogen monoxide
NO_2	nitrogen dioxide
NO_X	nitrogen oxides
O_3	ozone
SO_2	sulphur dioxide

UNITS:

ppb	parts per billion
ppm	parts per million
ppt	parts per trillion

Others:

ENSO	El Niño-Southern Oscillation
M/V	merchant vessel
R/V	research vessel
SOI	Southern Oscillation Index
SST	Sea Surface Temperature

LIST OF WMO WDCGG PUBLICATIONS

DATA REPORTING MANUAL:

WDCGG No. 1	January	1991

WMO WDCGG DATA REPORT:

			(period of data accepted)				
WDCGG No. 2 Part A	October	1992	October	1990	~	August	1992
WDCGG No. 2 Part B	October	1992	October	1990	~	August	1992
WDCGG No. 3	October	1993	September	1992	~	March	1993
WDCGG No. 5	March	1994	April	1993	~	September	1993
WDCGG No. 6	September	1994	September	1993	~	March	1994
WDCGG No. 7	March	1995	April	1994	~	December	1994
WDCGG No. 9	September	1995	January	1995	~	June	1995
WDCGG No.10	March	1996	July	1995	~	December	1995
WDCGG No.11	September	1996	January	1996	~	June	1996
WDCGG No.12	March	1997	July	1996	~	November	1996
WDCGG No.14	September	1997	December	1996	~	June	1997
WDCGG No.16	March	1998	July	1997	~	December	1997
WDCGG No.17	September	1998	January	1998	~	June	1998
WDCGG No.18	March	1999	July	1998	~	December	1998
WDCGG No.20	September	1999	January	1999	~	June	1999
WDCGG No.21	March	2000	July	1999	~	December	1999
WDCGG No.23	September	2000	January	2000	~	June	2000
WDCGG No.25	March	2001	July	2000	~	December	2000

WMO WDCGG DATA CATALOGUE:

WDCGG No. 4	December	1993
WDCGG No.13	March	1997
WDCGG No.19	March	1999
WDCGG No.24	March	2001

WMO WDCGG DATA SUMMARY:

WDCGG No. 8	October	1995
WDCGG No.15	March	1998
WDCGG No.22	March	2000
WDCGG No.26	March	2002
WDCGG No.27	March	2003
WDCGG No.28	March	2004
WDCGG No.29	March	2005
WDCGG No.30	March	2006
WDCGG No.31	March	2007
WDCGG No.32	March	2008

WMO WDCGG CD-ROM:

			(period of data accepted)				
CD-ROM No. 1	March	1995	October	1990	~	December	1994
CD-ROM No. 2	March	1996	October	1990	~	June	1995
CD-ROM No. 3	March	1997	October	1990	~	June	1996
CD-ROM No. 4	March	1998	October	1990	~	December	1997
CD-ROM No. 5	March	1999	October	1990	~	December	1998
CD-ROM No. 6	March	2000	October	1990	~	December	1999
CD-ROM No. 7	March	2001	October	1990	~	December	2000
CD-ROM No. 8	March	2002	October	1990	~	January	2002
CD-ROM No. 9	March	2003	October	1990	~	December	2002
CD-ROM No.10	March	2004	October	1990	~	December	2003
CD-ROM No.11	March	2005	October	1990	~	December	2004
CD-ROM No.12	March	2006	October	1990	~	December	2005

CD-ROM No.13	March	2007	October	1990	~	November	2006
CD-ROM No.14	March	2008	October	1990	~	November	2007